Design of the Tidal Power Plant between the North Sea and a tidal basin

As part of the Delta21 project

Research thesis

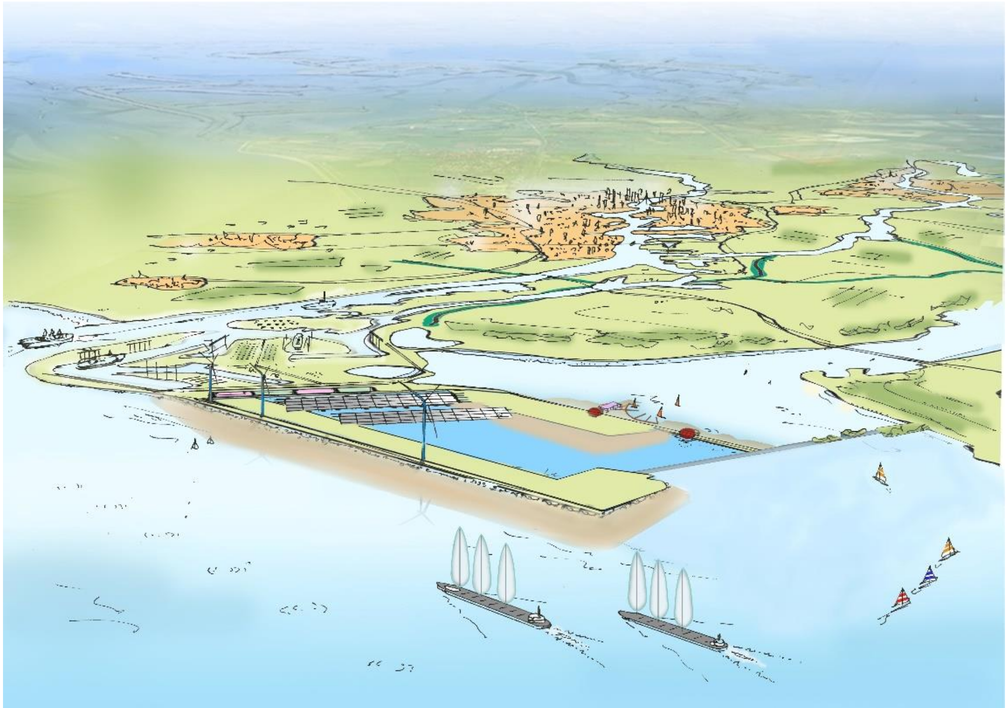

Author: Georges Dykmans

Student number: 00070477

Study year: 2018-2019

School: HZ University of Applied Sciences

Company supervisor: Huub Lavooij

Company: Delta21 & VolkerInfra

Supervisor: Joachim De Keijzer

Place & Date of publication: Vlissingen, August 2019

Report type: Final thesis

Preface

After being approached by my teacher S. van Schaick who proposed me the subject for this thesis, I was immediately on board with the Delta21 project idea of associating renewable energy production, hinterland flooding protection and nature restauration. I was given the task to design a tidal power plant for the project and soon realized the amplitude of the work it carried.

I would like to personally thank Huub Lavooij for his mentoring and always believing in me, as well as my thesis supervisor Joachim de Keijzer for pushing me forward, Samantha van Schaick without whom I would not have taken part in this great experience and the engineers, Raymond Meijnen, Hendrik Spek and Daan Van der Wiel for helping me throughout the thesis and answering my questions.

Georges Dykmans, Vlissingen, 02/08/2019

Summary

Meeting the Paris Climate Agreement goals for renewable energy, sea level rise protection and nature preservation require innovative multifunctional solutions in the Netherlands. As part of the Delta21 project, which looks at creating an energy storing reservoir and an energy producing tidal power plant while protecting the hinterland from flooding and restoring the Haringvliet fish migration, this research proposes the most optimal design for that tidal power plant. From three different alternatives comes the most suitable when considering fish-friendliness, costs, energy efficiency, maintenance efficiency and transportation of the caisson elements. The stability and strength of the caisson, during governing load situations, from the most suitable design, are then verified through calculations in two phases: transportation & immersion and commission. The results of this thesis thus provide a calculation methodology from civil engineering standards for a preliminary design of a tidal power plant.

Table of contents

1. Introduction 1
1.1 Background information 1
1.2 Problem Statement 2
1.3 Objectives and limitations 4
1.4 Research structure 5
2. Theoretical framework 6
2.1 Functional and technical requirements 6
2.1.1 Functional requirements 6
2.1.2 Technical requirements 6
2.2 Boundary conditions 8
2.2.1 Terrain data 8
2.2.2 Wind 9
2.2.3 Physical marine processes 10
2.2.4 Geological setting 15
2.2.5 Sea level rise and subsidence 16
2.3 Tidal power plants 17
2.3.1 Construction method 17
2.3.2 Dimensions 18
2.3.3 Turbines 24
2.3.4 Fish mortality 29
2.3.5 Gates 31
2.3.6 Joints 32
2.3.7 Piping 34
2.3.8 Bed protection 35
2.3.9 Stability checks during transport and immersion 38
2.3.10 Stability checks during commission 40
2.4 Risks and impacts 43
3. Method 44
3.1 Data collection 44
3.1.1 Literature research 44
3.1.2 Technical research 44
3.2 Data analysis 45

3.2.1 Calculations 45
3.2.2 Technosoft 45
3.3 Multi-Criteria Analysis 46
3.3.1 Alternatives 46
3.3.2 Criteria 47
3.3.3 Weighting factors 48
4. Results 50
4.1 Dimensions 50
4.1.1 Height 50
4.1.2 Length 51
4.1.3 Width 52
4.1.4 Thickness 53
4.1.5 Draught 54
4.2 Multi-Criteria Analysis 56
4.2.1 Fish friendliness 56
4.2.2 Costs 57
4.2.3 Energy efficiency 60
4.2.4 Maintenance efficiency 61
4.2.5 Transportation 62
4.2.6 Results 63
4.3 Ducted setup 67
4.3.1 Stoplogs 67
4.3.2 Stability checks during transport and immersion 69
4.3.3 Wave impact 72
4.3.4 Stability checks during commission 76
4.3.5 Bed protection 85
4.3.6 Preliminary design drawings 88
5. Discussions 94
6. Conclusion and recommendation 95
Bibliography 96
Appendix 1a: Venturi setup preliminary design A-A’ cross-section 1
Appendix 1b: Venturi setup preliminary design front view 2
Appendix 2a: Ducted setup preliminary design A-A’ cross-section 3
Appendix 1b: Ducted setup preliminary design front view 4

Appendix 3a: Hybrid setup preliminary design A-A’ cross-section 5
Appendix 3b: Ducted setup preliminary design front view 6
Appendix 4: SketchUp model of the Venturi setup in parallel projection from the front, the side and at an angle 7
Appendix 5: SketchUp model of the Ducted setup in parallel projection from the front, the side and at an angle 8
Appendix 6: SketchUp model of the Hybrid setup in parallel projection from the front, the side and at an angle 9

1. Introduction

Rapid carbon dioxide emission reductions are paramount in the current climate to meet the targets set by the Paris Climate Agreement. To reduce emissions while responding to the ever-growing energy demands, countries turn to renewable energies such as solar, eolian, hydraulic.

As part of the Delta21 project, the design of a structure must be defined to harness tidal energy through turbines. Different alternatives will be tested, and the end result will provide more than just guaranteed energy.

The following part of this chapter gives some background information on the problem. Then the problem statement of the research is drawn out specifying the main question and its derived subsequent questions. Thirdly, the objectives and limitations are defined and lastly, the structure of the research is stated to give an overview of the content each chapter is discussing.

1.1 Background information

Nowadays, the looming threat of climate change, energy crisis and the need to preserve natural environments and ecosystems bring projects such as the Delta21 project forward in an effort to develop and offer innovative solutions. For this reason, the Delta21 integral plan was created to primarily protect the Netherlands from flooding by proposing an alternative to the outdated concept of dike increases while remaining sustainable, energy efficient respecting the living ecosystems and their environment.

The investments only for dike heightening from 2029 to 2050 are estimated at € 2 billion and from 2029 to 2100 at over € 6 billion. The 800 km of dikes concerned will have to be raised to an average of approximately 0.8 m by 2100, partly due to the settlements. Moreover, if the sea level rises up to 1 m, then by 2100 more than € 11 billion extra can be saved on dike reinforcement and dike elevation. With Delta21, no additional investments in the dike reinforcements will be required in the area between the flood defenses and Gorinchem.

Delta21 is a spatial plan for the redevelopment of a part of the Dutch delta. It is mainly located west of the Haringvliet. It integrates several functions: flood protection, generation and storage of energy, fresh water buffer for the Rijnmond area and re-introduction of saline tides to restore the fish migration between the North Sea and the Rhine / Meuse back in the Haringvliet.

Figure 1. Span of the Delta21 works (Delta21, 2017)

As a result of the further settling of the polders, the geological settlement of the Netherlands, the appreciation of the land by increasing prosperity and population growth, the higher demands of agriculture and horticulture, the higher safety requirements of the residents and the sea level rise, Delta 21 found a solution for flood risk management: regulation of water levels through drainage, even in case of sea level rise.

The core of the Delta21 plan is the creation of a reservoir, where energy can be stored and again generated with help of pumps and turbines. In the reservoir with an installed pump/turbine capacity of about 1,8 GW and about 400 million cubic meters, sea water will be exchanged once a day. The large pump capacity can also be used to move superfluous river discharge into the North Sea. The other main point and energy source of the plan is the installation of a tidal power plant, on which the research will be focusing on, housing tidal turbines with an installed capacity of 60 MW that can generate energy using the tidal flows of the tidal basin and the Haringvliet. A floating solar panel park, optionally a wind farm and a warm water reservoir are part of the plan.

The gates of the Haringvliet sluices can always remain open, so the saline tide will be re-introduced in the Haringvliet, creating a saline water isotope. On the other hand, fresh water supply for Rotterdam and surroundings will be provided, creating possibilities for aqua cultures in the entire saline water area. Fish migration between North Sea and Rhine and Meuse will be enabled. The combination of all these functions will result in an attractive and healthy area for living and recreation.

1.2 Problem Statement

In the Netherlands, dikes are the primary defenses against the flooding of the hinterland. However, with the increase of the sea levels they need to be maintained and heightened to assure the safety of the country. With the current predictions for the sea level rise the heightening of dikes is expensive and not efficient over time. Multifunctional alternative solutions must be implemented to prepare for the rise in sea levels and answer the ever growing demand for energy and nature preservation.

The Delta Commission plans to heighten the dikes in the region surrounding the port of Rotterdam to meet the sea level rise predictions. The area south of the Maasvlakte 2 of the Port of Rotterdam constitutes the location for the Delta21 project and tidal power plant. The designing of the plant must provide a viable alternative to the heightening of dikes.

The aim of this research is to obtain a sustainable and efficient design of the tidal power plant providing a flow of water between the North Sea and the tidal basin. In the structure (concrete caisson) there will be 40 tidal turbines of 1,5 MW each, for a total of 60MW, these will create dynamic forces on the foundation and the structure itself, so, special consideration must be directed to these two elements.

A preliminary made design of the caisson was sketched as the picture below giving an impression of the possible caisson structure and how it could look like.

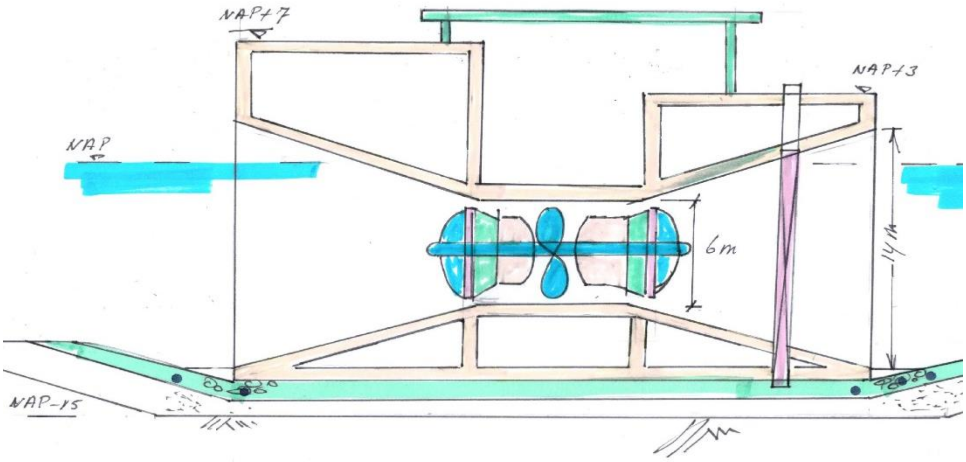

Figure 2. Preliminary design of the tidal power plant (Delta21, 2017)

Regarding the desired end result of this research, the thesis will be structured in a main research question and subsequent questions. Firstly, a theoretical background of the area will be outlined to learn about the environmental conditions the structure will be subjected to. Then, research will be carried out to determine the alternatives for the tidal structure by examining the subsequent questions. Finally, following suitable and relevant criteria, the optimal alternative answering the following main question will be drawn out and calculated:

What is the optimal design following the functional and technical requirements for the structure of the tidal power plant between the North Sea and the tidal basin to preserve water safety and the once ecologically rich Haringvliet estuary while providing sustainable energy with regards to fish-friendliness, costs and overall efficiency?

The following subsequent research questions are derived:

1. What are the functional and technical requirements of the tidal power plant housing turbines?
2. a) What are the boundary conditions shaping the project?

   b) Which external factors and forces acting on the structure need to be considered to ensure appropriate stability and a suitable design?
3. What are the risks and impacts of implementing the tidal power plant?
4. What are the possible alternatives and variants for designing an efficient and sturdy tidal power plant?
5. a) Which criteria are suitable for a relevant Multi-Criteria Analysis to find the ideal design?

   b) What are the weight factors of the different chosen criteria?
6. How will the design of the optimal alternative look like?

Firstly, research from different existing projects, European standards and experts is executed to obtain the functional and technical requirements of a tidal power plant. Secondly, external forces such as tides, waves, winds, storm conditions and their directions can be found in different sources such as waterboards websites or specific weather organizations reports. Thirdly, the alternatives are based on the difference of turbine system and channel setup. It results in varying structure designs which are compared to each other in the MCA. Finally, the optimal design is drawn out in AutoCAD and a model version of it is made in SketchUp for a better 3D perception.

1.3 Objectives and limitations

The main objective of this research is to obtain a sufficiently strong and well-founded design to help develop the Delta21 project further and provide them with solutions to problems that could arise if ever implemented.

The research will be limited in time and a choice has been made to take a civil engineer approach against a fluid mechanics one. So, the focus is made on the forces acting on the structure and how it will affect it rather than focusing on detailing and modeling the flow of water in the designed turbines ducts. The final product is also bound by defined competencies required to pass this research assignment. They go as follows:

BBE 1 Developing requirements for a design

CiT 1 Setting up and developing a schedule of requirements

BBE 2 Creating an integral design and justifying it

CiT 2 Setting up alternatives and variants

CiT 3 Assessing and choosing alternatives and variants

BBE 3 Specifying a design

CiT 4 Specifying calculations and drawings

Moreover, due to the short time period of the assignment, all the aspects of and surrounding the tidal power plant cannot be considered in the scope of the research. Therefore, the following limitations are set to define that scope:

- The subsoil composition at the location is considered from one borehole analysis, described later on, close to the subject area. A better soil analysis should be executed for the full integration of the design in the area.
- An Environmental Impact Assessment (EIA) should be drawn to ensure the best implementation of the design.
- The design of surrounding dunes is not considered.
- Any other requirements from potential stakeholders are not considered.
- The choice of turbine is already made: Pentair Fairbanks Nijhuis (PFN) turbines.
- The design of the gates will not be treated in this research.
- Only preliminary design of the structure will be drawn; however, details of specific elements will be made.

1.4 Research structure

In the following chapter, the theoretical framework presents a physical analysis of the area and its environment along with the general theory of tidal power plants providing a clearer understanding of their functionality and technicalities. The third chapter delivers the methodology employed during the research to obtain an optimal design. And finally, the results of the Multi-criteria Analysis and the calculations of the best alternative are laid out.

2. Theoretical framework

This chapter serves as the theoretical foundation to support the research by providing justification. First, the technical and functional requirements of the design will be set. Then, the physical analysis of the area is detailed in this chapter which includes the terrain data, the meteorological data, the physical marine processes, the geological setting, subsidence and sea level rise to highlight the boundaries conditions that will govern the choices made for the design of the structure. Thirdly, emphasis is made, after analysis of tidal power plants construction, on the actions the environment will act upon the structure. Then, the calculations and information surrounding the elements constituting the tidal power plant will be laid out. Finally, risks are assessed in a structural point of view.

2.1 Functional and technical requirements

Prior to the design phase, the requirements for the tidal power plant must be introduced. The functional and technical requirements serve as a base for the preliminary design and are defined in this chapter. The feasibility of the project has previously been done by Delta21 and from there are derived some of the described requirements.

2.1.1 Functional requirements

- The tidal power plant must create energy on demand.
- The tidal power plant must not reduce the water safety in the downstream region.
- The tidal power plant must not impede the flow of water between the North Sea and the tidal basin.
- The tidal power plant must assume the role of a primary defense according to the Dutch hydraulic standards.
- The gates of the turbine channels must be closed in case of extreme storm conditions.
- The gates must not impede with the flow of water through the channel when opened.
- The tidal power plant must be able to withstand during 1/10,000 storm events in addition to the sea level rise predictions.
- The tidal power plant must bring back tides in the Haringvliet.
- Access for maintenance must be made possible via a service road not open to the public for the time being.
- Gantry cranes or other relevant lifting mechanism for the gates and the turbines must be supported and fit in the structure.
- The turbines must be able to stop and start within 10 seconds.

2.1.2 Technical requirements

- The tidal power plant fish-friendliness allows for a mortality rate of fishes lower than 0.1%.
- The tidal power plant must be constructed for a functional lifetime of a 100 years.
- The tidal power plant must be long enough to house 40 turbines, a first given estimation specifies the length of the structure at 400 m.
- Minimal sediment transportation must be allowed through the channels.
- The turbines have a life expectancy of 50 to 60 years.
- The turbines must be demountable for easier installation and maintenance.
- Total replacement of turbines must be possible.
- The turbines must be fully submerged.
- An opening must be made possible to access the turbines in a dry environment or to lift the turbines up altogether via cranes for maintenance in a turbine housing.
- Maintenance activities must be able to be completed in a safe environment no matter what environmental conditions.

- The gates should preferably be placed at the end of the caisson.
- The stopping of the rotor must not impede the flow of the water.
- The turbines must be bi-directional and serve as pumps if needed.
- The Gantry crane for the turbines must be able to slide out of the structure to load carrier trucks for maintenance of turbine parts.
- The mechanical elements, the gates, the turbines and the cranes, must comply to the EU machine directive for health and safety.
- Overtopping must be of very low hindrance, lower than 10-20 l/s/m.
- Design and maintenance must conform to the Werkwijzer Ontwerpen Waterkerende Kunstwerken.

2.2 Boundary conditions

In order to determine the main dimensions and characteristics of the structure, the boundary conditions are required and laid down in this paragraph.

2.2.1 Terrain data

The case area is located south of the port of Rotterdam and west of the Haringvliet in the Netherlands.

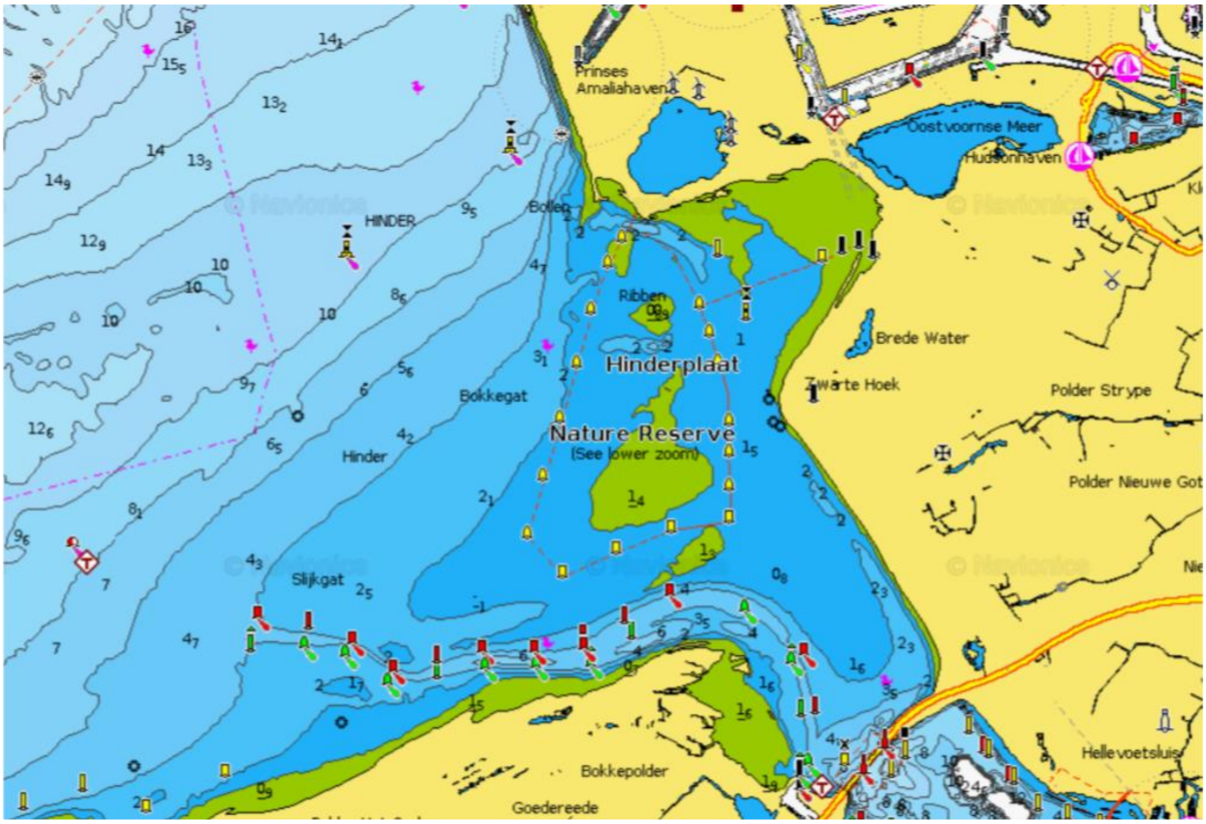

Figure 3. Bathymetry of the subject area (Garmin, 2019)

2.2.2 Wind

Below are the wind statistics at the Lichteiland Goeree/Renesse station on the Windfinder website which is the closest to the project location and provides a good correlation to the subject area. The website also offers a wind direction distribution in percentage with the dominant direction West South-West reaching 13.1% of the winds. The statistics are based on observations taken between 08/2001 - 02/2019 daily from 7am to 7pm local time.

Month of year	Jan 01	Feb 02	Mar 03	Apr 04	May 05	Jun 06	Jul 07	Aug 08	Sep 09	Oct 10	Nov 11	Dec 12	Year 1-12
Dominant wind direction													
Wind probability >= 4 Beaufort (%)	81	79	74	68	69	65	63	61	65	80	81	83	72
Average Wind speed (kts)	18	18	16	14	15	14	14	14	15	17	19	19	16
Average air temp. (°C)	6	5	7	9	13	15	18	18	17	14	10	7	11

Figure 4. Wind statistics at the Lichteiland Goeree/Renesse station (Windfinder, 2019)

The heaviest gust of wind in a hundred years was measured during a storm in Hoek van Holland, according to the KNMI, where the meter shot out at 162 kilometers per hour on November, 6 1921, that is 45 m/s gusts of wind with highest hourly average wind speeds of 32 m/s. Hoek Van Holland lying north of the Maasvlakte of the port of Rotterdam is relatively close to the subject location hence the assumption that the area was also hit by the same wind speeds from a West South-West direction.

In shallow seas, deltas, closed off creeks, and lakes, wind fields can influence the water level quite considerably by damming up the water (wind set-up).
Figure 5 shows a model to approximate the wind set-up.

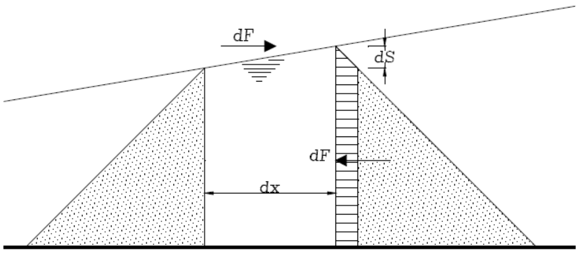

Figure 5. Balance of the forces in case of wind set-up (Voorendt, Bezuyen, & Molenaar, 2011)

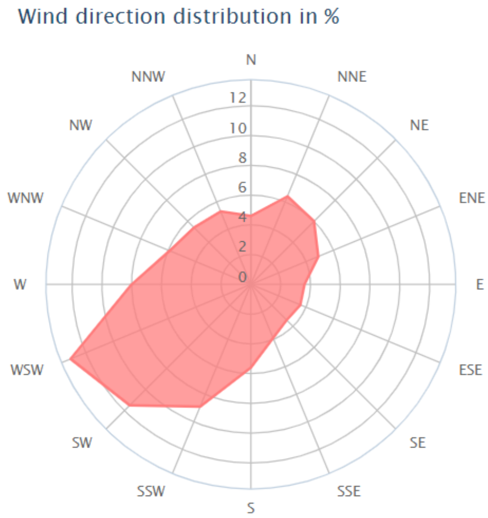

Figure 6. Wind distribution for the Lichteiland Goeree/Renesse station (Windfinder, 2019)

The wind set-up in the equilibrium state is approximately:

$$S = C_2 \cdot \frac{u^2}{g \cdot d} \cdot dx$$

With:
- S total wind set-up [m]
- C_2 constant ≈ 3.5·10^{-6} to 4·10^{-6} [-]
- d water depth [m]
- dx fetch [m]
- u wind velocity [m/s]

2.2.3 Physical marine processes

Astronomical tides

The tidal fluctuations depend on moon and sun cycles in combination with the oceanic configuration. They can be predicted fairly reasonably and are published by various authorities. (Voorendt, Bezuyen, & Molenaar, 2011). The Rijkswaterstaat offers an array of data recorded by their meteorological stations from which historical data can be retrieved. The Haringvliet 10 station is perfectly located to provide accurate information on the subject area.

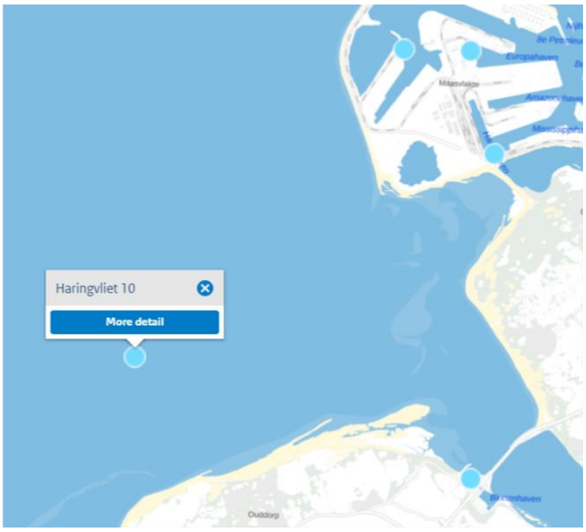

Figure 7. Location of the Haringvliet 10 station (Rijkswaterstaat, 2019)

In the following table is an overview of the water levels recorded by the station Haringvliet 10 between March 1st 2018 and March 1st 2019 which are considered as base for the dimensioning of the tidal power plant. Therefore, additional data access would be needed to thoroughly determine the most probable water levels.

Parameter	Value	Unit
Maximum tidal range	+2.99	m
Average tidal range	+2.11	m
Maximum High Water Level	+1.77	m NAP
Minimum High Water Level	+0.53	m NAP
Average High Water Level	+1.26	m NAP
Maximum Low Water Level	-0.48	m NAP
Minimum Low Water Level	-1.20	m NAP
Average Low Water Level	-0.84	m NAP

Table 1. Water levels recorded by Haringvliet 10 station (Rijkswaterstaat, 2019)

The maximum tidal range is the largest that has ever been recorded by the station and thus will be considered for the purpose of the research.

Maximum water levels, necessary for the assessment of the crest elevation, must take into account maximum tidal levels, wind setup, storm surge, wave runup and any long term variation in mean water levels that may be anticipated. […] The significant wave height is computed as the mean of the largest one-third of the waves for each storm condition evaluated. The maximum individual wave may be about twice the significant wave height. […]

Minimum water levels may be computed from tabulated tidal data and estimates of wind set down and wave drawdown. Minimum tidal levels would be lower, low -water level, low tide, or LLWLT. The same wind setup and significant wave evaluations used for selecting structural crest elevations can be used in the opposite sense for assessing minimum water levels. For single effect, ebb-tide generation, avoidance of turbine cavitation is a critical consideration at the point in operating cycle when the seaside water level is at its lowest. The minimum seaside water level would be the minimum tidal levels less a wind set down, with an appropriate exceedance frequency determined from the wind spectrum analysis. The turbine manufacturer will specify a minimum setting for the turbines below the lowest water level that would produce no cavitation (Clark, 2007).

Waves

The document *Hydraulische Randvoorwaarden primaire waterkeringen* (Waterstaat, 2007), developed by the Rijkswaterstaat provides design data for primary defenses in the Netherlands. In our case the Dike ring area 25, located in the province of South Holland, which broadly covers the area of the island Goeree-Overflakkee with the North Sea and the Haringvliet on the north side is used as reference as it comes closest to our subject area.

Wind waves are displayed with a characteristic wave height, wave period and an angle of wave incidence (the Wave Limit Conditions). The angle of wave incidence is shown in degrees relative to the direction perpendicular to the flood defense. The wave direction is shown in degrees with respect to the wind direction North (clockwise direction, see Figure 8). The wave height is expressed as the significant wave height (Hs or Hm0). The peak period ($T_{m-1.0}$) is used for the wave period

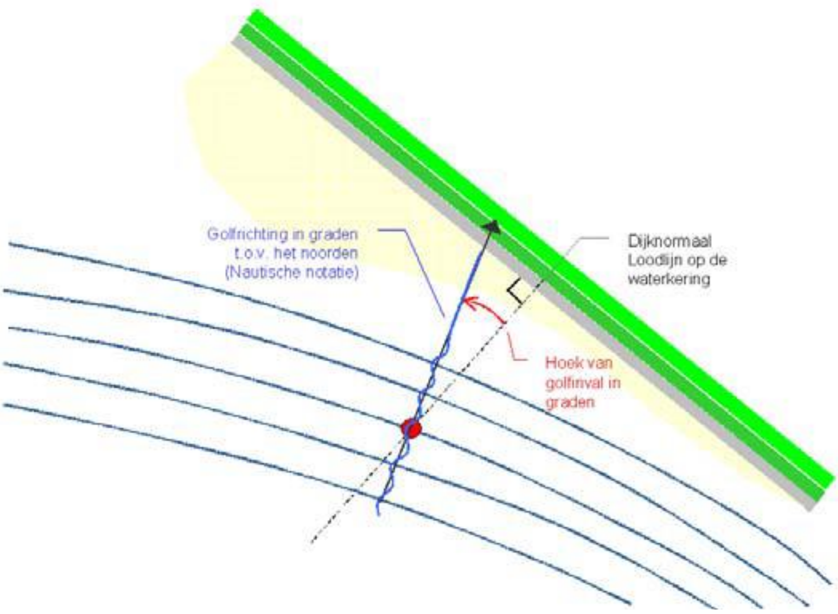

Figure 8. Angle of wave incidence (Waterstaat, 2007)

The data gathered from the document is presented in the following table with a probability of 1/4000:

Location	Design Water Level [m+NAP]	Significant wave height H_{m0} [m]	Wave period $T_{m-1.0}$ [s]	Incoming wave β [°]
Flaauwe Werk	5.0	2.9	10.2	20

Table 2. Data from HR2006

Figure 9 indicates the location where the data was retrieved in Flaauwe Werk. It is the closest station to the subject are and thus its data is considered.

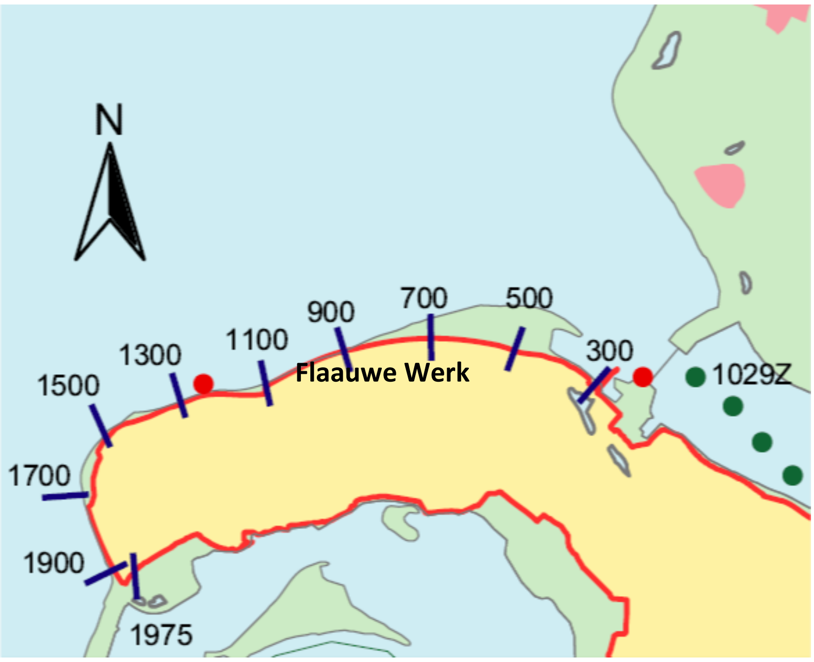

Figure 9. Location of the data recovery point Flaauwe Werk (Waterstaat, 2007)

Design wave height

The significant wave height H_s is the average of the highest 1/3 of the waves. This wave occurs regularly and is therefore a much lower than the design wave height H_d. If the effects of shallow water can be disregarded with a small wave height, a Rayleigh distribution can be assumed. The probability of exceedance of a given wave height within a given wave field is:

$$\Pr(H > x) = e^{-2\left(\frac{x}{H_s}\right)^2}$$

Therefore, the probability that the design wave height H_d is exceeded during a storm with N waves is:

$$\Pr(H > H_d) = 1 - e^{-Ne^{-2\left(\frac{H_d}{H_s}\right)^2}}$$

For a storm along the coast one can assume $T_{storm} = 2$ h. Using the time period of the incoming waves T_{wave}, the number of waves N along the coast is:

$$N = \frac{T_{storm}}{T_{wave}}$$

If one allows an exceedance probability $\Pr(H > H_d) = 0.10$, the design wave height H_d is:

$$H_d = \sqrt{-\frac{\ln\frac{\ln(1-0.10)}{-N}}{2}} \cdot H_s$$

To ascertain the design wavelength, one may assume that the shape of the energy spectrum essentially does not change for light and heavy storms, so:

$$L_d \approx L_s$$

Wave impact

During the operation phase, when the structure is affected by storm surges throughout which the gate must be closed, the wave impact represents the major wave load. As the gate is closed, the caisson is thus assumed to be a vertical breakwater. To calculate the wave impact, Goda's expression, modified by Tanimoto, is used in helping to determine the wave pressures at several locations in front of the caisson. In case of breaking waves on top of the sill Takahashi adopted a couple of factors obtained by Goda.

Goda (1985, 1992) made a general expression for the wave pressure on a caisson on a rockfill sill. This expression can also be used for broken and breaking waves. Worldwide Goda's equations are used often for the design of vertical breakwaters, see figure 10. Combining Goda and Takahashi leads to the following equations: (Van Saase, 2018)

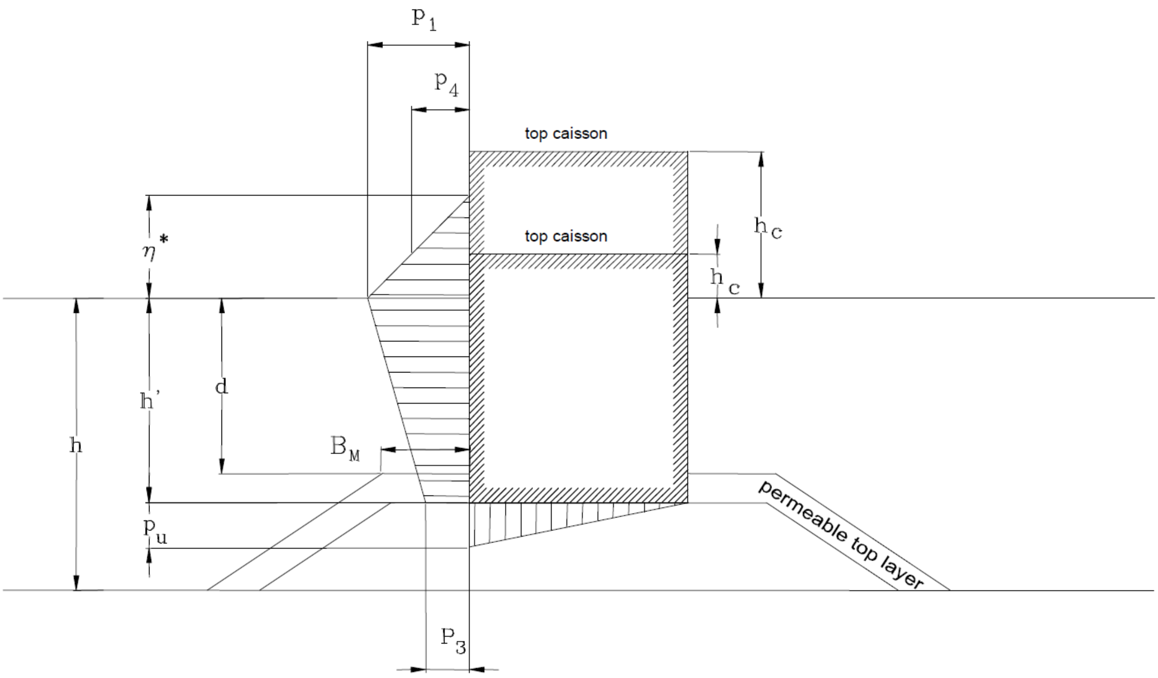

Figure 10. Goda (modified by Tanimoto): wave pressure (Molenaar & Voorendt, 2016)

The sill height is $h - d$.
The sill width is B_M.
The maximum wave pressures are:

$$p_1 = 0.5(1 + \cos\beta)(\lambda_1\,\alpha_1 + \lambda_2\alpha_2\cos^2\beta)\rho h H_D$$

$$p_3 = \alpha_3 p_1$$

$$p_4 = \alpha_4 p_1$$

$$p_u = 0.5(1 + \cos\beta)\lambda_3\alpha_1\alpha_3\,\rho h H_D$$

$\eta^* = 0.75(1 + \cos\beta)\lambda_1 H_D$ the elevation at which the wave pressure is exerted

$$\alpha_1 = 0.6 + 0.5\left(\frac{4\pi h/L_D}{\sinh(4\pi h/L_D)}\right)^2$$

$$\alpha_2 = min\left(\frac{(1-\frac{d}{h_b})(\frac{H_D}{d})^2}{3}, \frac{2d}{H_D}\right)$$

$$\alpha_3 = 1 - \left(\frac{h'}{h}\right)\left(1 - \frac{1}{\cosh(\frac{2\pi h}{L_D})}\right) \approx \frac{1}{\cosh(kd)} \quad \text{(without sill)}$$

$$\alpha_4 = 1 - \frac{h_c^*}{\eta^*}$$

$$h_c^* = \min(\eta^*, h_c)$$

With:

β	[°]	the angle of the incoming wave
$\lambda_1, \lambda_2, \lambda_3$		the factors dependent on the shape of the structure and on wave conditions; (vertical wall and non-breaking waves: $\lambda_1 = \lambda_2 = \lambda_3 = 1$)
		λ_1 the reduction or increase of the wave's slowly-varying pressure component
		λ_2 the changes in the breaking pressure component
		λ_3 the changes in the uplift pressure
h_b	[m]	water depth at a distance $5H_D$ from the wall
H_D	[m]	design wave height
L_D	[m]	design wavelength
d	[m]	water depth above the sill
h'	[m]	water depth above the wall foundations plane
h	[m]	water depth in front of the sill
T	[s]	wave period

Using the linear wave theory laid down in Table 3, the design wavelength is calculated from which the relative depth characteristics are determined.

Relative depth characteristics	Shallow Water $\frac{h}{L} < \frac{1}{20}$	Transitional water depth $\frac{1}{20} < \frac{h}{L} < \frac{1}{2}$	Deep water $\frac{h}{L} > \frac{1}{2}$
Wave length	$L = T\sqrt{gh}$	$L = \frac{gT^2}{2\pi}\tanh kh$	$L = L_0 = \frac{gT^2}{2\pi}$
Wave number		$k = \frac{2\pi}{L}$	

Table 3. Linear wave theory and wave characteristics (Voorendt, Bezuyen, & Molenaar, 2011)

2.2.4 Geological setting

The subsoil information of an area is crucial before implementing any structure and the DINOloket portal provides extensive data from the Dutch subsurface thanks to many analyses of borehole measurements and drilling profiles.

From the geological drilling survey BS031207 done the 13th of June 1996 a drill sample profile and 12 grain size analyses can be retrieved.

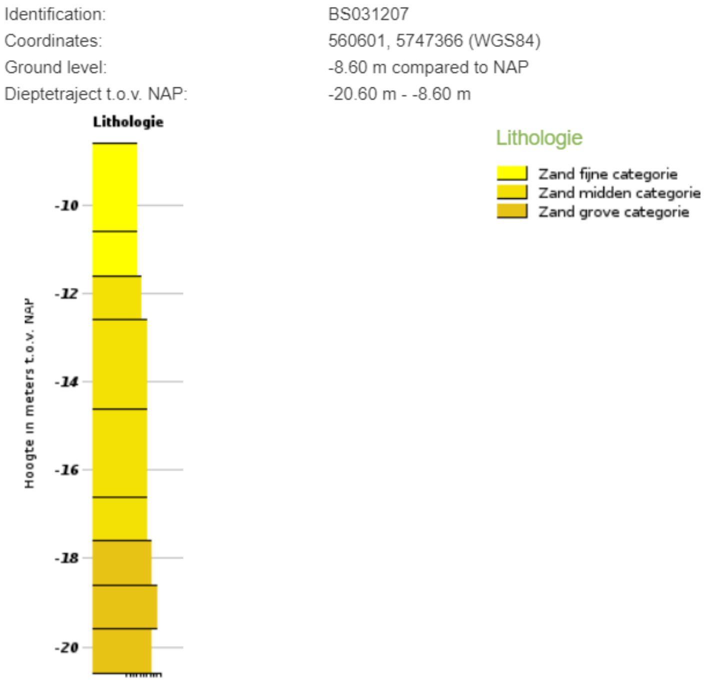

Layer	Properties
-8.6; -10.6	Very fine sand
-10.6; -11.6	Very fine sand
-11.6; -12.6	Moderately fine sand
-12.6; -14.6	Moderately coarse sand
-14.6; -16.6	Moderately coarse sand
-16.6; -17.6	Moderately coarse sand
-17.6; -18.6	Very coarse sand
-18.6; -19.6	Extremely coarse sand Clay
-19.6; -20.6	Very coarse sand Clay

Figure 11. Lithology of subject area subsoil (Netherlands Organization for Applied Natural Sciences Research TNO, 2019)

The grain size analyses provide the particle size distribution of the sand in the subject area. From the data it can be concluded that the soil is mainly composed of fine to coarse sand. The sand has a particle diameter of 0.063<D<2 mm.

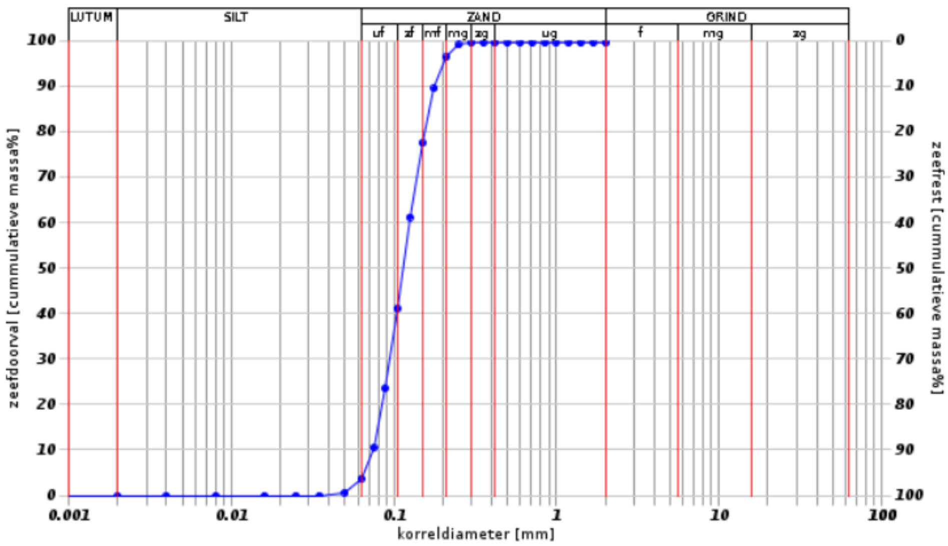

Figure 12. Grain size distribution for the first subsoil meter (Netherlands Organization for Applied Natural Sciences Research TNO, 2019)

Due to a lack of precise bathymetric analysis, the previous borehole survey is taken as governing for the entire structure's surrounding bed level. Therefore, the bed level is taken at -8.60 m NAP.

2.2.5 Sea level rise and subsidence

For a low-lying delta like the Netherlands, the possible impacts of sea level rise induced by climate change are a major concern. Global mean sea level rise is mainly caused by steric changes (changes in in ocean density, predominantly due to thermal expansion), and eustatic changes (changes in ocean mass), due to mass changes in small continental glaciers and ice sheets, and in the Antarctic Ice Sheet and Greenland Ice Sheet. (Katsman, Sterl, Beersma, & al., 2011).
This article weighs and evaluates whether the Netherlands' flood protection strategy is capable of coping with future climate conditions, focusing on sea level rise in case of low-probability/high impact scenarios. From their analyses, they develop a plausible high-end scenario of 0.40 to 1.05 m rise on the coast of the Netherlands by 2100 without considering land subsidence.

Moreover, the Delta Committee predicts sea level rises from 0.65 to 1.3 m by 2100 and from 2 to 4 m by 2200 including land subsidence. (Deltacommissie, 2008). Meaning, by 2100 a sea level rise of 1.2 m with a 10 cm subsidence is chosen as design value. Those values represent the possible upper limits, so by taking them into account during the design process ensures a long term sustainability of the structure.

Because we determined a lifetime of 100 years for the structure, the aim is to find the level of the sea by 2120. If we follow the trend predicted by the Delta Committee in 2008, it results in a rise in sea level of 1.3 cm/year and if the rise reaches 1.2 m in 2100 then it can be expected that by 2120 the sea level rise will attain 1.46 m. Following the same process for the subsidence predicted by the Delta Committee, the subsidence rate is 1.09mm/year. Consequently, by 2120 the subsidence would have reached 12.2 cm.

The addition of the sea level rise and the subsidence gives the relative sea level rise. In this case the relative sea level rise attains 1.58 m.

Parameter	Value	Unit
Maximum tidal range	+2.99	m
Average tidal range	+2.11	m
Maximum High Water Level	+3.35	m NAP
Minimum High Water Level	+2.11	m NAP
Average High Water Level	+2.84	m NAP
Maximum Low Water Level	+1.10	m NAP
Minimum Low Water Level	+0.38	m NAP
Average Low Water Level	+0.74	m NAP

Table 4. Water levels applicable to the 2120 scenario with a 1.58 m relative sea level rise (Rijkswaterstaat, 2019)

2.3 Tidal power plants

2.3.1 Construction method

The construction method for this project is construction in the “wet” that is, prefabricated caisson in a dry dock. The chosen dry dock is located at the former RSV shipyard, and now the Damen ship repair and conversion shipyard, in the port of Rotterdam for the current project. This choice resulted from discussions with Huub Lavooij and Leen Berke. The wet construction method was chosen for the caissons because it presents less perturbation through time to the entrance of the estuary and its flow. Building in the “dry” would require the closing off of the estuary to be able to build the all structure in-situ.

By choosing the wet construction method, the caisson needs to be transported from the dry dock to the location with minimum risks regarding water depth and draught. The following figure gives the route the caissons must take to arrive to destination.

Figure 13. Length of floatation route (https://www.google.com/maps)

According to Mohamed A. El-Reedy in his book, Offshore Structures (El-Reedy, 2012), tugboats run at speed from 12 to 15 knots, that is, between 22.2 km/h and 27.8 km/h. By averaging, it is assumed that the tugboats carrying the caissons run at 25 km/h.

With 51 km to go from the dry dock to the location, approximately 2 hours are necessary to complete the transportation. To tally any dredging activities regarding keel clearance between the bottom of the structure and the seabed, the floating phase is carried out during High Water Level, starting an hour before and finishing an hour after to exploit fully the maximum water depth. It is known as slack water as nearing the peak of the tide, the increase in water depth is the lowest following the rule of twelfths. The rule of twelfths is an approximation presuming that the increase in depth in the six hours between low and high water is: first hour: 1/12, second: 2/12, third: 3/12, fourth: 3/12, fifth: 2/12, sixth: 1/12.

2.3.2 Dimensions

Experience taught that a 'standard recipe' for the design of caissons cannot be given. Specific project requirements and local circumstances generally differ too much to make the design that simple. However, an overall approach that in most cases leads to good results is a two-step approach: first determine the main dimensions and then, step 2, check the dimensions based on a number of basic engineering calculations. It cannot be avoided that some steps have to be repeated if requirements are not met: In that case the initial dimensions have to be reconsidered and previously done checks have to be repeated.

Figure 14 illustrates how the design process gets into iteration when determining the dimensions of the caisson. (Voorendt, Bezuyen, & Molenaar, 2011)

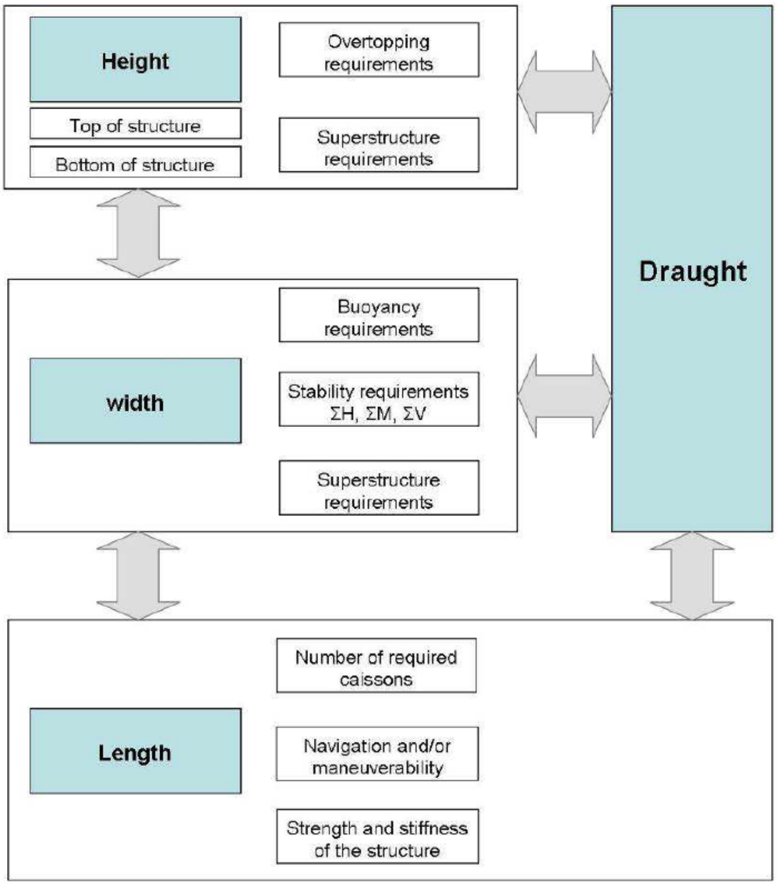

Figure 14. Iteration to find the caissons main dimensions (Voorendt, Bezuyen, & Molenaar, 2011)

Height

The height by simple definition is the difference between Top of Structure (ToS) and Bottom of Structure (BoS); so, determining the height comes down to finding these two levels. To start with the latter: BoS for caissons used in breakwaters and quay walls, usually depends on the original bed level or on the level of the sill or soil improving (gravel) bed constructed on the original bottom.

ToS for breakwaters and quay walls (i.e., uncovered caissons) depends on:

- astronomical tide
- wind set-up
- height of wind waves
- refraction, shoaling, breaking, reflection and diffraction of wind waves
- overtopping (and eventually wave run-up)

and occasionally:

- extra freeboard
- seiches
- shower oscillations and shower gusts
- relative sea level rise

To calculate the overtopping of a structure, two different methods can be used: the steep slope approach and the gentle slope approach. In the research case, a gentle slope would lead to an unwanted increase of the width of the caissons. The 2018 EurOtop (van der Meer, et al., 2018) gives information on the allowed overtopping of a structure, depending on its purpose, its slope and its allowed overtopping, to find an appropriate freeboard.

A certain overtopping discharge could be allowed as only the tidal basin lies behind the tidal power plant and the overflowing at the reservoir provides security regarding excess of water in the basin. No public roads nor public access has been decided so it is supposed that the crest is only allocated by a service road and room for maintenance activities for now. Future public access is in discussion, so this aspect is not considered for the design.

The 2018 EurOtop manual gives limits for overtopping not to be exceeded.

Hazard type and reason	Significant wave height H_{m0} (m)	Mean discharge q (l/s per m)	Max volume Vmax (l per m)
Cars on seawall / dike crest	3	<5	2000
	2	10-20	2000
	1	<75	2000

Table 5. Limits for overtopping for people and vehicles

With a significant wave height of 2.9 m at the location, a maximum flow rate of 5 l/s/m or 0.005 $m^3/s/m$ at the design water level +5 m NAP is selected.

However, because overtopping in the present situation does not affect the proper functioning of the tidal power plant and the road on top of the structure is a service road, slack can be given to the maximum flow rate going over the crest. Moreover, the design presents no grass slope, subject to erosion in case of overtopping, as it is all made in concrete and it leads to no significant effects on the water level in the tidal basin. The range 10-20 l/s/m is therefore chosen as maximum overtopping flow rate.

As overtopping is expected to occur during storm surges, it is assumed that the gates of the turbine channels will be closed off in such events, so we consider a structure with vertical walls.

For a design approach, with vertical walls and without foreshore influence nor breaking waves, the following formula should be used:

$$\frac{q}{\sqrt{g \cdot H_{m0}^3}} = 0.054 \cdot \exp[-\left(2.12 \frac{R_c}{H_{m0}}\right)^{1.3}]$$

With:

$\frac{q}{\sqrt{g \cdot H_{m0}^3}}$ the dimensionless overtopping discharge [-]

$\frac{R_c}{H_{m0}}$ the relative crest freeboard [-]

q the maximum overtopping discharge [l/s/m]

R_c the crest height [m]

H_{m0} the significant wave height [m]

$$R_c = \frac{\sqrt[1.3]{-\ln\left(\frac{q}{0.054\sqrt{g \cdot H_{m0}^3}}\right)} \cdot H_{m0}}{2.12}$$

Adding the newly found crest height to the previously found design water level and significant wave height gives the level of the top of the structure.

Width

The lecture notes by Voorendt & al. (Voorendt, Bezuyen, & Molenaar, 2011) on caissons denote that the width should be determined for the transportation process first. As the preferred construction method to build the caissons is in a dry environment instead of a wet environment, they will be floated on location.

Once the caisson height has been selected, the width of the caisson must be determined considering the required keel clearance during the floating transport stages of the caisson; this appears to be governing in most cases. In the equilibrium equation for floating objects (weight = buoyant force) the weight of the caisson must be verified using a best guess for the width in order to be able to compute the draught.

An additional factor to consider for determining the width of the caisson is piping under the structure. Using Bligh's and Lane's formulas, a safe seepage distance can be established and thus provide a minimum width for the structure. The piping mechanism and the process to calculate the seepage length are defined and developed in more detailed in the paragraph 2.3.7 Piping.

Length

Voorendt & al. indicate that based on experience and construction practices a length/width ratio of 3/1 can be used as first magnitude and proved efficient for comparable projects. The length/width ratio of 2.2 / 1 of the Veersche Gat unity caissons was less favorable with respect to maneuverability. Relatively, much power was needed to control the floating caissons under all circumstances. For the closure of the Brouwersdam, caissons were used with a length/width ratio of 3.8 / 1, which proved to be easily navigable. Tow tests at the Maritime Research Institute Netherlands (MARIN) showed that a length/width ratio of 3 / 1 is sufficient for navigation.

Another factor to consider is that longer caissons reduce the number of immersions thus diminishing the risks that procedure represents in relation with other previously immersed caisson along with a decrease in the number of joints or shear-keys necessary for the stability of the structure. Detailing of the application of joints is made in the paragraph 2.3.6 Joints.

Nonetheless, longer length can hinder the positioning and immersion processes, especially in currents. Therefore, for safer maneuverability of the caissons, the length must be limited.

More accurately and realistically, the immersion and navigation characteristics during transport and the resulting caisson strength and stiffness should be taken into consideration. And provision is made on the estimated length using the provided rule of thumb by means of stability checks during transportation and immersed situation.

Thickness

The same lecture notes, as stated previously (Voorendt, Bezuyen, & Molenaar, 2011), stipulate that the thickness of the external concrete elements: walls, roof and floor, is governed by the load situation occurring during the floating phase. This can be explained due to the absence of water or soil ballast on the inside of the structure thus providing no counter load to the forces acting on the outside by the water.

If, however, the bed under the caisson is not smooth, the governing load condition could occur when the fully loaded caisson rests on eventual bumps or big boulders on the bed. The caisson in this case, is not evenly supported by the subsoil, which causes concentrated loads. This implies a considerable increase of bending moments and stresses in the concrete, compared to the floating phase, which is not unlikely to cause torsion of the entire caisson.

Additional precautions must then be taken to ensure a leveled and smooth bed accomplished by accurate dredging or precise rumble dumping followed by follow-up treatment and monitoring. Extra thickness can also be applied to the walls and the bottom plate to bear eventual concentrated loads. However, in this case, it is assumed that the sill's surface is smooth.

The thickness of the concrete elements is tested subsequently via stability checks.

Draught

If the found dimensions conflict with the required maximum draught, there are three main methods to reduce the draught of the caisson:

- reduction of the weight, generally by decreasing the thickness of walls or bottom slab, but it may result in finishing caisson construction ‘after’ immersion as well
- increase buoyancy of the structure, generally by increasing the width and/or the length of the caisson
- adding additional buoyancy during transport, for instance with help of drift bodies

Thus, values for the caisson height, width and length are found, plus the estimated wall and bottom thicknesses. However, it should be checked if these dimensions suffice with respect to all load situations that can be expected.

The draught (d) of the caisson is limited by the required minimum keel clearance. This means the buoyant force should be large enough. To determine the buoyant force (F_b), the under-water volume of the caisson (V_{uw}) has to be computed:

$$V_{uw} = b \cdot l \cdot d \; [m^3]$$

A length-width ratio of $l = 3b$ has proven reasonable with respect to navigability, so:

$$V_{uw} = b \cdot 3b \cdot d = 3b^2 \cdot d \; [m^3]$$

The buoyant force then is:

$F_b = V_{uw} \cdot \gamma_w = 3b^2 \cdot d \cdot \gamma_w \; [kN]$, where b and d are unknown parameters.

The allowable draught must be determined considering various bed and water levels. Two situations that have to be examined anyway are transport and positioning & immersion.

During transport there should be at least 1.00 m keel clearance while during the positioning above the sill, the maneuvers will be more careful, so a keel clearance of 0.50 m suffices. The positioning will take place immediately before immersion, so at mean low water.

The transport and positioning & immersion condition should be both valid, so the draught of the caisson should be smaller than the minimum draught out of the two conditions.

2.3.3 Turbines

The tidal power plant must house 40 turbines and the choice was made by Delta21 to include Pentair Fairbanks Nijhuis turbines in the project. The *Conceptual Design and Comparison of Two Propeller Turbine Configurations* (Meijnen & Arnold, 2015), offers a description of the two bulb turbines used in two different setups: a ducted setup and a venturi setup.

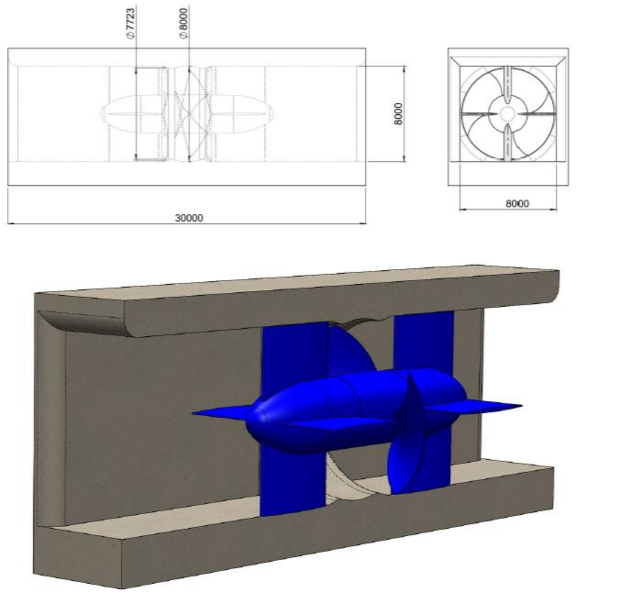

Figure 15. Dimension drawing of turbine in ducted setup (8.00 m diameter rotor) (Meijnen & Arnold, 2015)

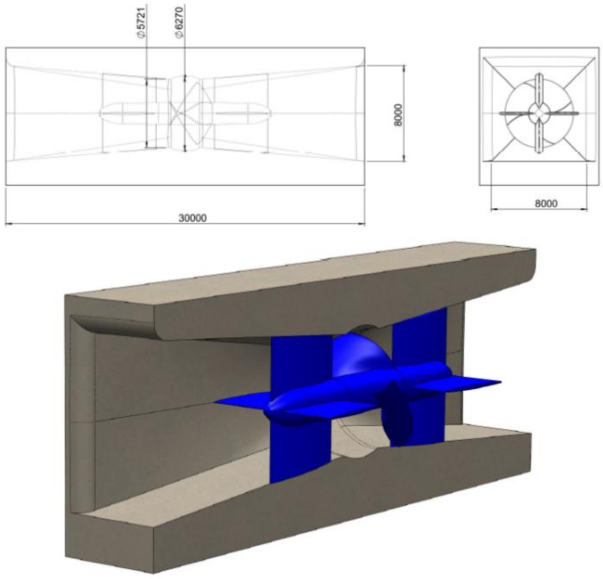

Figure 16. Dimension drawing of turbine in venturi setup (5.80 m diameter rotor) (Meijnen & Arnold, 2015)

In this report a turbine design is presented for both a venturi (diffuser) type channel and a ducted channel. With the aid of CFD, it is examined which performance differences are to be expected and what influence this will have on the civilian part of the tidal power plant. Also, costs for both turbine variants are estimated.

The manufacturer suggests, that the axis of the turbine should be minimally submerged by one time the diameter of the rotor below minimum water level to ensure good functioning and cavitation.

For the current research, the results of the previously described report are assumed and integrated. The difference in setups will serve as basis for the alternatives to be analyzed in the Multi Criteria Analysis which is developed further in the third chapter under 3.3 Multi-Criteria Analysis.

These turbines are chosen for their fish-friendliness, bi-directional profile and capacity to turn into pumps if the necessity arises.

Design flow rates

The report describes the flow through turbines and the effect of the latter on the former.

In figure 17, a schematic representation of a guided flow water turbine is presented. The turbine with a rotor surface A_r is placed in or behind a channel or passage opening with cross-sectional area A_s, the flow velocity being determined by the prevailing pressure difference H.

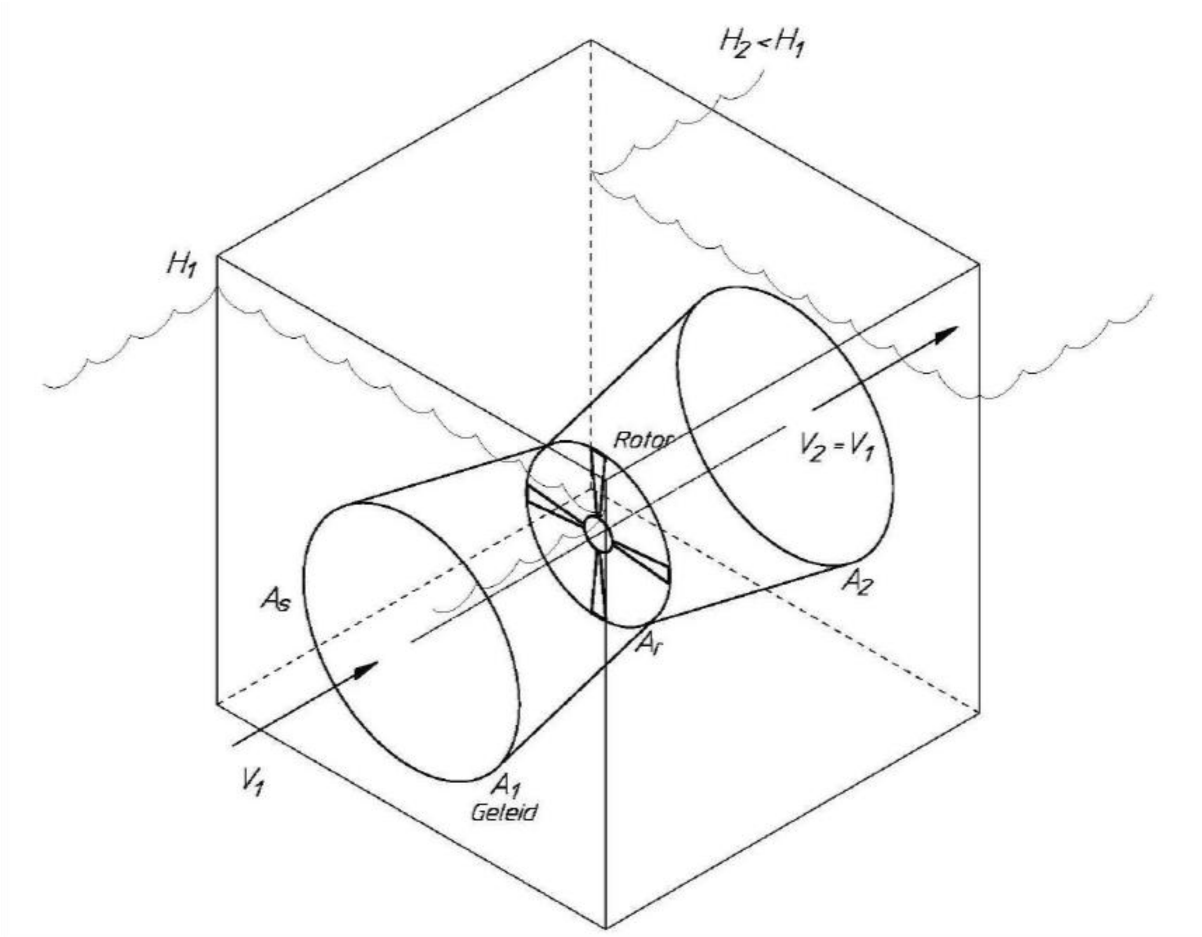

Figure 17. Schematic presentation of a direct current turbine (Meijnen & Arnold, 2015)

A turbine placed in, or in the vicinity of a passage opening, lowers the pressure gradient. This results in a reduction in flow. For a conduction current turbine, $h_2 < h_1$ and $v_2 = v_1$. The theoretical capacity and the pressure gradient are then:

$$P = \rho Q(h_2 - h_1)$$

$$H_r = (h_2 - h_1) = fH$$

With: H_r the energy added or withdrawn by the rotor

f the degree of reaction of the turbine (0 – 1)

Nevertheless, if all (pressure) energy is withdrawn (f = 1), the flow stops and $Q = 0$ and $P = 0$. So, only a fraction f of the system pressure level can be used. The fraction f of the available system pressure difference H can be used varying between 0 and 1, with an optimum somewhere. The flow rate is then:

$$Q_{sred} = A_s\sqrt{\frac{2g(|H| - H_r)}{C}} = A_s\sqrt{\frac{2g|H|(1-f)}{C}}$$

With: C the loss coefficient due to friction and turbulence in the passage opening

From their research, Meijnen and Arnold gathered that for the maximum power $f = \frac{2}{3}$ and the resulting reduction in flow is approximately of 42%.

Because both setups presented in the Meijnen and Arnold report are used it is assumed that:

$A_s = 8 * 8 = 64$ [m^2] opening cross sectional area for both setups
$C_{ducted} = 1.25$
$C_{venturi} = 1.35$

Moreover, as a rough indication for the average tide, assumed and calculated previously, on the North Sea side: HW = 1.77 m NAP and LW = -1.20 m NAP. The current target level on the tidal basin side is 0.00 m NAP.

Thus, the static head at HWL = 1.77 + 0.00 = 1.77 m NAP; and the static head at LWL = 1.20 - 0.00 = 1.20 m NAP. The average static head, taken as the design head for the turbines, becomes $H = \frac{1.77+.120}{2} = 1.49$ m.

$$H_r = \frac{2}{3}H = 0.99$$

Ducted variant design flow rate: $Q_d = 179\ [m^3/s]$

Venturi variant design flow rate: $Q_d = 172\ [m^3/s]$

Proportionately, Hybrid variant design flow rate: $Q_d = 175.5\ [m^3/s]$

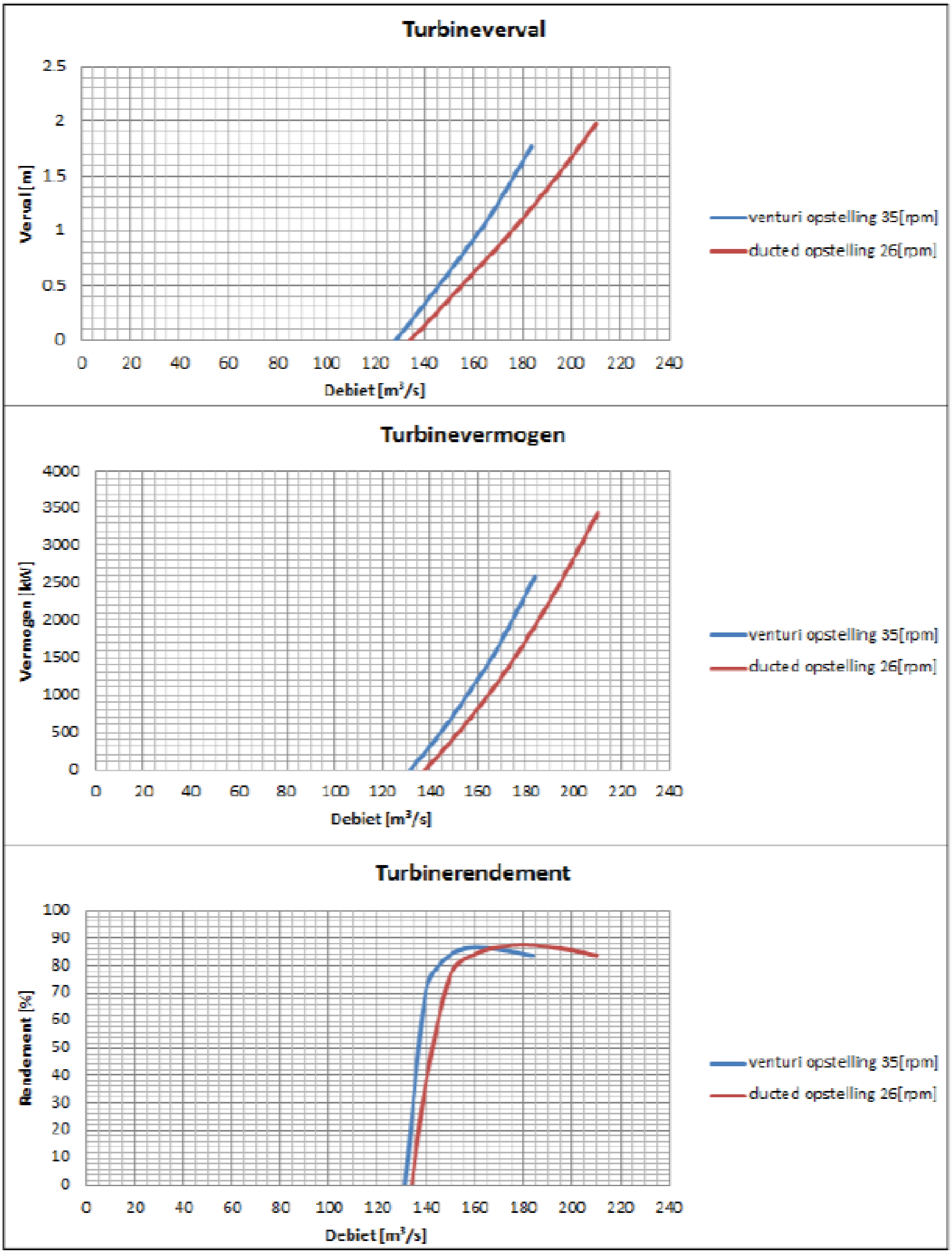

Figure 18. Comparison of the performance of the venturi and ducted turbine designs (Meijnen & Arnold, 2015)

Design depth

After conversating with R. Meijnen on the design of the Pentair Fairbanks Nijhuis turbines, he suggested that the turbine axis should be minimally 1*D submerged, with D the diameter of the turbine, i.e. the top tip of the rotor should be 1*r submerged, with r the radius of the turbine.

Therefore, for the ducted setup, with an 8 m diameter turbine, the top of the shaft should be 4 m below minimum water level. For the venturi setup, with a 5.8 m diameter turbine, the top of the rotor should be 2.9 m below minimum water level.

Hybrid setup

As a third alternative, a hybrid of the venturi and ducted setup is explored. Mainly the structural part of this setup is touched as a thorough analysis leading to the calculation of the yield would take a lot of time but could be studied further if found to be a viable option. In this case, an optimal turbine design could also be made for this set-up in a later stage.

With the insight of Pentair engineer, Raymond Meijnen, working on the aforementioned Pentair Fairbanks Nijhuis turbines, a 7 m diameter turbine is used for the hybrid setup as a starting point. From this, the civil design of the duct can be made which allows to get insight in price consequences of the setup. Based on the three setups, a decision can be made as to which is the closest to optimum, price wise, when comparing them.

2.3.4 Fish mortality

In 1994, the US Department of Energy's Advanced Hydropower Turbine Systems (AHTS) program lead to an increase in research on the mechanisms responsible for damage on fish and their mortality passing through pumps and turbines.

The primary cause of damage to fish passing through turbines is mechanical injuries by blade strike leading to bruises, hemorrhage or the severing of the body. Strike probability models can be used to estimate the probability of a fish being hit by a blade. This theoretical blade strike probability is subsequently corrected with a factor to account for the mutilation rate following blade strike, to arrive at the probability of severe injury and/or mortality (van Esch, 2015).

The Model-based study of fish damage for the Pentair Fairbanks Nijhuis Modified Bulb Turbine and the Water2Energy Cross Flow turbine study made by B.P.M van Esch, assumes that blade strike is the most important cause of fish damage.

The Nijhuis turbine owes its improved fish-friendliness to the shape of the runner blades. The specific shape of the blades serves to reduce the collision speed, effectively by reducing the velocity of impact in a direction normal to the leading edge. An example can be seen in the two-bladed model of the figure below.

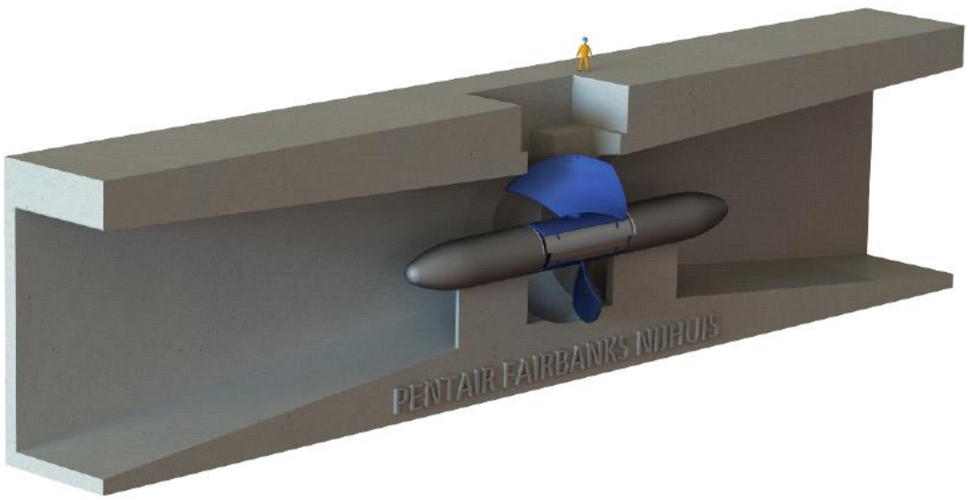

Figure 19. CAD drawing showing the specific shape of the blades of the bi-directional runner (van Esch, 2015)

For this study, the fish mortality tests were done at model-scale in an effort to establish the turbines' fish handling performance before full-sized turbines tests. However, up-scaling of the test results to full-scale turbines requires both geometric and dynamic similarity between the two scales. Therefore, the researcher established in the Pro-Tide project to use model-based predictions of fish mortality and compare the results of these calculations with fish tests at model-scale. Since the calculated values agree fairly well with measured fish mortality, it was considered feasible to use the blade strike model to predict the expected fish mortality in the full-sized turbines (van Esch, 2015).

The model predicts the mortality of salmon or trout smolts of 15 cm, sea bass of 25 cm and eel of 75 cm at the Brouwersdam location and therefore, the results are considered for the current research as the two location are close to each other and of similar boundary conditions.

The model uses an 8.0 m diameter Nijhuis turbine and the results of blade strike model calculations, with a flow rate of 235 m^3/s, a shaft speed of 13 rpm and a head of 1.0 m, go as follow:

Type of fish	Fish mortality [%]
Smolts 15 cm	< 0.1
Bass 25 cm	0.19
Eel 75 cm	< 0.1

Table 6. Calculated expected mortality for the Nijhuis full-scale turbine operating at rated condition (van Esch, 2015)

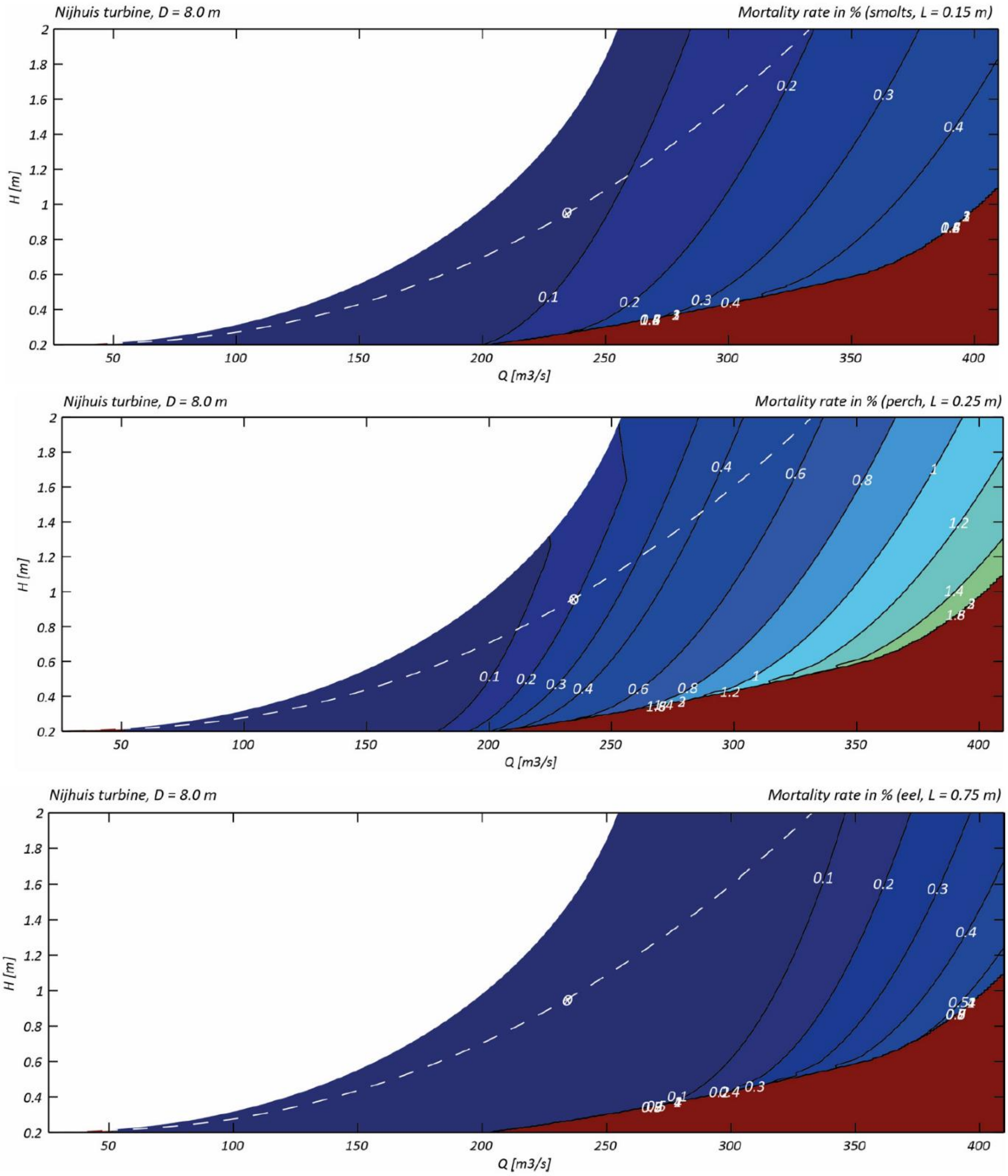

Figure 20. Estimated mortality Pm for smolts (15 cm), bass (25 cm), and eel (75 cm) in the Nijhuis turbine at full scale. The rated operating condition at H = 1 m is indicated in the graphs (van Esch, 2015)

2.3.5 Gates

In his book, Robert H. Clark (Clark, 2007) states that two types of gates are most suitable for tidal-electric operation: the radial gate and the vertical-lift gate.

Radial gates

The selected design guidelines for water control structures (Mack, Slack, & Llorca, 2004), prepared by Mack, Slack & Associates Inc. under contract with Alberta Transportation, give information on radial gates.
Also called Tainter gates, the radial gates rotate around a horizontal axis. Although, they require a lower hoisting force, they do not require gate slots, which can become plugged with ice or debris and can cause cavitation. Even though the radial gates can typically be less expensive than vertical lift gates, they involve a more complex fabrication, result in high concentrated loads at the pivot point and require a more significant amount of space both in vertical and horizontal directions to rotate freely.

Vertical lift gates

The gate slots of vertical-lift gates create hydraulic problems at high velocity flow, whereas radial gates do not require slots. In spite of this advantage, vertical-lift gates are often selected because of the installation problems associated with radial gates. Moreover, vertical lift gates get a more even distribution of the gate water loads and they require an overhead structure to host them which in the case of a tidal power plant can serve as overtopping defense (Lewin, 2001).

Thus, the choice is made on vertical lift gates and to ensure a streamlined flow in the channels, the gates are set in the overhead gate housing while in their resting position and strips and seals are installed in the slots to avoid any hydraulic disruptions.

The gates are located on the seaside of the tidal power plant where the wave action, water pressures and water levels are maximum. They are closed during extreme storm conditions at the North Sea guaranteeing safety from flooding of the hinterland, by functioning as the primary water retaining defense of the tidal power plant. The gate in open position is hoisted in the gate housing above its closed position, allowing it to move vertically.

Provisions are made on the possibilities of additional gates as part of the alternatives discussed in the Multi Criteria Analysis:

- One vertical lift gate on the seaside.
- One vertical lift gate on the seaside and one temporary gate/stoplog on the basin side for dry maintenance environment in the channels.

2.3.6 Joints

Because the design consists of several caissons, they need to be locked solidly together as well as being watertight. The more joints needed the higher the risk of failure. Hence, particular attention must be brought on the design of the interlocking joints.

According to the report *Civil Engineering for Underground Rail Transport* (Edwards, 1990), starting points for the design are:

1. Simple design to minimize building risks;
2. Minimal dimensions;
3. Adaptability to all possible combinations of tolerances;
4. Watertight construction;
5. Flat surfaces of both caisson front faces while sinking;
6. Limited mutual movement of adjoining caissons (in a metro design in Amsterdam the movement was set at 10mm in all directions).

Shear keys in the outer wall of the caissons can transfer the shear forces in transverse direction through the segment joints. The water tightness can be achieved by adding a seal profile such as the GINA profile which must be able to resist water pressure increasing with the water depth.

A study published on the Journal of the Korean Society of Civil Engineers by Sung Hoon & al. (Sung Hoon, Min Su, Youn Ju, & Yoon Koog, 2019) shows an interlocking system on caissons with the use of shear keys.

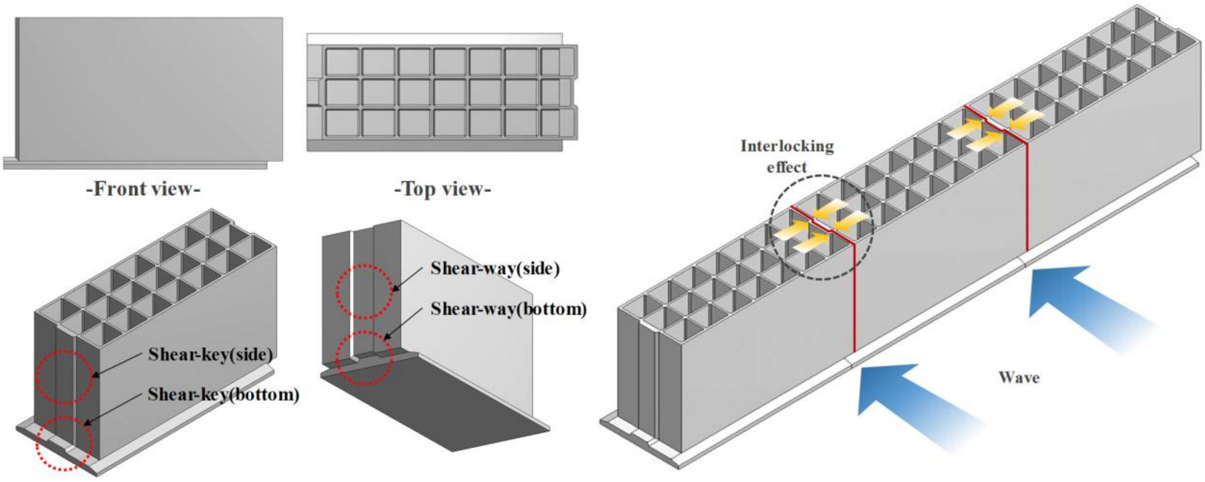

(a) Shape and features (b) Interlocking effect

Figure 21. Interlocking caissons with a shear-key (Sung Hoon, Min Su, Youn Ju, & Yoon Koog, 2019)

Figure 21 shows the shape and characteristics of the interlocking caisson of the shear-key type. A shear-key interlocking caisson has a shear-key and shear-way configuration on the side wall of the caisson and the protruding bottom plate for interlocking with adjacent caissons, see Figure 21 (a). The caisson is interlocked with the adjacent caisson by the vertical and horizontal shear keys, extending the structure. Therefore, the interlocking caisson breakwaters reduce the maximum wave power by the smoothing effect of the wave like a single pole caisson. In addition, the interlocking effect of the shear key improves the activity and conduction resistance of the caisson to the wave, see Figure 21 (b). This shear-key system is advantageous in its interlocking effect while in commission and facilitating the mounting operation because the shear keys act as a guide.

The research done by Sung Hoon & al. shows that the X and Y maximum displacements increased with increasing shear angle and decreased with vertical (0 °). The slope of the maximum displacement according to the shear tilt angle shows a tendency to increase at a shear tilt angle of 45 ° or more, see in figure 22 (a). Therefore, it is considered that it is advantageous to design the shear inclination angle of the shear key below 30 °. The X and Y maximum displacements were constant with varying shear length and shear length ratio as seen in the figures 22 (b) and (c).

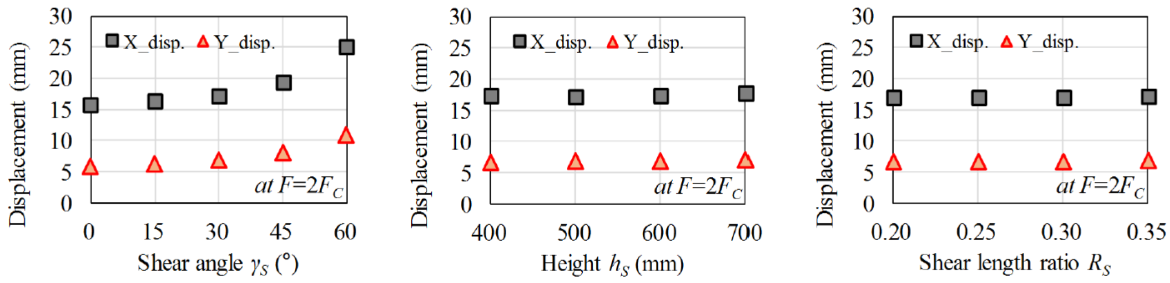

(a) Shear Angle (b) Shear-Key Height (c) Shear Length Ratio

Figure 22. Maximum displacement results (F = 2Fc) (Sung Hoon, Min Su, Youn Ju, & Yoon Koog, 2019)

Therefore, the angle chosen for the interlocking shear key is 30 °, the shear key height is 500 mm and the shear/length ratio is 0.2.

2.3.7 Piping

Groundwater flow under or besides a water or soil retaining structure is caused by a potential difference across the structure. Piping can occur at the plane separating the impermeable structure and a loose grain layer (Figure 23). Piping is the flow of water through a pipe like channel that has been created by internal erosion. This phenomenon can occur along the foundation plane of a structure but also along a retention wall (Molenaar & Voorendt, 2016).

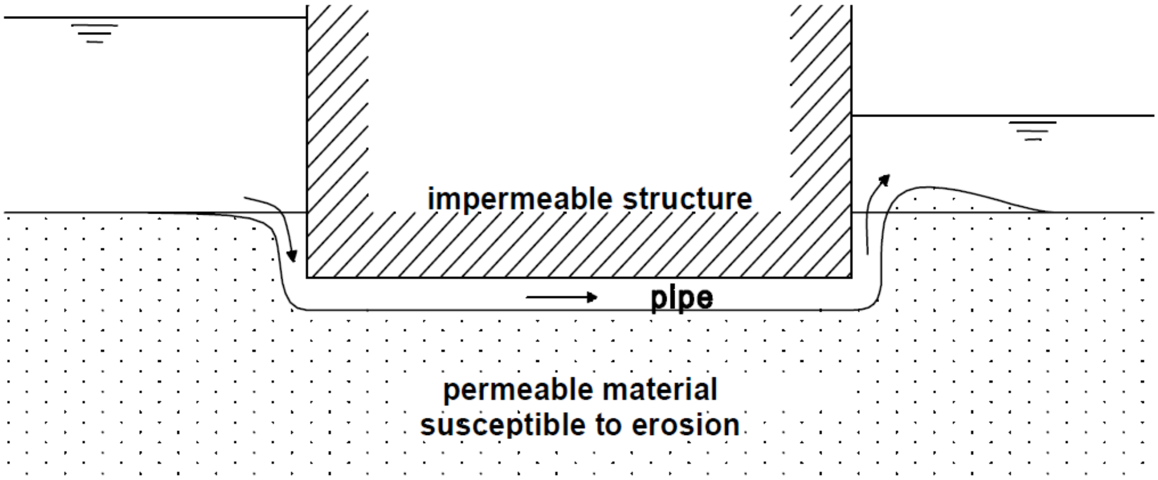

Figure 23. Piping process (Voorendt, Bezuyen, & Molenaar, 2011)

Empirical formulas based on research describe the critical situations in which piping can occur. The most famous are the Bligh and Lane formulas.
The two methods are presented in the following table:

Piping Method	Bligh		Lane	
Criterion	$L \geq \gamma \cdot C_B \cdot \Delta H$		$L \geq \gamma \cdot C_L \cdot \Delta H$	
Used seepage length	$L = \sum L_{vert} + \sum L_{hor}$		$L = \sum L_{vert} + \sum \frac{1}{3} L_{hor}$	
	C_B	i_{max}	C_L	i_{max}
Soil type:				
Very fine sand/silt/sludge	18	5.6%	8.5	11.8%
Fine sand	15	6.7%	7.0	14.3%
Middle fine sand	-	-	6.0	16.7%
Coarse sand	12	8.3%	5.0	20.0%
(Fine) gravel (+sand)	5-9	11.1 – 20.0%	4.0	25.0%

Table 7. Safe seepage distance for piping (Voorendt, Bezuyen, & Molenaar, 2011)

With:	L	[m]	the total seepage distance, which is the distance through the soil where the water flow is impeded by the soil structure
	C_B	[-]	Bligh's constant, depends on soil type
	C_L	[-]	Lane's constant, depends on soil type
	ΔH	[m]	differential head across structure
	γ	[-]	= 2.0, Lane's safety factor for primary flood defense systems (NEN 9997-1)
	i_{max}	[-]	maximum (allowed) hydraulic gradient = DH / L

In the Dutch design practice, both methods are being applied. Bligh's method is most suitable for the design of dikes, whereas Lanes' method is used to estimate whether piping will occur under water retaining structures because of the possibility of vertical piping lines.

A solution could be the implementation of a sheet pile wall to prevent the seepage and is developed further in the Results and Discussion chapter.

2.3.8 Bed protection

Because closing the estuary and allowing the water to only flow through the tidal power plant increases flow velocities, protection needs to be applied to the nearby bed as the structure becomes a primary defense of which the stability is of paramount importance. Higher velocities lead to a higher sediment transportation and local scour. To counter such effects, different protective layers need to be used and are detailed in this paragraph.

Foundation bed

The soil beneath the structure is assumed as compact, especially in case of dredging activities opening deeper layers which are naturally more compacted, leading to no settlement. A better understanding of the soil layers and their properties would allow settlement calculations.

Foundations, or substructure, are the part of an engineered system that transmits to, and into, the underlying soil or rock the loads supported by the foundation and its self-weight. The resulting soil stresses—except at the ground surface—are in addition to those presently existing in the earth mass from its self-weight and geological history (Bowles, 1997).

For the tidal power plant, its caissons are laid on a rubble mound foundation. The stability of the armor units for rubble mounds against wave action must then be investigated by calculating its stability coefficient. The stability coefficient N_s depends on such variables as shape of armor unit, manner of placing, shape of rubble mound foundation, wave conditions (height, period, direction) and so on. Tanimoto et al. (1982) proposed a formula to calculate the stability coefficient for two layers of quarry stones based on analytical considerations and the results of random wave experiments. Takahashi et al. (1990) modified Tanimoto's formula so it can be applied to obliquely incident waves (Tanimoto & Takahashi, 1994). That is,

$$N_s = max\left\{1.8, \left[1.3\left(\frac{1-\kappa}{\kappa^{\frac{1}{3}}}\right)\left(\frac{h'}{H_s}\right) + 1.8\exp(-1.5\left(\frac{1-\kappa}{\kappa^{\frac{1}{3}}}\right)\left(\frac{h'}{H_s}\right)(1-\kappa)\right]\right\}$$

$$\kappa = \frac{(\frac{4\pi h'}{L'})}{\sinh\left(\frac{4\pi h'}{L'}\right)} \cdot max\left\{0.45\sin^2\beta\cos^2\left(\frac{2\pi x}{L'}\cos\beta\right), \cos^2\beta\sin^2\left(\frac{2\pi B_M}{L'}\cos\beta\right)\right\}$$

With:	L'	[m]	the wavelength corresponding to the significant wave period at the depth h'
	x	[m]	the distance from the wall $\leq B_M$
	B_M	[m]	the berm width

From the stability coefficient the armor nominal diameter can be calculated:

$$D_{n50} = \frac{H_s}{N_s}$$

The layer thickness of the rubble mound is assumed sufficient with two times the armor nominal diameter. Moreover, geotextile as permeable filter layer should be added on top of the rubble mound but its thickness is considered as negligible and thus is not included in the overall thickness of the foundation sill.

Scour protection

To prevent scour on both sides of the tidal power plant the required length of the bottom protection can be calculated with:

$$L \geq \gamma \cdot n_s \cdot h_{max}$$

With:	γ	[-]	a safety factor (≥1.0)
	$1{:}\,n_s$	[-]	the average slope of the slide
	h_{max}	[m]	the maximum scouring depth

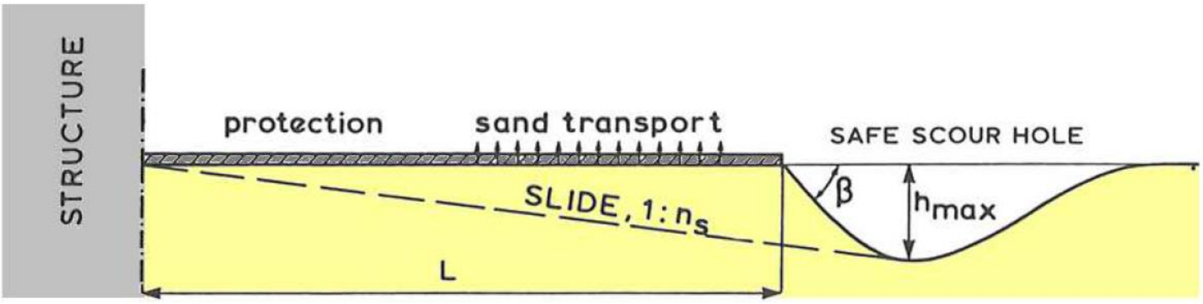

Figure 24. Length of bottom protection (Voorendt, Bezuyen, & Molenaar, 2011)

$n_s \approx 6$ for densely packed, or cohesive material, $n_s \approx 15$ for loosely packed material.

The upper scour slope, β, is usually much less steep than the natural slope of sediment under water. Usual values for β vary between 18° and 26°.

The time dependent scour formula of Breusers requires quite some information, which is difficult to obtain. A simplification can be achieved by calculating the equilibrium depth of the scour hole and assuming that there is no sand coming from upstream (clear water scour) (Molenaar & Voorendt, 2016).

In that case the maximum (= equilibrium) scour depth is given by:

$$\frac{h_{max}}{h_0} = \frac{(0.5 \cdot \alpha \cdot u) - u_c}{u_c} \; for \; (0.5 \cdot \alpha \cdot u) - u_c > 0$$

With:	h_0	[m]	the initial water height
	h_{max}	[m]	the maximum scouring depth (= equilibrium depth)
	u	[m/s]	the depth-averaged flow velocity at the end of the bed protection
	u_c	[m/s]	the critical velocity regarding begin of motion of sand particles
	α	[-]	a coefficient to include turbulence effects. The value of a is in the order of 3

The critical velocity u_c can be calculated with the Shields equation:

$$u_c = C\sqrt{\psi_c \cdot \Delta \cdot D_{n50}}$$

With:	D_{n50}	[m]	the median nominal diameter of sand particles $D_{n50} = 0.84D_{50}$
	C	[√m/s]	Chézy coefficient: $C = 18 \cdot \log\left(12\frac{R}{k_r}\right)$
	k_r	[m]	the equivalent sand roughness ≈ $2 \cdot D_{n50}$
	Δ	[-]	the relative density: $\Delta = \frac{\rho_s - \rho_w}{\rho_w}$
	ψ_c	[-]	Shields (stability) parameter

The Shields parameter depends on the dimensionless grain diameter $d*$:

$$d* = D_{50} \cdot \sqrt[3]{\frac{\Delta \cdot g}{\nu^2}}$$

With: ν [m2/s] the kinematic viscosity

Figure 25 shows the relation between the Shields parameter ψ_c and the dimensionless grain diameter $d*$ (lower horizontal axis). For normal circumstances (temperature, density), the value of ψ_c can be directly related to D_{50} (upper horizontal axis). Line 1 in this graph should be used for determining the scour depth. It indicates the threshold of motion of all grains. Line 2 should be used for stability calculations of the bed protection, because it indicates the threshold where no grains at all are moving (Molenaar & Voorendt, 2016).

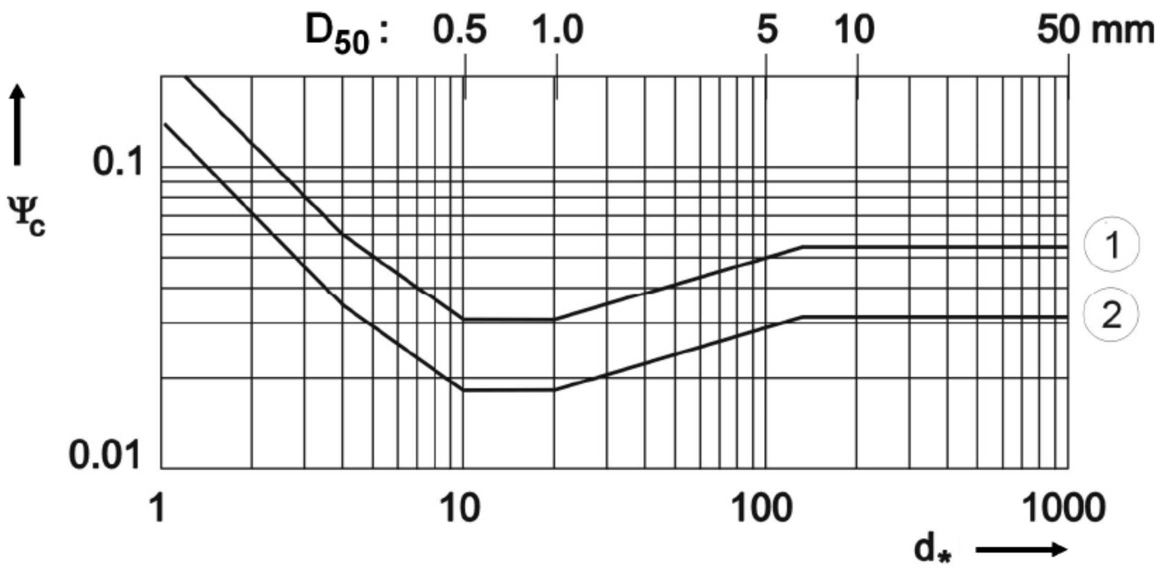

Figure 25. Relation between the Shields parameter and $d*$ or D_{50} for usual conditions (Schiereck, 1993)

From the borehole analysis presented earlier, D_{50} is assumed to be 0.12 mm for the first meter of sand below the seabed.

2.3.9 Stability checks during transport and immersion

Stability checks are effectuated in the different conditions the caissons are subjected to during the overall construction process. The preferred construction method for the design is in a wet environment, meaning the caissons are floated to location. Hence, the stability of the elements needs to be checked during floatation as well as during immersion and once the tidal power plant is implemented.

To ensure that floating elements do not undesirably move or rotate, they should be statically and dynamically stable. The stability of a floating element depends on forces and moments, and the shape of the element.

Static stability

The Manual of Hydraulic Structures (Molenaar & Voorendt, 2016) gives an overview of the different design checks required.

- **Equilibrium of vertical forces**

Vertical forces establish an equilibrium if the buoyant force equals the weight of the floating body (including all ballast). This buoyant force has the same magnitude as the weight of the displaced volume of fluid (Archimedes' principle: a floating body displaces its own weight of fluid).

- **Equilibrium of moments**

To avoid unwanted tilting in an unacceptable degree during the floating transport or the immersing procedure, assurance must be made on the equilibrium of moments: the sum of the moments must equal zero with the use of ballasts.

- **Metacentric height**

A check of the equilibrium of moments (previous paragraph) is sufficient if an element is floating in still water. In reality, however, this is rarely the case. This is why also the sensitivity to tilting has to be taken into account. A measure for the resistance to tilting is given by the metacentric height.

The calculation steps are:

1. Calculate the weight of the caisson and the position of the gravity center point of the caisson with reference to the intersection of the Z-axis with the bottom line of the caisson, this distance is KG.

2. Locate the center of buoyancy and calculate its position above the bottom of the element. This distance is KB.

3. Determine the shape of the area at the fluid surface and compute the smallest area moment of inertia for that shape.

$$I = \frac{1}{12} \cdot l \cdot b^3$$

Now BM can be computed by dividing the moment of inertia by the volume of displaced fluid, V.

$$BM = \frac{\frac{1}{12} \cdot l \cdot b^3}{V}$$

4. Now the metacentric height h_m can be computed by:

$$h_m = KB + BM - KG$$

If $h_m > 0$ the caisson is theoretically stable, while $h_m > 0.5$ is preferred.

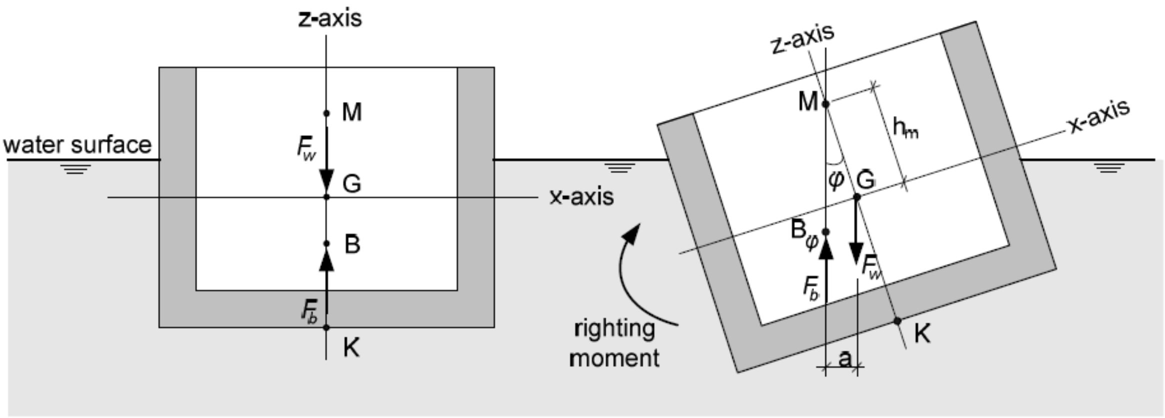

Figure 26. Floating element (Voorendt, Bezuyen, & Molenaar, 2011)

Dynamic stability

Not only the static stability but also the dynamic stability should be checked. If an element is transported over water, it will be affected by waves or swell. This can cause the element to sway, which can cause problems with respect to navigability and keel clearance.

- **Sway**

If the length or the width of a floating element are too small compared to the length of the waves or swell, the element will start swaying on the waves. In practice, the following rule of thumb is being used:

$L_w < 0.7 \cdot l_e$ and $L_w < 0.7 \cdot b_e$ (dependent on the direction of the waves relative to the caisson)

With:	L_w	[m]	the wavelength
	l_e	[m]	the length of the floating element
	b_e	[m]	the width of the element

- **Natural oscillation**

The dynamic stability can also be threatened in the case when the natural oscillation period of the element is close to the period of the water movements. The natural oscillation period of the element then needs to be much greater than the one of the waves or swell and can be calculated using the following formula:

$$T_0 = \frac{2\pi j}{\sqrt{h_m g}}$$

With:	T_0	[s]	the natural oscillation period
	h_m	[m]	the metacentric height
	g	[m/s²]	the gravitational constant
	$j = \sqrt{\frac{I_{polar}}{A}}$	[m]	the polar inertia radius of the element
	A	[m²]	the area of concrete in a vertical cross section
	$I_{polar} = I_{xx} + I_{zz}$		
	I_{xx}	[m⁴]	the polar moment of inertia around the z-axis in relation with G
	I_{zz}	[m⁴]	the polar moment of inertia around the x-axis in relation with G

2.3.10 Stability checks during commission

Shear criterion caisson-subsoil

The total of the horizontal forces acting on a caisson (on a shallow foundation) should be transferred to the subsoil (Figure 27). The friction force of the subsoil should resist the resulting total horizontal force. This friction force is determined by the total of the forces acting on the caisson in the vertical direction (or the vertical components of the forces), multiplied by a friction coefficient f. In equation form:

$$\sum H < f \sum V$$

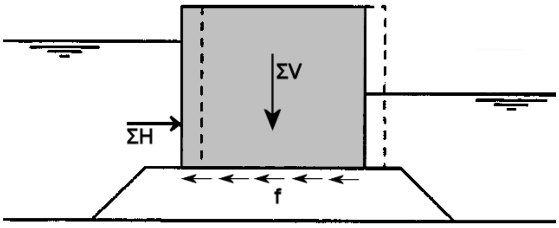

Figure 27. Slide-off principle sketch (Voorendt, Bezuyen, & Molenaar, 2011)

The friction coefficient f takes several mechanisms into account. The most critical of these should be used:

1. friction between structure and subsoil: f = tan(δ), with δ = friction angle between structure and subsoil. If δ is unknown, it can be approximated: δ ≈ ⅔ ϕ (ϕ is angle of internal friction of the subsoil). The friction coefficient for caisson-rubble is about 0.5.
2. Internal friction of the subsoil: f = tan(ϕ), where ϕ is the angle of internal friction of the subsoil.
3. A deeper soil layer with a low sliding resistance (Voorendt, Bezuyen, & Molenaar, 2011).

The impact of waves should also be considered in the force and moment equilibriums.

Rotational stability

Contrary to compression stresses perpendicular to bottom of the structure and friction acting in the plane of the structure (bottom) and the soil, tensile stresses perpendicular to the bottom of the structure cannot develop. Considering the stability of shallow foundations, a tensile force between structure and the soil will not enter the force equilibrium equation. Especially the adhesive and cohesive properties of sand are very poor. If the resulting action force intersects the core of the structure, the soil stresses will be positive (= pressure) over the entire width. The core is defined as the area extending to 1/6 b on both sides of the gravity center line, see Figure 28.

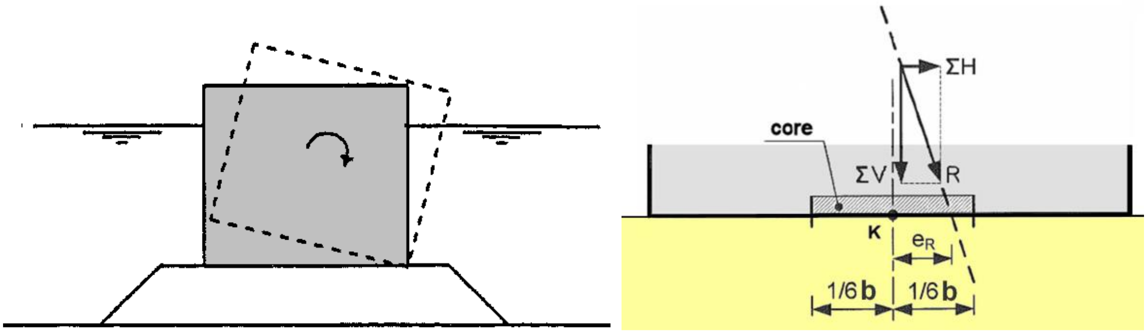

Figure 28. The action line of the resulting force should intersect the core of the structure (Voorendt, Bezuyen, & Molenaar, 2011)

It should be checked that:

$$e_R = \frac{\sum M}{\sum V} \leq \frac{1}{6} b$$

With: e_R the distance from the moment centre (K) to the intersection point of the resulting force with the bottom line [m]

$\sum V$ the total of the acting vertical forces (or vertical components) per structural element [kN]

$\sum M$ the total of the moments, preferably around point K, per structural element [kNm]

b the width of the structural element [m] (Voorendt, Bezuyen, & Molenaar, 2011)

Vertical stability

The required vertical effective soil stress should not exceed the maximum bearing capacity of the soil, otherwise the soil will collapse. The maximum acting stress on the soil can be calculated with:

$$\sigma_{k,max} = \frac{F}{A} + \frac{M}{W} = \frac{\sum V}{b \cdot l} + \frac{\sum M}{\frac{1}{6} l b^2}$$

With: F the normal force [kN]

A the area perpendicular to the normal force [m²]

M the acting moment [kNm]

W the section modulus [m^3]

$\sum V$ the total of the acting vertical forces (or vertical components) [N]

b the width of the structural element [m]

l the length of the structural element [m]

$\sum M$ the total of the moments, preferably around point K, halfway the width [kNm]

The bearing capacity can be calculated according to TGB 1990 (NEN 6744), which gives the Brinch Hansen method for determining the maximum bearing capacity of a foundation. This method takes into account the influence of cohesion, surcharge including soil coverage and capacity of the soil below the foundation (Voorendt, Bezuyen, & Molenaar, 2011).

The maximum bearing capacity can be approximated by:

$$F_{max} = p'_{max} \cdot A$$

With: $p'_{max} = c' N_c s_c i_c + q' N_q s_q i_q + 0.5 \gamma' B \cdot N_\gamma s_\gamma i_\gamma$

consisting of contributions from cohesion (index $_c$), surcharge including soil coverage ($_q$) and capacity of the soil below the foundation ($_\gamma$).

The bearing capacity factors are:

$$N_c = \left(N_q - 1\right) \cot \emptyset' \qquad N_q = \frac{1+\sin \emptyset'}{1-\sin \emptyset'} e^{\pi \tan \emptyset'} \qquad N_\gamma = 2(N_q - 1) \tan \emptyset'$$

The shape factors ($B \leq L \leq \infty$) are:

$$S_c = 1 + 0.2 \frac{B}{L} \qquad S_q = 1 + \frac{B}{L} \sin \emptyset' \qquad S_\gamma = 1 - 0.3 \frac{B}{L}$$

The inclination factors to deal with an eventual inclined direction of the resulting force (B ≤ L ≤ ∞) are:
For drained soil:

For H parallel to L and L /B ≥ 2:

$$i_c = \frac{i_q N_q - 1}{N_q - 1} \qquad i_q = i_\gamma = 1 - \frac{H}{F + Ac' \cot \emptyset'}$$

For H parallel to B:

$$i_c = \frac{i_q N_q - 1}{N_q - 1} \qquad i_q = \left(1 - \frac{0.70H}{F + Ac' \cot \emptyset'}\right)^3 \quad i_\gamma = \left(1 - \frac{H}{F + Ac' \cot \emptyset'}\right)^3$$

For undrained soil:

$$i_c = 0.5\left(1 + \sqrt{1 - \frac{H}{Af_{undr}}}\right)$$ for the rest, see drained soil, above.

Only the part of the foundation slab which has effective stresses underneath is included in the effective width B. The factors for the bearing force are also given in the figure below.

$\emptyset_{e;d}$	N_c	N_q	N_γ
0°	5	1	0
5°	6.5	1.5	0
10°	8.5	2.5	1
15°	11	4	2
20°	15	6.5	4
22.5°	17.5	8	6
25°	20.5	10.5	9
27.5°	25	14	14
30°	30	18	20
32.5°	37	25	30
35°	46	33	46
37.5°	58	46	68
40°	75	64	106
42.5°	99	92	166

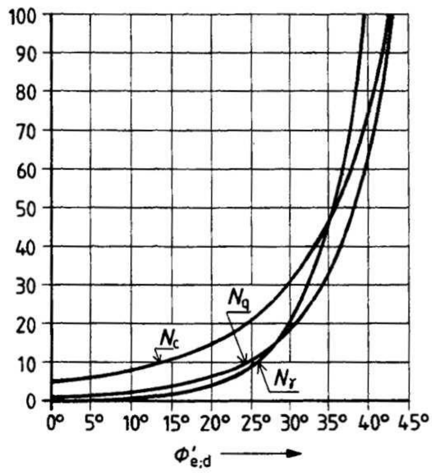

Figure 29. Bearing capacity factors as functions of the angle of internal friction (Voorendt, Bezuyen, & Molenaar, 2011)

With:

p'_{max}	[kPa]	the maximal average effective stress on the effective foundation area
$\emptyset'$	[°]	the (weighted) effective angle of internal friction
A	[m^2]	the effective foundation area
c'	[kN/m^2]	the (weighted) cohesion (design value) = 0 for sand
q'	[kPa]	the effective stress at the depth of but next to foundation surface (design value)
γ'	[kN/m^3]	the (weighted) effective volumetric weight of the soil below construction depth (design value)
H	[kN]	the shear force [kN]
F	[kN]	the component of the exerted force perpendicular to the foundation surface (design value)
f_{undr}	[kPa]	the design value of the undrained shear strength $= c_u$
L	[m]	the length of the effective foundation area, for circular slabs: L = B
B	[m]	the width of the effective foundation area, for circular slabs: L = B

2.4 Risks and impacts

Risk is generally defined as the probability of a hazard multiplied by its consequence. Risks in maritime construction can be more likely than on land, and the consequences can be greater. Good management of risks is therefore essential (Hawkswood & Allsop, 2009).

To reduce risks due to unforeseen circumstances it is highly advisable to draw up a work plan in advance. The aspects to be considered depend highly upon the specific circumstances, but the following list gives a first idea of what could be included in the plan (Deltadienst, 1957-1987):

- Closure moment if possible, during low slack water
- Maximum flow velocity
- Maintaining position during the immersion process (e.g., use of an anchored pontoon)
- Procedure for the inlet of ballast water
- Planning of the ballasting with sand and the application of rubble (including delivery)
- The fill-up of the space between the joints of the caissons.
- Tolerances

3. Method

This chapter introduces the methods and tools used in this research to recover the data needed and how this information is further analyzed and implemented to answer the main question.

3.1 Data collection

In order to start thinking of and create a design, data needs to be gathered to familiarize oneself with the subject, the boundary conditions, existing standards and projects and the calculations required. Hence the following methods are used:

- Literature research
- Technical research (Experts)

3.1.1 Literature research

In order to opt for an optimal design, data needs to be gathered from scientific sources. Reliable literature can be found on different search engines such as Google Scholar, ScienceDirect or Research Gate when providing key words relevant to the research. Moreover, the Rijkswaterstaat website, DINOLoket or the Pro-Tide website are most profitable for they provide accurate data sets and relevant research papers needed for the collecting of a trustworthy theoretical framework to better identify the design as a whole.

3.1.2 Technical research

Although deskresearch is a paramount aspect of the data collection, it must be corroborated with external knowhow from experts. Professional in their field provide expertise and valuable feedback based on their experience throughout their career.

The experts that are consulted and involved during the research are as follow:

- Huub Lavooij, Initiator of the Delta21 project
- Joachim de Keijzer, Lecturer/Researcher Civil Engineering at the HZ University of Applied sciences
- Raymond Meijnen, Engineer Research & Development at Pentair Fairbank Nijhuis
- Hendrik Spek, Engineer at VolkerWessels
- Daan Van der Wiel, Engineer at VolkerInfra

3.2 Data analysis

3.2.1 Calculations

All the data collected is processed to find the relevant measurements for the structure and the forces that act upon it. This information is reported in the Results chapter of the research by means of the execution of the additional required calculations and assumptions necessary, to achieve the most suitable design for the subject area, and the incorporation of the conditions and situations for the loads operating on the structure.

Excel is used for the calculation process in order to be able to easily change previously assumed measurements without having to recalculate all the follow up computations. Moreover, the results can be reported into the thesis more straightforwardly.

3.2.2 Technosoft

Once all the forces are calculated, they are entered into Technosoft to verify the stability of the structure and from which can be extracted information on the moments, shear forces and the reaction forces to check the strength of members of the caisson.

3.3 Multi-Criteria Analysis

In order to decide on the optimal variant for the structure of the tidal power plant from the three designs a Multi Criteria Analysis (MCA) is implemented. The MCA is a tool to obtain the best alternative out of a set of predefined variants according to criteria relevant to the project and the client desires. The alternative with the highest score is chosen as the optimal option as it best meets the selected criteria.
In this chapter, the alternatives are laid down and the criteria and their allocated weight are described.

3.3.1 Alternatives

The different variants selected for the MCA go as follow:

- A ducted setup with an 8.0 m diameter turbine

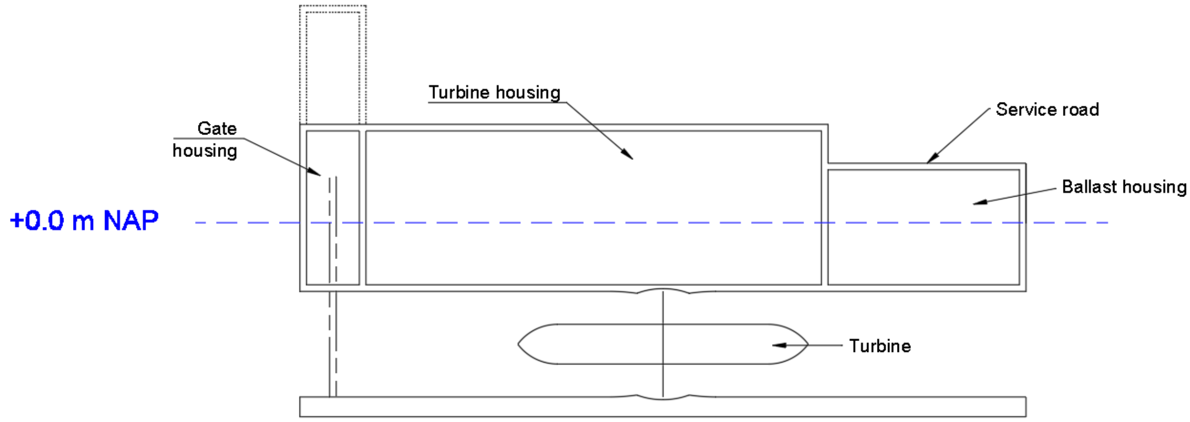

- A venturi setup with a 5.8 m diameter turbine

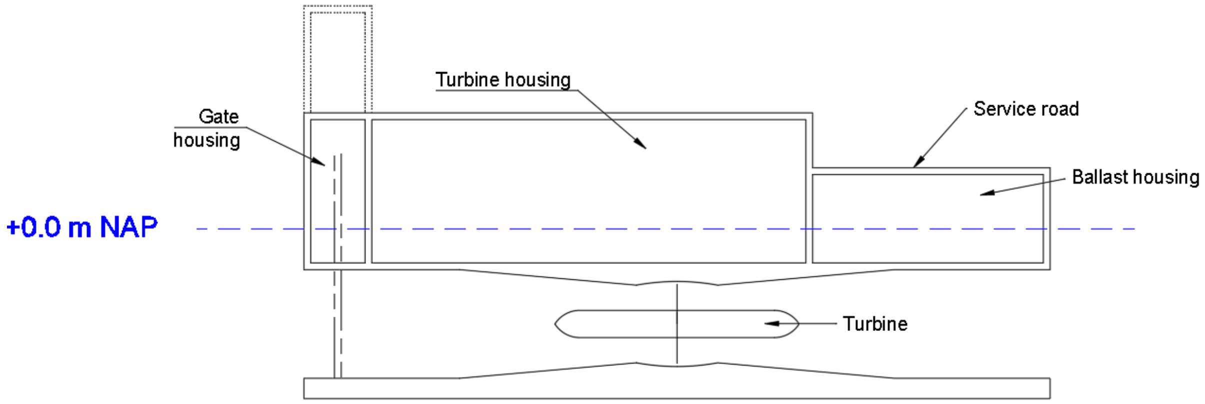

- A hybrid setup with a 7.0 m diameter turbine

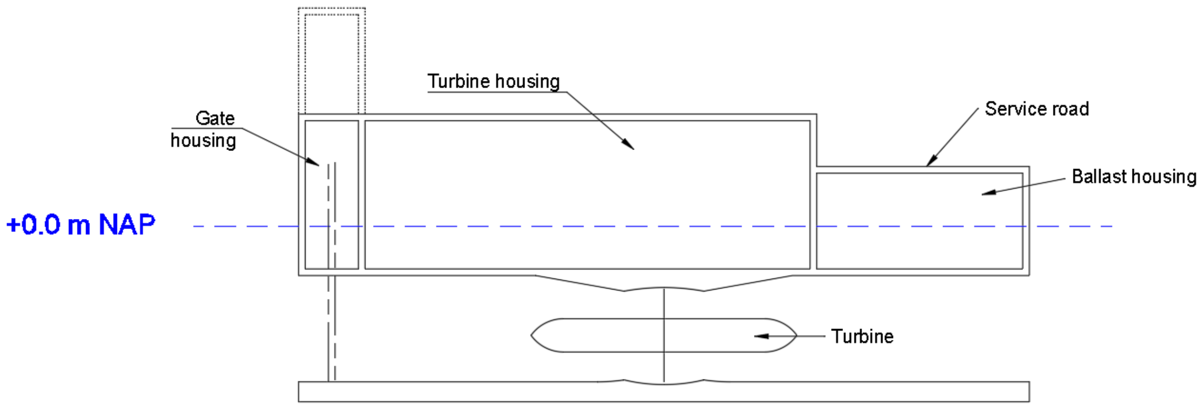

3.3.2 Criteria

Deciding criteria are chosen relevantly to the Delta21 project and discussions that occurred. The MCA is divided into five criteria:

- the fish-friendliness
- the costs
- the energy efficiency
- the maintenance efficiency
- the transportation

Fish-friendliness

Estuarine and delta river ecology is valuable and strict thresholds for allowable mortality for fish and sea mammals are set. The current criterion is 0,1 % allowable mortality for fish, for a single passage. The fish-friendliness of the structure and turbines is a deciding factor because of the fish migration that will occur upon operation and a key factor to the restauration of the Haringvliet ecosystem. The alternatives differ in their setup and thus affect the fish population differently.

Costs

Costs are usually always a criterion for a construction project and serve to find the cheapest alternative without hindering the quality and efficiency. The alternatives differ in the implementation of the gates and in their setup diverging on the turbines' diameter and depth of construction altering the amount of concrete per variant. The costs will not include maintenance costs for the structure maintenance operations as it is assumed that they are the same for all the alternatives, however, the costs for the cranes and the turbines are taken into consideration.

Energy efficiency

The efficiency of the design differs in the setup as each has a different channel shape that induces different losses as well as the turbine choice. Each turbine thus gives a distinctive energy yield. The energy yield of each setup is thus compared to reveal the most energy efficient variant.

Maintenance efficiency

The decision on the alternatives considering the gates also plays on the efficiency of the design in maintenance operation ease and the safety of the structure. The alternatives vary in turbine size and thus turbine weight which amounts to more difficult maintenance operations and logistic.

Transportation

The transportation criterion refers to the ease of the caissons' transport phase from the dry dock to location. The setups differ in overall concrete volume and thus in weight which will play a major role during that phase of the project relative to keel clearance, maneuverability and stability. The draught of each caisson is thus assessed to underline the variant that would need more dredging operations.

3.3.3 Weighting factors

The criteria are graded on a scale of 1 to 10, 1 being the worse and 10 being the highest score to distinguish the different alternatives from one another. The evaluation scale is detailed as follows: 1 - Very poor; 2.5 - Poor; 5- Average; 7.5 - Good; 10 - Very good.
The MCA allows the comparison of the different aspects of the designs whilst simultaneously giving the criteria the appropriate weight in the overall decision. This is achieved by giving the sum of the criteria a percentage of 100% and allocating representative percentages that are in line with the relative importance of the criteria in terms of the total project.

Due to the multitude of potential criteria in such a large scale project, five are chosen, considered the most vital and in line with the client's requirements, for an optimal design and are given the following weights after approval by Huub Lavooij from Delta21.

- Fish friendliness: 25%
- Costs :33%
- Energy efficiency: 16%
- Maintenance efficiency: 16%
- Transportation: 10%

The weights as referred to above are allocated for several reasons explained in the table below.

Criteria	Weight factor (%)	Explanation
Fish-friendliness	25	The fish friendliness is the second most important criterion as required by Delta21 for an unaltered and protected fish migration. It is a necessary criterion to ensure the nature preservation aspect of the Delta21 project. Therefore, it amounts to a quarter of the criteria total score.
Costs	33	The costs criterion is given the highest weight as wasteful designs where the costs are not considered will not be realized making the rest of the work irrelevant. Moreover, it accounts for many aspects of the project, such as the transportation costs, dredging costs, material and equipment differing from an alternative to another. Labor and structure maintenance costs will not be taken into account as it is assumed they are the same for each variants. Therefore, it is given a third of the criteria total score.
Energy efficiency	16	The efficiency of both energy and maintenance are given equal weights due to the fact that they are equally important since if maintenance operations are not efficient, the energy yield is compromised which is the main purpose of a tidal power plant. Therefore, energy efficiency is given a sixth of the criteria total score.
Maintenance efficiency	16	The maintenance efficiency is an important criterion as it is influential to the continued and successful functioning of the tidal power plant as well as preserving its longevity. Therefore, maintenance efficiency is given a sixth of the criteria total score.
Transportation	10	The transportation criterion is regarded as the least significant in this study as it only focuses on the floating phase of the caissons to location and thus do not amount to the amplitude of the project. But it is a key requirement nonetheless as the chosen method of construction is in a dry dock and thus requires a floated transportation which leads to dredging activities to allow the caisson to reach its destination without damage.

Table 8. Weighting factors for each criterion

	Ducted setup 8.0 m diameter turbine			Venturi setup 5.8 m diameter turbine			Hybrid setup 7.0 m diameter turbine		
	Grade	Weight	Score	Grade	Weight	Score	Grade	Weight	Score
Fish-friendliness		0.25			0.25			0.25	
Costs		0.33			0.33			0.33	
Energy efficiency		0.16			0.16			0.16	
Maintenance efficiency		0.16			0.16			0.16	
Transportation		0.10			0.10			0.10	
Total									

Table 9. MCA matrix

The above matrix will be filled in the results part of the research and the total score per variant comes from the multiplication of the grades by the allocated weight given to the criterion then summed to give the final grade out of 10.

4. Results

4.1 Dimensions

4.1.1 Height

In order to find the height of the structure the top and bottom levels need to be calculated. The first step is to calculate the overtopping of the caisson.

With a chosen overtopping discharge of 0.02 $m^3/s/m$, the significant wave height of 2.9 m and the constant of gravity of 9.81 m/s^2, the crest height $R_c = 3.77$ m

Now to find the design wave height the number of waves N occurring during a storm needs to be calculated. With a storm time period of two hours and the waves period $T_{wave} = 10.2$ s,

$N = 705.88$ is the number of waves during the storm event and by allowing an exceedance probability $\Pr(H > H_d) = 0.10$, the design wave height $H_d = 6.09$ m.

With the predicted relative sea level rise of 1.58 m, the design water level of +5.00 m NAP added to the crest height and the design wave height, the top of the structure ToS amounts to for the three variants:

$ToS = 1.58 + 3.77 + 6.09 + 5.00 = +16.43$ m NAP.

The bottom of the structure BoS level is however different for the three alternatives due to the fact that they have different turbines of differing diameters. The level is calculated with regard to cavitation. Cavitation occurs with the rapid changes of pressure in the water leading to the formation of vapor-filled pockets. As the turbine blades move through the water, low-pressure areas are formed as the fluid accelerates around and moves past the blades. As it reaches vapor pressure, the fluid vaporizes and forms small bubbles of gas. When the bubbles collapse, they can cause very strong local shock waves in the fluid, which may damage the blades. To avoid this undesirable event, the turbines need to be positioned at the design depth. The design depth for each of the variants is one turbine radius from tip of the blade to minimum water level. From this can be retrieved the axial depth of each turbine

The minimum water level recorded by the station is -1.20 m NAP.

Venturi setup	Ducted setup	Hybrid setup
With a 5.8 m diameter turbine, the axial depth is -7.00 m NAP.	With an 8.0 m diameter turbine, the axial depth is -9.20 m NAP.	With a 7.0 m diameter turbine, the axial depth is -8.20 m NAP.
The entry of the sluiceway being 8 m wide and 8 m high and with a floor slab of 1.5 m thick, the bottom of the structure level is -12.5 m NAP.	The entry of the sluiceway being 8 m wide and 8 m high and with a floor slab of 1.5 m thick, the bottom of the structure level is -14.7 m NAP.	The entry of the sluiceway being 8 m wide and 8 m high and with a floor slab of 1.5 m thick, the bottom of the structure level is -13.2 m NAP.
The total height thus amounts to 28.93 m.	The total height thus amounts to 31.13 m.	The total height thus amounts to 29.63 m.

On the tidal basin side, not suspect to the sea wave attack, the level of the top of the ballast housing is at +3.00 m NAP due to the fact that the top of the locks for the overflow into the energy storage is leveled at +3.00 m NAP.

These heights result in necessary dredging works on the location to implement the tidal power plant. It is assumed the caissons are to be constructed on top of a rubble foundation bed. The sill is assumed to be 2 m thick. Therefore, with the assumed terrain level at -8.60 m NAP, the dredging depth below each variant can be calculated.

Venturi setup	Ducted setup	Hybrid setup
The bottom of the structure level minus the sill height leads to a required depth of -14.5 m NAP. The bed level previously assumed at -8.60 m NAP results in a dredging depth of 5.90 m.	The bottom of the structure level minus the sill height leads to a required depth of -16.7 m NAP. The bed level previously assumed at -8.60 m NAP results in a dredging depth of 8.10 m.	The bottom of the structure level minus the sill height leads to a required depth of -15.2 m NAP. The bed level previously assumed at -8.60 m NAP results in a dredging depth of 6.60 m.

For maneuverability during the transportation phase, the wall element making the required height on the North Sea side is built in situ once the caissons are immersed. The deck level during floatation is then chosen regarding the gate housing and turbine housing requirements. Space must be allocated on the top of the housings' interior for lifting mechanisms and cranes necessary for the functioning of the gates and maintenance operation. Assumption is made that a minimum of 2.50 m is necessary for the gate lifting mechanism while a minimum height of 4.00 m must be allocated for the wall of the turbine housing leading to the service road for maintenance operations to extract, repair and/or replace defective turbine parts that would be brought in and out via trucks through the service road.

Venturi setup	Ducted setup	Hybrid setup
With a minimal margin of 2.50 m over the gate, the wall between the top deck and the top of the ballast housing measures 5.00 m.	With a minimal 4.00 m wall height between the top deck and the top of the ballast housing, the clearance above the gate is 3.70 m.	With a minimal margin of 2.50 m over the gate, the wall between the top deck and the top of the ballast housing measures 4.30 m.

4.1.2 Length

The length of once caisson is determined by minimizing the total number of caissons for the tidal power plant as more caissons make for more risks during the immersion phase. The requirement ordered by Delta21 is 400 m long tidal power plant housing 40 turbines. The choice is made to divide it into 3 caissons of 135 m. The thickness of the inner and outer walls is 0.5 m, the shafts are 8.0 m wide and the interlocking shear keys are 500 mm wide on each side. 16 turbines can fit if the middle caisson is made 137 m long and the two outer caissons 131.5 m long housing each 12 turbines. The middle caisson is then the focus of the calculations as it is longer and thus heavier.

4.1.3 Width

Following the practices, the length/width ratio 3/1 is used to estimate the width. When considering the previously 135 m caisson, the width becomes 45 m. However, the width is adjusted in the different designs in order to fulfill the requirement of a maximum allowable draught during the floating phase. The chosen width is therefore 55 m.

Enough room for housing the gate, when it is lifted to open the channels, and the turbine, when it is lifted for maintenance, is needed. From estimations given by Pentair engineer, Raymond Meijnen, as the detailed mechanical design of the turbines has not been executed yet, the rough dimensions of the turbines go as follow:

- The length of the rotor itself is 6 m
- The bulbs are each 6 m for the venturi setup and 8 m for the ducted setup. As no mechanical design of the turbine for the hybrid setup has ever been made, it is agreed upon to take proportionate measures; therefore, the bulbs length for the hybrid setup is 7 m. This length depends on the installed generator power, as more power means longer bulbs. With a low head difference, the bulbs length is thus assumed to be sufficient.

The total length of the turbines is then calculated as bulb + rotor + bulb.

Venturi setup	Ducted setup	Hybrid setup
18.0 m	22.0 m	20.0 m

Table 10. Length of the turbines for each setup

The turbine housing thus needs to host the turbine in its entirety during maintenance operations. Placing the turbine in the center of the tidal power plant, and adding a 1 m margin, the turbine housings of each setup becomes:

Venturi setup	Ducted setup	Hybrid setup
32.0 m	34.5 m	33.5 m

Table 11. Length of the turbine housing of each setup

The gate housing is assumed to be 4 m wide with a 1 m thick gate. Margins of 1.5 m are allocated on both sides of the gate inside the gate housing for maintenance operations within the chamber.

A criterion to check if the width of the caisson is sufficient is the piping length under the structure. The maximum theoretical head difference between the North Sea side and the tidal basin reaches 4.5 m with the design water level at +5.00 m NAP on the sea side and the tidal basin level being kept as low as possible during a storm event or high river discharge so around +0.50 m NAP and +1.50 m NAP.

The geological survey provides the soil types at location and the prevailing types after dredging operations are fine sand, middle fine sand and coarse sand.

Soil type	Bligh's method			Lane's method		
	C_B	γ	L [m]	C_L	γ	L [m]
Fine sand	15	1.0	67.5	7.0	2.0	63.0
Middle fine sand	-	1.0	-	6.0	2.0	54.0
Coarse sand	12	1.0	54.0	5.0	2.0	45.0

Table 12. Safe seepage distance

From the results, a safe seepage distance cannot be assured for the caissons as their width is 55.0 m. However, to counter piping, a sheet-pile wall can be driven at the foot of the structure. Therefore, adding 13.0 m long sheet piles in front of the caissons would increase the used seepage length to 68.0 m assuring a safe seepage distance.

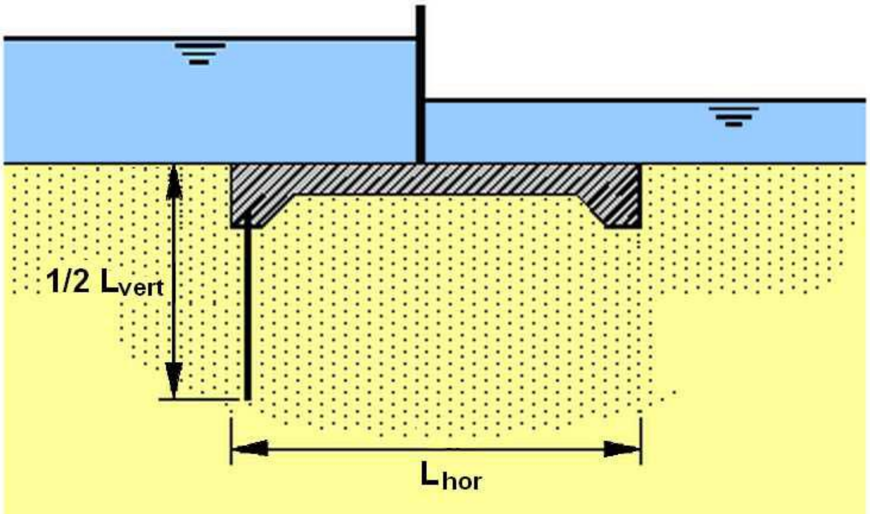

Figure 30. Horizontal and vertical seepage paths (Molenaar & Voorendt, 2016)

4.1.4 Thickness

The thickness for all walls and upper decks is chosen as 0.5 m for the calculations previous to the MCA and once the most optimal variant is highlighted, checks are carried to evaluate the stability of the structure.

A preliminary design of each setup can be viewed in Appendix 1a: Venturi setup preliminary design A-A' cross-section, Appendix 2a: Ducted setup preliminary design A-A' cross-section, Appendix 3a: Hybrid setup preliminary design A-A' cross-section.

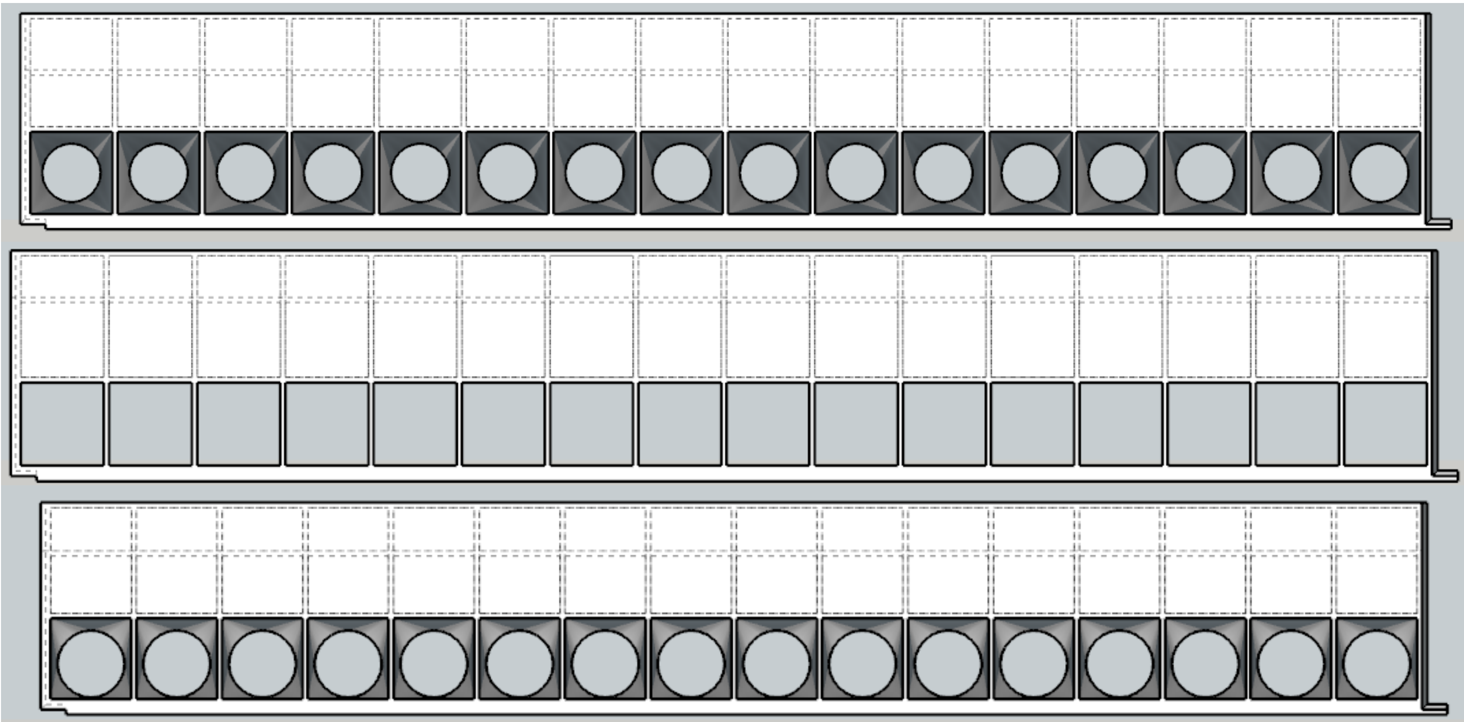

Figure 31. SketchUp models of the venturi, ducted and hybrid variants respectively

4.1.5 Draught

The draught of the caisson during the floating phase is an important factor to take into account as it leads to the creation of possible dredging activities and the under-water volume of the floating structure necessary to calculate the buoyancy and stability of the caisson throughout the transportation stage.

The different designs are adjusted in order to fulfill the requirement of a maximum allowable draught. Therefore, in order to comply, the upper decks are constructed in-situ to decrease the total weight of concrete during the transportation phase. The volume of concrete of each variant is calculated through the modeling of the caissons in the drawing software SketchUp. The models can be viewed in Appendix 4: SketchUp model of the Venturi setup in parallel projection from the front, the side and at an angle, Appendix 5: SketchUp model of the Ducted setup in parallel projection from the front, the side and at an angle and Appendix 6: SketchUp model of the Hybrid setup in parallel projection from the front, the side and at an angle. The general material property for reinforced concrete is taken as 25.0 kN/m³ following EN1992-1-1 §3.1. The draught can be calculated using the following formula:

$$d = \frac{F_{w,Total}}{b \cdot l \cdot \gamma_w}$$

With:

d	[m]	the draught
$F_{w,Total}$	[kN]	the total weight of the caisson
b	[m]	the width of the caisson
l	[m]	the length of the caisson
γ_w	[kN/m³]	= 10.29, the density of saltwater

	Venturi setup	Ducted setup	Hybrid setup
Total concrete volume [m³]	37,058.52	26,921.20	31,396.88
Reinforced concrete unit weight [kN/m³]	25.0	25.0	25.0
Weight of the concrete element [kN]	926,463.10	673,030.00	784,921.90
Draught [m]	11.95	8.68	11.14

Table 13. Draught calculation per variant

During transportation, a keel clearance of 1.00 m is needed. Therefore, the draught must be 1.00 m lower than the bottom of the structure level.

The water level is assumed to be at +0.00 m NAP.

	Venturi setup	Ducted setup	Hybrid setup
Transportation required draught [m]	11.50	13.70	12.20
Required draught > Draught?	No	Yes	Yes
Difference [m]	0.45	- 5.02	- 1.06

Table 14. Verification of the allowable draught per variant during transportation

During immersion, a keel clearance of 0.25 m is allowed because the sinking operation is more accurate. Therefore, the draught must be 0.25 m lower than the bottom of the structure level.

	Venturi setup	Ducted setup	Hybrid setup
Immersion required draught [m]	12.30	14.50	13.00
Required draught > Draught?	Yes	Yes	Yes
Difference [m]	- 0.30	- 5.77	- 1.81

Table 15. Verification of the allowable draught per variant during immersion

From tables 13 and 14, it can be concluded that only the venturi setup during transportation does not comply with the allowable draught. However, the difference is only 0.45 m. Therefore, the transportation phase for this variant must be undergone during tidal levels above +0.45 m NAP. From the astronomical data retrieved from the Rijkswaterstaat, the average water level is at +1.26 m NAP which leaves ample room to navigate.

4.2 Multi-Criteria Analysis

4.2.1 Fish friendliness

The fish friendliness of the turbines is an important factor to take into consideration for the Delta21 project and following the Pro-Tide research on fish mortality of Pentair Fairbanks Nijhuis turbines, the assessment of the alternatives can be achieved.

The turbines of each variant have a design flow rate of:

- Ducted variant design flow rate: $Q_d = 179\ [m^3/s]$
- Venturi variant design flow rate: $Q_d = 172\ [m^3/s]$
- Hybrid variant design flow rate: $Q_d = 175.5\ [m^3/s]$

Therefore, looking at the graphs in Figure 20 in the paragraph 2.3.4 Fish mortality, it can be assumed that the turbines of the three alternatives have a mortality rate lower than 0.1 % for all the types of fish, even the bass, which fulfills the fish-friendliness requirement set for the project.

The test results of the model-scale turbines show higher percentage of mortality due to the fact that they are smaller with the approximately same fish lengths as the full-scale tests. Hence, it can be inferred that a smaller turbine diameter leads to an increase in fish mortality.

For the assessment of the alternatives the highest grade will then be given to the ducted setup as it has the lowest mortality rate, followed closely by the hybrid setup and lastly the venturi setup having the smallest turbine diameter.

	Venturi setup	Ducted setup	Hybrid setup
Turbine diameter [m]	5.8	8.0	7.0
Grade	7	10	8.5

Table 16. Fish friendliness grades per alternatives

4.2.2 Costs

The determination of the costs per variant comes from the difference in volume of concrete, dredging activities and turbine model with its allotted crane.

Concrete

Although the cubic meter price of reinforced concrete varies as it depends strongly on the location, the volumes, the amount of steel used and the construction method, € 1000/m^3 is applied for this estimation of the costs after discussion and agreement with Huub Lavooij.

	Venturi	Ducted	Hybrid
Volume of concrete [m^3]	40,826.02	30,688.70	35,164.38
Unit price of concrete [€/m^3]	1,000	1,000	1,000
Total concrete costs [€]	40,826,024.05	30,688,700.00	35,164,376.18

Table 17. Total concrete costs per caisson per variant

Dredging

Assuming that for each variant, the same dredger and equipment would be used, the dredging costs are calculated by the amount of sand to dig up. The total length of the tidal power plant is 400 m and it is assumed that the dredging of the bed will expand 250 m on each side of the tidal power plant, thus the total dredging area becomes:

$$A_{dredge} = (250 * 2 + 55) * 400 = 222{,}000 \text{ m}^2$$

The volume of sand to be dredged out is calculated using the difference of levels between the assumed bed level and the bottom of the structure level with the sill layer in consideration. The price of a cubic meter of dredged sand is estimated at 2.5 €/m^3 with a trailing suction hopper dredger (TSHD) according to the Bodemrichtlijn website (Bodemrichtlijn, 2019) providing knowledge for specific situations. The TSHD is adequate in this situation as the geological setting surveys fine sand to coarse sand as it can reach dredging depths from 5 m to 50 m.

	Venturi	Ducted	Hybrid
Dredging depth [m]	5.90	8.10	6.60
Dredging area [m^2]	222,000	222,000	222,000
Total excavated sand volume [m^3]	1,309,800	1,798,200	1,465,200
Unit price of dredged sand [€/m^3]	2.5	2.5	2.5
Total dredging costs [€]	3,274,500	4,495,500	3,663,000

Table 18. Total dredging costs for the tidal power plant per variant

Turbines

The study on the Pentair Fairbanks Nijhuis turbines done by R. Meijnen & J. Arnold, gives an overview of the cost per turbines. To determine the costs, the three designs are based on a directly linked permanent magnet generator that is placed in the bulb of the turbine. This bulb is sealed and forms a dry space cooled down by the flowing water on the bulb's wall. The generator will be regulated at speed by means of a frequency converter. The installed capacity for the three turbine designs is 2000 [kW]. The construction is based on carbon steel with galvanic protection, which has been applied with great success in the French La Rance tidal power plant since the 1960s.

The cost price is determined with the following formula:

$$Costprice = n_{turbines}(Mass(0.8C_{turbine} + 0.2C_{divers}) + Power(C_{electric}))\left(1.05 + \frac{0.25}{\sqrt{n_{turbines}}}\right)$$

With:

$n_{turbines}$	[-]	the number of turbines
$Mass$	[kg]	total mass per turbine
$C_{turbine}$	[€/kg]	cost factor for the construction of the turbine unit
C_{divers}	[€/kg]	cost factor for the construction parts (bearings, seals, etc.)
$C_{electric}$	[€/kW]	cost factor for E-part

The following table gives an overview of the aforementioned variables.

	Venturi	Ducted	Hybrid
$n_{turbines}$ [-]	1	1	1
$Mass$ [kg]	127,000	250,000	190,000
$C_{turbine}$ [€/kg]	15	15	15
C_{divers} [€/kg]	30	30	30
$C_{electric}$ [€/kW]	300	300	300

Table 19. Variables used and calculated for cost price calculation (Meijnen & Arnold, 2015)

The cost price determined with the previous formula is calculated as hardware cost in the following tables. The prices showed in those tables are based on European materials and processing prices without including the VAT:

- Hardware: electromechanical turbine construction (steelwork, including generator, VSD and required regulators)
- Project costs: design, engineering, project management, model tests, quality control
- Installation: placing and commissioning
- KPI: Key Performance Indicators
- Maintenance: average maintenance costs per year over lifetime

Nr Turbines [-]	Hardware [€/Turbine]	Project costs [€/Turbine]	Installation [€/Turbine]	KPI [€/kW]	Maintenance [€/Turbine /year]
1	3,752,000	800,000	50,000	1,996	74,000
4	3,391,000	429,000	49,000	1,668	67,000
10	3,258,000	284,000	47,000	1,543	64,000
20	3,192,000	208,000	46,000	1,479	63,000
40	3,144,000	152,000	44,000	1,433	62,000
60	3,123,000	127,000	43,000	1,412	61,000

Table 20. Cost price (excluding VAT) per turbine for the Venturi setup (Meijnen & Arnold, 2015)

Nr Turbines [-]	Hardware [€/Turbine]	Project costs [€/ Turbine]	Installation [€/ Turbine]	KPI [€/ kW]	Maintenance [€/Turbine/year]
1	6,630,000	800,000	100,000	3,104	130,000
4	5,993,000	429,000	97,000	2,670	117,000
10	5,758,000	284,000	94,000	2,506	112,000
20	5,640,000	208,000	91,000	2,423	110,000
40	5,557,000	152,000	89,000	2,363	108,000
60	5,520,000	127,000	86,000	2,336	107,000

Table 21. Cost price (excluding VAT) per turbine for the Ducted setup (Meijnen & Arnold, 2015)

Nr Turbines [-]	Hardware [€/Turbine]	Project costs [€/ Turbine]	Installation [€/ Turbine]	KPI [€/ kW]	Maintenance [€/turbine/year]
1	5,226,000	800,000	75,000	2,550	102,000
4	4,724,000	429,000	73,000	2,169	92,000
10	4,539,000	284,000	71,000	2,025	88,000
20	4,446,000	208,000	69,000	1,951	87,000
40	4,380,000	152,000	67,000	1,898	85,000
60	4,351,000	127,000	65,000	1,874	84,000

Table 22. Cost price (excluding VAT) per turbine for the Hybrid set-up proportionately to the other two setups

The tidal power plant requires 40 turbines in total, thus by adding all the different costs for a 40 turbines installation, the total cost per setup per turbine can be found.

	Venturi setup	Ducted setup	Hybrid setup
Total cost [€/Turbine]	4,835,000	8,269,000	6,582,000

Total costs

The total costs per alternatives are calculated by summing the concrete costs times three for the three caissons, the dredging costs and the turbine costs times forty for the number of turbines housed in the tidal power plant.

The venturi setup is given a 10 as it has the lowest total costs overall. By taking a margin of 2.50 points for a 100,000,000 the other grade can be calculated with a cross product. The ducted setup gets a 2.70 points reduction out of 10 and the hybrid setup gets a 1.33 points reduction out of 10. The final grades are laid in the following table.

	Venturi setup	Ducted setup	Hybrid setup
Total costs [€]	319,152,572.2	427,321,600.0	372,436,128.5
Grade	10	7.30	8.77

Table 23. Costs grades per alternatives

4.2.3 Energy efficiency

Following the study by Meijnen & Arnold, the setups do not have big differences in energy yield, but a difference exists, nonetheless. Figure 18 in the 2.3.3 Turbines paragraph shows the difference between the venturi and ducted setups turbines with regards to turbine decay, power and efficiency.

The turbine efficiency at the design point is almost the same for both the ducted and venturi setups. Due to lower flow losses for the ducted variant, the design flow rate is somewhat higher than for the venturi variant (164 [m^3 / s] vs 157 [m^3 / s]). As a result, the energy production per turbine for the ducted version will be slightly higher than for the venturi version, about 5 % greater (Meijnen & Arnold, 2015).

The hybrid setup being not included in the study, proportionality is assumed, as previously stated, leading to a 2.5 % variation of energy production between the two other setups. Therefore, the ducted setup is given a 10 as it is the most efficient. The hybrid setup is given a 9.5 to still highlight the difference, as small as it may be. The same goes for the venturi setup to which is assigned a 9 grade.

	Venturi setup	Ducted setup	Hybrid setup
Grade	9	10	9.5

Table 24. Energy efficiency grades per alternatives

Further investigation with full-scale models of the different turbines should be carried to assert the energy yield more precisely.

4.2.4 Maintenance efficiency

For maintenance of the shafts, the choice lies in either to do maintenance in a dry or wet environment. The dry environment is achieved by closing the gate on the sea side and adding a stoplog or temporary gate on the tidal basin side. The wet environment maintenance can be achieved by means of divers, however, daily pay rate to employ divers can go as high as GBP £600 per day in the North Sea controlled by the Offshore Diving Industry Agreement (ODIA) according to the Professional Diving Academy website (Professional Diving Academy, 2019). Therefore, a temporary gate may be the better option as it leads to no extra diving precautions or equipment like decompression chamber for the returning divers.

The maintenance of the turbines from each setup differs in the weight of the parts. Heavier turbines require equipment that can withstand the extra weight during transportation to location or during hoisting in the turbine housing. Thus, the ducted setup having the heaviest turbine gets the lowest grade while the venturi setup gets a 10 points grade. With a margin of 2.5 points for 100,000 kg, the ducted setup gets a reduction of 3.07 points out of 10 and the hybrid setup gets a reduction of 1.57 points out of 10. The allocated grades can be seen in the following table:

	Venturi setup	Ducted setup	Hybrid setup
Mass of the turbine [kg]	127,000	250,000	190,000
Grade	10	6.93	8.43

Table 25. Maintenance efficiency grades per alternatives

4.2.5 Transportation

Transportation of the caissons consists of floating each caisson from the dry dock in the Port of Rotterdam to location where it can be immersed. That is why the draught of the caisson is an important factor to take into account. The bigger the draught, the more additional dredging works have to be carried out to ensure a safe clearance between the bottom of the structure and the seabed.

A water level of +0.53 m NAP is assumed during the transportation phase as transportation is effectuated during high water levels and according to the data gathered from the Rijkswaterstaat website, the chosen water level is the lowest high water level recorded between March 1st 2018 and March 1st 2019.

The following table denotes the water levels of the structure and the required depth from the water level to the bed noting that a 1 m clearance is required.

	Venturi setup	Ducted setup	Hybrid setup
Draught [m]	11.95	8.68	11.14
Required water depth [m]	12.95	9.68	12.14
Bottom of the structure level during transport [m NAP]	-11.42	-8.15	-10.61

Table 26. Water depth and NAP levels of the caissons during transportation per setup

The Ducted setup requires the least water depth and is therefore appointed a 10 points grade. A margin of 1.5 points per water depth meter is appointed as grading because the higher the required water depth the more likely it indicates a need for dredging activities along the transportation route, increasing greatly the costs of the project. The venturi setup then gets a reduction of 4.90 points out of 10 and the hybrid setup gets a reduction of 3.69 points out of 10. The allocated grades can be seen in the following table:

	Venturi setup	Ducted setup	Hybrid setup
Grade	5.10	10	6.31

Table 27. Transportation grades per alternatives

4.2.6 Results

Using the grades found in the criteria assessment tables and the weights, a score per alternative is calculated. Summing the scores of each criterion gives a final score for the alternative. The variant with the highest score is decisive. The results are presented in following Table.

	Ducted setup 8.0 m diameter turbine			Venturi setup 5.8 m diameter turbine			Hybrid setup 7.0 m diameter turbine		
	Grade	Weight	Score	Grade	Weight	Score	Grade	Weight	Score
Fish-friendliness	10	0.25	2.50	7	0.25	1.75	8.5	0.25	2.13
Costs	7.30	0.33	2.41	10	0.33	3.30	8.77	0.33	2.89
Energy efficiency	10	0.16	1.60	9	0.16	1.44	9.5	0.16	1.52
Maintenance efficiency	6.93	0.16	1.11	10	0.16	1.60	8.43	0.16	1.35
Transportation	10	0.10	1.00	5.10	0.10	0.51	6.31	0.10	0.63
Total			**8.62**			**8.60**			**8.52**

Table 28. Final MCA matrix

By looking at the table, it can be concluded that the most optimal and decisive alternative is the ducted setup as even though it is not the most cost or maintenance effective design it is the most fish-friendly setup which is a paramount factor for Delta21 as well as being the most energy efficient and transportation friendly. The cost leading potential dredging activities for the transportation phase will be greater for the venturi and hybrid setup which would reduce the gap for the costs' grades making the ducted setup even more prone to be the best variant. In order to accurately calculate the transportation dredging costs, the exact bathymetry of the seabed should be known all along the floating route.

To ensure the correct assessment of the alternatives and a clear and significant optimal design, as the result of assessment do not differ greatly, three sensibility checks of the MCA are realized.

Sensibility check 1

Criteria	Weight factor (%)	Explanation
Fish-friendliness	33	The fish friendliness becomes the most important factor of the project as one of the three Delta21 project's main focus is the nature restauration of the Haringvliet by fish migration. Therefore, it is given the highest score in this check.
Costs	25	The costs criterion is decreased to leave the fish friendliness the highest score relative to the importance of the latter.
Energy efficiency	12	The efficiency of both energy and maintenance are still given equal weights due to the fact that they are equally important. Their scores are decreased to give more importance to the transportation criterion in that check.
Maintenance efficiency	12	To sensibly reflect the MCA assessment the maintenance efficiency criterion is given the lowest score with the energy efficiency to emphasis the fish friendliness and transportation factors as maintenance is a prerequisite of a project anyhow.
Transportation	18	The transportation criterion's score is slightly increased to accentuate the importance of the floatation phase during the project.

	Ducted setup 8.0 m diameter turbine			Venturi setup 5.8 m diameter turbine			Hybrid setup 7.0 m diameter turbine		
	Grade	Weight	Score	Grade	Weight	Score	Grade	Weight	Score
Fish-friendliness	10	0.33	3.30	7	0.33	2.31	8.5	0.33	2.81
Costs	7.30	0.25	1.83	10	0.25	2.50	8.77	0.25	2.19
Energy efficiency	10	0.12	1.20	9	0.12	1.08	9.5	0.12	1.14
Maintenance efficiency	6.93	0.12	0.83	10	0.12	1.20	8.43	0.12	1.01
Transportation	10	0.18	1.80	5.10	0.18	0.92	6.31	0.18	1.14
Total			**8.96**			**8.01**			**8.29**

Sensibility check 2

Criteria	Weight factor (%)	Explanation
Fish-friendliness	25	For this check, the fish friendliness and transportation criteria have the highest score as fish friendliness remains an important factor to Delta21.
Costs	18	The costs criterion for this check is lowered to underline the other aspects of the project like energy efficiency, paramount for an energy production that will return on the investment, and transportation that requires strong logistics throughout the floating phase.
Energy efficiency	20	The energy efficiency criterion is raised for this check to highlight the importance that is energy production efficiency as it is the main role of a tidal power plant.
Maintenance efficiency	12	Maintenance efficiency becomes the lowest criterion for this check as it represents only a small part of the project.
Transportation	25	Transportation weight factor is heightened for this check to focus on the transport prominence and all the difficulties that come with it during the project.

	Ducted setup 8.0 m diameter turbine			Venturi setup 5.8 m diameter turbine			Hybrid setup 7.0 m diameter turbine		
	Grade	Weight	Score	Grade	Weight	Score	Grade	Weight	Score
Fish-friendliness	10	0.25	2.50	7	0.25	1.75	8.5	0.25	2.13
Costs	7.30	0.18	1.31	10	0.18	1.80	8.77	0.18	1.58
Energy efficiency	10	0.20	2.00	9	0.20	1.80	9.5	0.20	1.90
Maintenance efficiency	6.93	0.12	0.83	10	0.12	1.20	8.43	0.12	1.01
Transportation	10	0.25	2.50	5.10	0.25	1.28	6.31	0.25	1.58
Total			**9.14**			**7.83**			**8.20**

Sensibility check 3

To check further, all the criteria are given the same weight highlighting their performance score per criterion and therefore underline their efficiency as a design without weighting factors.

Criteria	Weight factor (%)
Fish-friendliness	20
Costs	20
Energy efficiency	20
Maintenance efficiency	20
Transportation	20

	Ducted setup 8.0 m diameter turbine			Venturi setup 5.8 m diameter turbine			Hybrid setup 7.0 m diameter turbine		
	Grade	Weight	Score	Grade	Weight	Score	Grade	Weight	Score
Fish-friendliness	10	0.20	2.00	7	0.20	1.40	8.5	0.20	1.70
Costs	7.30	0.20	1.46	10	0.20	2.00	8.77	0.20	1.75
Energy efficiency	10	0.20	2.00	9	0.20	1.80	9.5	0.20	1.90
Maintenance efficiency	6.93	0.20	1.39	10	0.20	2.00	8.43	0.20	1.69
Transportation	10	0.20	2.00	5.10	0.20	1.02	6.31	0.20	1.26
Total			**8.85**			**8.22**			**8.30**

The performance of the sensibility checks denotes that the ducted setup is indeed the most suitable alternative when it comes to the chosen criteria. Therefore, the ducted setup is the chosen and assessed as the most optimal design of this research.

4.3 Ducted setup

4.3.1 Stoplogs

In order to carry maintenance operations in the tidal power plant's shafts, divers or stoplogs are necessary. The choice is made on a dry maintenance environment thus turning the attention on the use of stoplogs. Consequently, an assumed 1.50 m increment on the tidal basin side is required to host the 0.50 m wide temporary gate. To keep the turbine in the center of the structure, preventing any asymmetrical weight once in commission, 1.50 m is added on the North Sea side bringing the total width of the caisson to 58 m leading to a reduction from 13 m to 10 m of the length of the sheet pile wall countering the piping effect. The turbine housing becomes 36.0 m long.

During transportation both ends of the shaft must be closed to ensure a dry and empty environment increasing buoyancy. Therefore, the gates and the stoplogs on each side of the tidal power plant must be placed before floating. Following the calculation by M.H. van Saase in his Master thesis report The Conceptual Design of a Tidal Power Plant in the Brouwersdam (van Saase, 2018) on the vertical gates, it is assumed that the gate for the North Sea side weighs 200 kN. The stoplogs weight is estimated at 100 kN as they do not require to be as strong as the gate subject to the sea and are used only during the transportation phase or maintenance operations.

This leads to a change in concrete volume and total weight thus resulting in an increase of the draught of the caisson.

	Ducted setup
Total concrete volume [m^3]	28,054.79
Reinforced concrete unit weight [kN/m^3]	25.0
Weight of the concrete element and gates [kN]	706,169.75
Draught [m]	9.11
Transportation required draught [m]	13.70
Required draught > Draught?	Yes
Difference [m]	- 4.59
Immersion required draught [m]	14.50
Required draught > Draught?	Yes
Difference [m]	- 5.34

Table 29. Ducted setup draught calculation and transportation and immersion clearance verification

The ducted setup is still compliant with the allowable draught during transportation.

In case of maintenance, the stoplogs are then lowered and hosted into sockets by cranes located on the service road, as shown in figure 32.

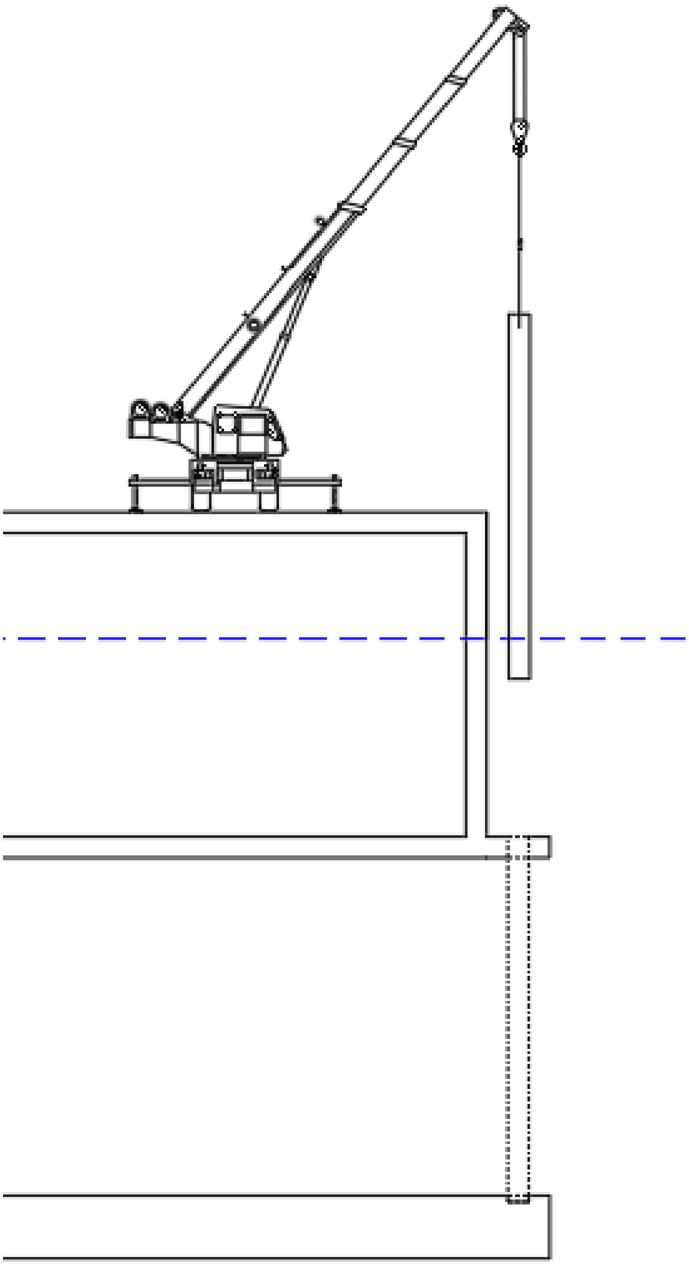

Figure 32. Positioning of the stoplogs in case of maintenance operations

To ease the placement process of the stoplogs when the caissons are submerged, a guide such as the one used for underwater pile driving should be added.

4.3.2 Stability checks during transport and immersion

Static stability

During transport, the stability of the caisson must be assured thus the weight of the structure must be spread evenly. The inlet and outlet of the structure are closed off from sea water to increase the buoyancy. The ballast housing ensures additional weight on the tidal basin side to counter the extra weight from the North Sea side elements.

- **Equilibrium of vertical forces**

Vertical forces establish an equilibrium if the buoyant force equals the weight of the floating body (including all ballast). To ensure the equilibrium of moments, explained below, a sand ballast of 18.01 cm is necessary in each ballast housing resulting in a new draught of 9.18 m which is still compliant with the keel clearance check.

The buoyant force is then calculated:

$$F_b = V_{uw} \cdot \gamma_w = b \cdot l \cdot d \cdot \gamma_w \; [kN]$$

$$F_b = 58 \cdot 137 \cdot 9.18 \cdot 10.29 = 750{,}596.64 \; kN$$

- **Equilibrium of moments**

To prevent the caisson form tilting during floatation, the moments' equilibrium must be achieved. To attain this equilibrium, the summation of the moments around the point of rotation taken as the center of the caisson must equal to zero.

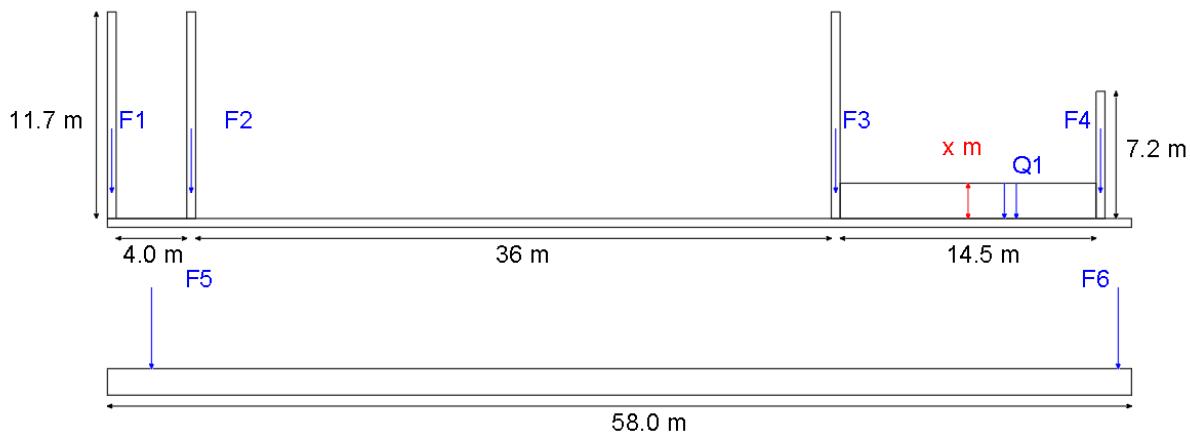

Figure 33. Transportation structure vertical loads sketch

With unit weights for sand of 16 kN/m^3 and concrete of 25 kN/m^3, F1=F2=F3= 146.25 kN and F4= 90 kN.
F5 represents the gate on the North Sea side and F6 the temporary gate on the tidal basin side placed to close the shaft during transportation, respectively weighing 200 kN and 100 kN.
With the equilibrium of moments from the center equal to zero, the resultant of the Q load, RQ1= 302.90 kN. Therefore, Q1= 2.88 kN/m^2 which leads to a sand layer of 18.01 cm.

So, by applying an 18.01 cm ballast sand layer in the ballast housing, stability is reached during transportation.

- **Metacentric height**

Following the calculation steps presented in the theoretical framework:

1. the center of gravity point of the caisson with reference to the intersection of the Z-axis with the bottom line of the caisson gives the distance KG.

   $KG = \frac{\sum V_i \cdot e \cdot \gamma_i}{\sum V_i \cdot \gamma_i} = 4.99\ m$ above the underside.

2. The center of buoyancy B is found by halving the draught of the caisson. The draught of the element is 9.18 m so:

   $KB = \frac{1}{2} \cdot d = 4.59\ m$

3. BM is found by dividing the area moment of inertia of the area that intersects the water surface by the volume of the displaced fluid:

   $$BM = \frac{\frac{1}{12} \cdot l \cdot b^3}{V}$$

   $I = 2{,}227{,}529\ m^4$ and $V = 72{,}944.28\ m^3$

   Therefore, $BM = 30.54\ m$

4. the metacentric height h_m can be computed by:

   $$h_m = KB + BM - KG$$

   If $h_m > 0$ the caisson is theoretically stable, while $h_m > 0.5$ is preferred.

   $h_m = 30.14\ m$, so, there is no problem with the static stability.

Dynamic stability

- **Sway**

Considerable swinging of the caisson on the waves or swell should be avoided. Based on experience, the following rule of thumb is often used for a check:

$L_w < 0.7 \cdot l_e$ and $L_w < 0.7 \cdot b_e$

If this condition does not apply, problems due to swaying of the element can be expected.

In our case: $L_w < 0.7 \cdot 137 = 95.9\ m$, if the wave direction is parallel to the length axis of the caisson.
In our case: $L_w < 0.7 \cdot 58 = 40.6\ m$, if the wave direction is perpendicular to the length axis of the caisson.

Actual local wave data should be checked to ensure minimal swaying of the element. Transportation should be carried during a calm day to minimize risks of swaying.

- **Natural oscillation**

It should also be avoided that the periods of wave movements come close to the natural oscillation period of the structure. Hence the natural oscillation period must be calculated using the Steiners theorem:

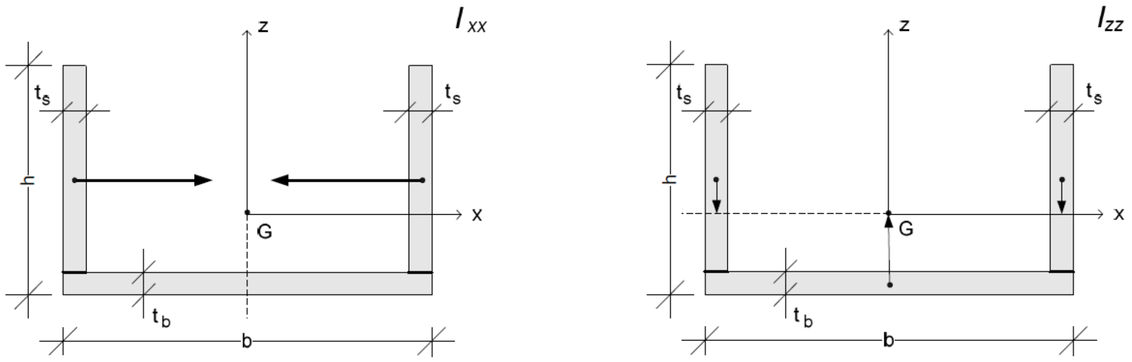

Figure 34. Indication of translation direction for application of Steiners theorem for Ixx (left) and for Izz (right) (Voorendt, Bezuyen, & Molenaar, 2011)

First I_{xx} around the z-axis (vertical axis) is calculated:

$$I_{xx} = 51{,}411.4\ m^4$$

I_{zz} is around the x-axis, the horizontal axis in width direction:

$$I_{zz} = 4{,}903.2\ m^4$$

The polar moment of inertia: $I_p = I_{xx} + I_{zz} = 56{,}314.6\ m^4$

The area of concrete in the cross-section is: $A_c = 147.76\ m^2$

The polar inertia radius then is: $j = \sqrt{\frac{I_p}{A_c}} = 19.52\ m$

The natural oscillation period is:

$$T_0 = \frac{2\pi j}{\sqrt{h_m g}} = 7.13\ s$$

Transportation is thus only allowed when the natural oscillation period is significantly larger than the wave period. So, as for swaying, transportation should be carried out during a calm day to minimize risks.

4.3.3 Wave impact

Using the method of Goda the wave impact on the structure during commission can be computed. The calculations focus on the extreme storm condition with a design water level of +5.00 m NAP plus the sea level rise taken into consideration, for a total design water level of +6.58 m NAP. During such events, the gates on the North Sea side are closed, thus the caisson is assumed to be a vertical wall.

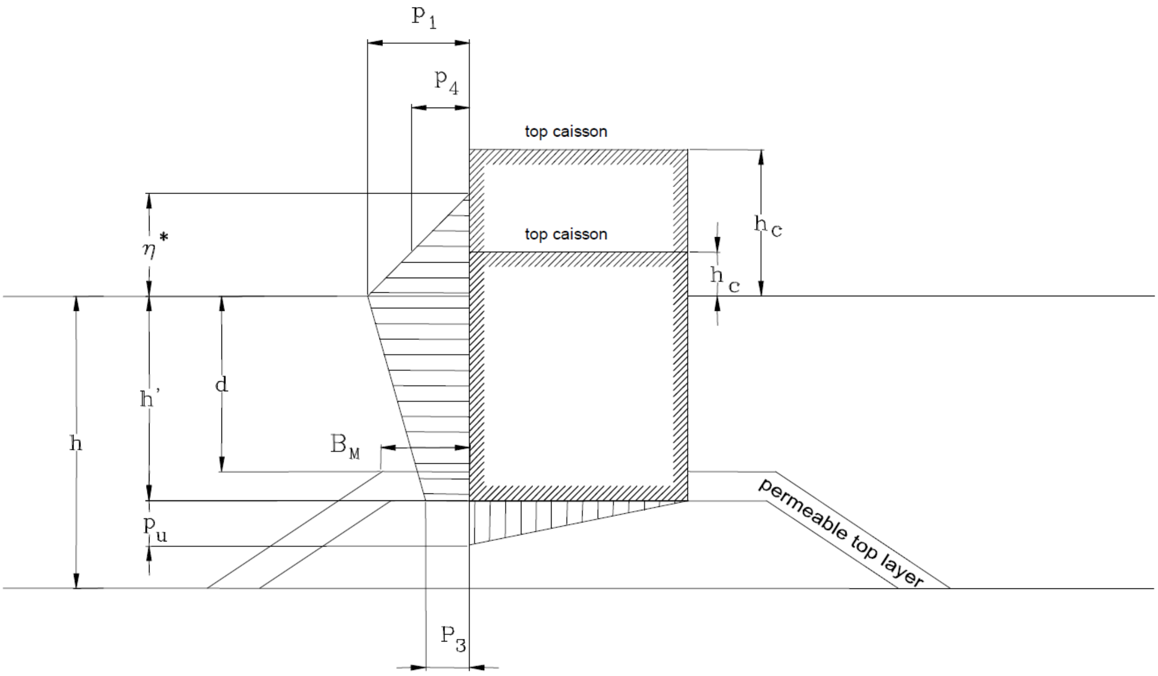

Figure 35. Goda (modified by Tanimoto): wave pressure (Molenaar & Voorendt, 2016)

Parameters	Symbol	Input
Water level [m NAP]		+6.58
Bottom of the structure [m NAP]		-14.7
Bottom rubble foundation [m NAP]		-16.7
Design wave height [m]	H_d	6.09
Significant wave height [m]	H_s	2.9
Angle of incoming wave [°]	β	0
Water depth above the sill [m]	d	$h' - 2D_{n50}$
Water depth above the wall foundations plane [m]	h'	21.28
Water depth in front of the sill [m]	h	23.28
Wave period [s]	T	10.2
Berm width [m]	B_M	5
Shape factors [-]	$\lambda_1, \lambda_2, \lambda_3$	1

Table 30. Input parameters for the wave impact calculation

To determine the wavelength of the incoming waves, it is required to figure out the relative depth characteristic of the structure.

For shallow waters, the wavelength $L' = T\sqrt{gh} = 147.37\ m$, thus $\frac{h'}{L} = 0.14$ which is not smaller than $\frac{\mathbf{1}}{\mathbf{20}}$ therefore it is not considered shallow waters.

For deep waters, the wavelength $L' = L_0 = \frac{gT^2}{2\pi} = 162.44\ m$, thus $\frac{h'}{L} = 0.13$ which is not higher than $\frac{1}{2}$ therefore it is not considered to be deep waters.

For transitional water, the wavelength $L' = \frac{gT^2}{2\pi} \tanh kh'$, with $k = \frac{2\pi}{L}$ the wave number.

By means of iteration, it is then possible to calculate the wavelength of the incoming waves in transitional waters.

The wavelength at depth h' then becomes $L' = 127.11\ m$, with $k' = 0.04943$

Parameters	Symbol	Input
Wavelength at depth h' [m]	L'	127.11
Design wavelength [m]	L_D	130.99
Wave number at depth h' [-]	k'	0.04943
	κ	0.0312
Stability coefficient [-]	N_s	29.36
Armor nominal diameter [m]	D_{n50}	0.09877
Water depth above the sill [m]	d	21.08
Height wave impact above water level [m]	η^*	9.14
Freeboard [m]	h_c	9.85
Freeboard min(η^*,h_c) [m]	h_c^*	9.14
Water depth at a distance $5H_D$ from the wall [m]	h_b	23.28
Pressure 1 [kN/m]	p_1	87.92
Pressure 3 [kN/m]	p_3	55.08
Pressure 4 [kN/m]	p_4	0.0
Pressure bottom [kN/m]	p_u	54.84

T able 31. Output parameters for the wave impact calculation

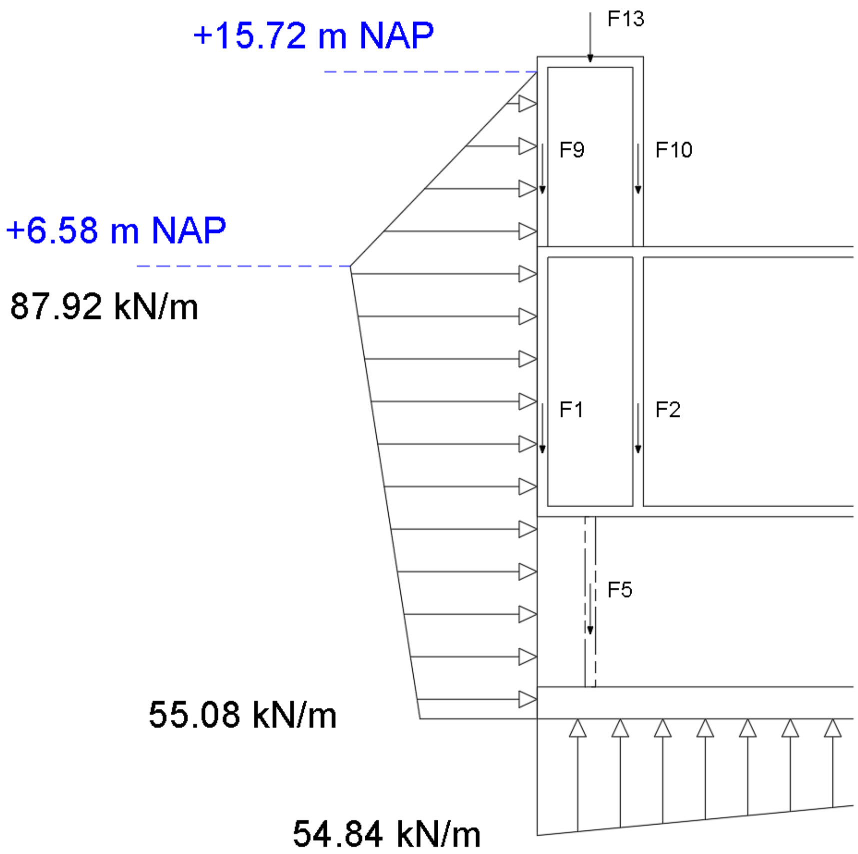

Figure 36. load distribution of the wave impact at North Sea level +6.58 m NAP

The hydrostatic pressure can be calculated using the following formula:

$$p = \rho * g * h$$

Tidal basin side	
Density of water [kg/m³]	1,029
Water depth [m]	15.20
Gravity [m/s²]	9.81
Water pressure [kN/m]	153.44

Table 32. Hydraulic pressure at the tidal basin side

North Sea side	
Density of water [kg/m³]	1,029
Water depth [m]	21.28
Gravity [m/s²]	9.81
Water pressure [kN/m]	214.81

Table 33. Hydraulic pressure at the North Sea side

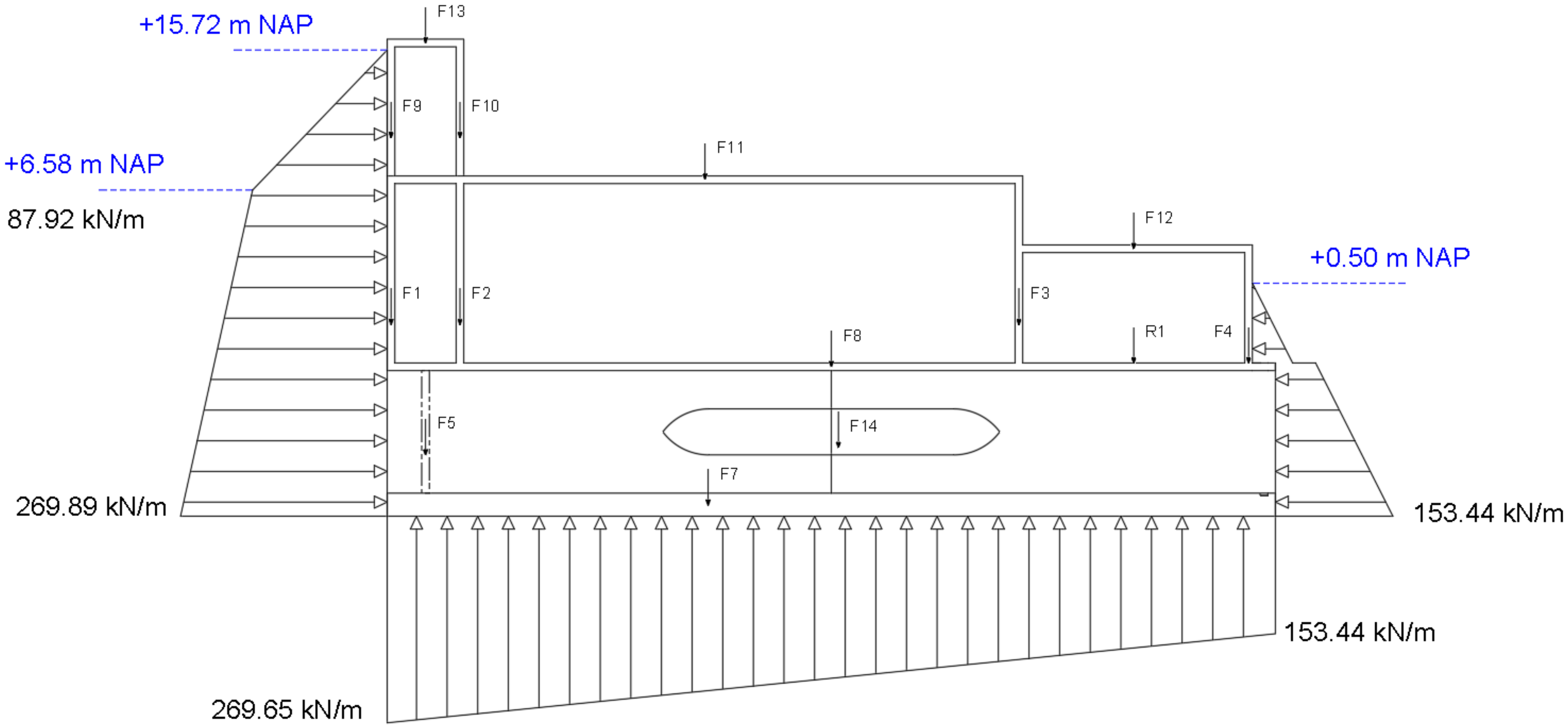

Figure 37. Combination of wave impact and hydraulic pressures for a North Sea water level at +6.58 m NAP

4.3.4 Stability checks during commission

Shear criterion caisson-foundation

Using the caisson-rubble friction coefficient of 0.5, the horizontal stability in commission can be checked by multiplying it to the dead weight of all the elements of the tidal power plant and the product must exceed the total of the horizontal forces during the extreme storm conditions. The infrastructure elements: gates, turbines and concrete, are given a 10% increase for possible operational equipment needed in the tidal power plant.

In order to sink the caisson to its resting position, the ballast must be filled to counter the buoyancy force. The water leveled assumed is +4.58 m NAP corresponding to the highest High Water Level recorded plus the sea level rise in order to find the maximum draught the caisson must be subjected to during commission. Using the following formula with a draught of 19.28:

$$F_b = V_{uw} \cdot \gamma_w = b \cdot l \cdot d \cdot \gamma_w \ [kN]$$

$$F_b = 58 \cdot 137 \cdot 19.28 \cdot 10.29 = 1{,}576{,}416.48 \ kN$$

The total weight of the structure is 1,585,369.95 kN which is higher than the buoyancy force therefore does not require more ballast to counteract the buoyancy effect.

The total vertical load of the tidal power plant can then be calculated by subtracting the average water pressure under the caisson to the structure's total weight. The resulting vertical force per caisson is:

Element	Weight [kN]
Total weight of the concrete elements	927,463.08
Total weight of the North Sea side gates	3,520.00
Total weight of the water in the sluiceways	605,875.20
Total weight of the turbines	43,164.00
Total weight of the transportation ballasts	5,347.67
Total average water pressure under the caisson	243,823.01
Total vertical load	1,341,546.94

Table 34. Total vertical load of the tidal power plant

Forces	Weight [kN]
Total horizontal force on the North Sea side	576,603.05
Total horizontal force on the Tidal Basin side	159,757.82
Total horizontal load	416,845.23

Table 35. Total horizontal load of the tidal power plant

To be stable, the following formula must be checked:

$$\frac{\sum H}{f \sum V} < 1.0 \Leftrightarrow \frac{416{,}845.23}{0.5 * 1{,}341{,}546.94} = 0.62 < 1.0$$

Therefore, the tidal power plant is horizontally stable during extreme storm events.

Rotational stability

For this check, the turn-over criterion must verify $e_R = \frac{\sum M}{\sum V} \leq \frac{1}{6}b$.

Therefore, all the vertical forces are summed to find their total and the sum of the moments of the vertical and horizontal forces towards K is calculated.

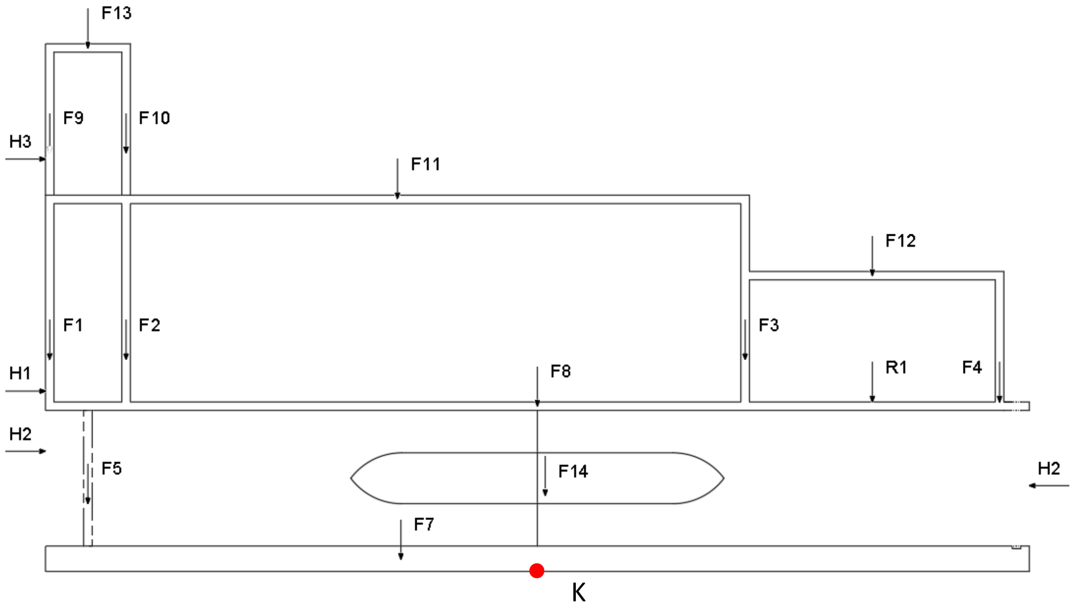

Figure 38. Overview of the vertical loads of the tidal power plant

The sum of the vertical forces is: $\sum V = 5{,}161.15\ kN/m$.

And the sum of the moments towards K is: $\sum M = 26{,}909.24\ \ kNm/m$ clockwise.

Therefore, $e_R = \frac{26{,}909.24}{5{,}161.15} = 5.21\ m \leq \frac{1}{6} * 58 = 9.67\ m$.

The caisson is thus rotationally stable.

Vertical stability

The required vertical effective soil stress should not exceed the maximum bearing capacity of the soil, otherwise the soil will collapse. The maximum acting stress on the soil can be calculated with:

$$\sigma_{k,max} = \frac{F}{A} + \frac{M}{W} = \frac{\sum V}{b \cdot l} + \frac{\sum M}{\frac{1}{6} l b^2}$$

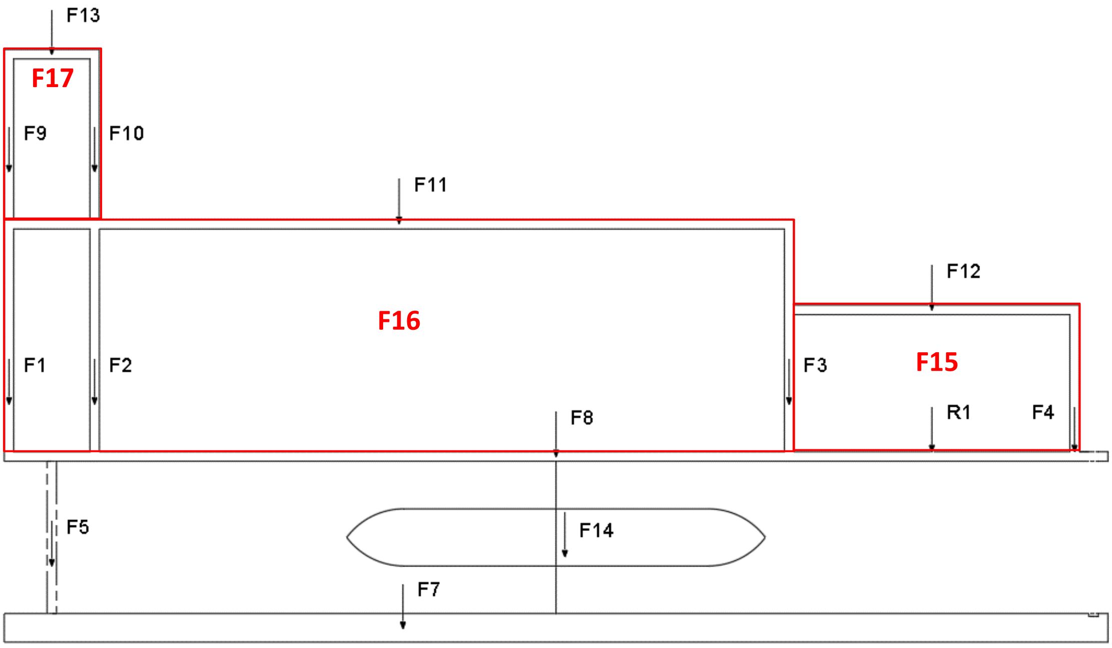

Figure 39. Total vertical forces along the caisson length

With F15, F16 and F17 the vertical forces of the side walls necessary to calculate the total moment towards K.

Parameter	Value
Total vertical forces [kN]	1,341,546.94
Total moment towards K [kNm]	2,796,215.61
Area [m²]	7,946.00
Section modulus [m³]	76,811.33
Maximum acting stress [kN/m²]	205.24

Table 36. Calculation of the maximum acting stress under the caisson

However, due to the presence of the sill, the vertical load has to spread through it. It is spread under an assumed angle of 45°.

This infers that the maximum acting stress on the soil layer below the sill should be compared with the bearing capacity. This means that $\sigma_{k,max}$ reduces with a factor $\frac{b}{b'}$ due to the caisson weight, but an extra pressure should also be taken into account because of the weight of the sill above the area with width $b' = 62.00\ m$. The unit weight for the sill is assumed as saturated gravel:

$$\gamma'_{sill} = 20\ kN/m^3$$

$$\sigma'_{k,max} = \frac{b}{b'} * \sigma_{k,max} + \gamma'_{sill} * h_{sill} * 1 * 1 = \frac{58}{62} * 205.24 + 20 * 2.00 * 1 * 1 = 232.00\ kN/m^2$$

This new maximum effective soil stress should not exceed the vertical bearing capacity.

$$p'_{max} = c'N_c s_c i_c + q'N_q s_q i_q + 0.5\gamma' B \cdot N_\gamma s_\gamma i_\gamma$$

The cohesion of sand is assumed negligible. The effective soil stress next to the caisson is also assumed to be negligible, because the sill is not present over the entire width of the sliding plane and it would be too favorable if its effect would be taken fully into account. Thus, the Prandtl & Brinch Hansen bearing capacity equation can be simplified to:

$$p'_{max} = 0.5\gamma' b' \cdot N_\gamma s_\gamma i_\gamma$$

Parameter	Symbol	Value
Relative weight [kN/m³]	γ'	$\gamma_s - \gamma_w = 20 - 10 = 10$
Angle of internal friction [°]	$\emptyset'$	30
Bearing capacity factor [-]	N_q	18.40
Bearing capacity factor [-]	N_γ	20.09
Shape factor [-]	s_γ	0.86
Inclination factor (for H parallel to b) [-]	i_γ	0.33
Bearing capacity [kN/m²]	p'_{max}	1,762.90

Table 37. Calculation of the maximum bearing capacity of the subsoil

Thus, even in this critical phase, it can be concluded that the bearing capacity of the soil beneath the tidal power plant is amply adequate to support its weight.

Caisson strength check

Assuming that the caisson rests on a flat bed after immersion, the commission phase of the project is most likely governing for the moments and stresses in the side walls of the caisson. This is due to the combination of the water pressure outside and the lack of pressure working from the inside of the empty caisson to the outside. The wave impact and the hydraulic pressures on the North Sea side of the tidal power plant during a storm event are expected to be the governing load situation.

Therefore, a strength check is effectuated for the portion of outer wall most subjected to external forces:

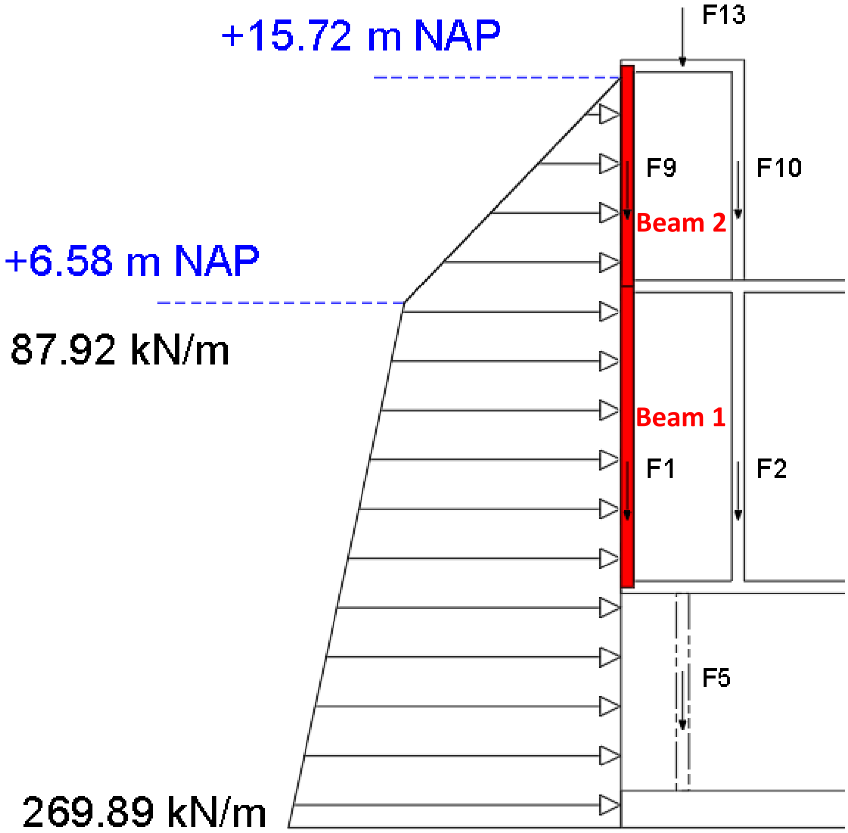

Figure 40. Wall section with beam 1 and beam 2 checked for strength

By entering the horizontal loads in Technosoft after drawing the structure and its elements, the moments, shear stress and axial loads can be extracted.

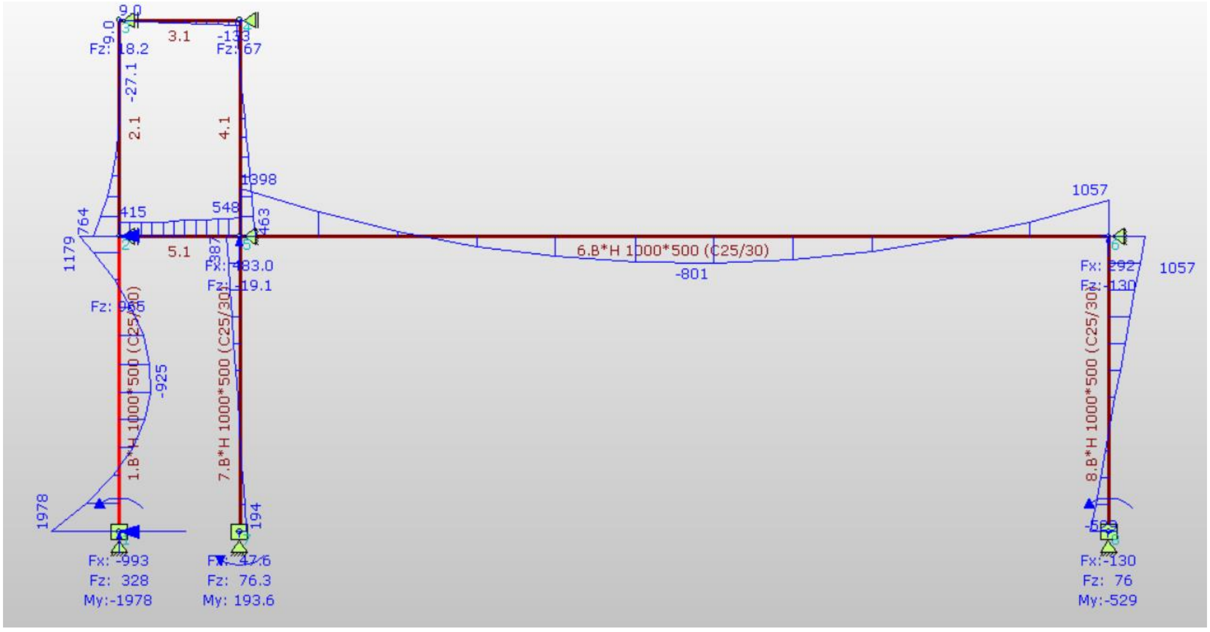

Figure 43. Output of the external forces acting on the portion of wall

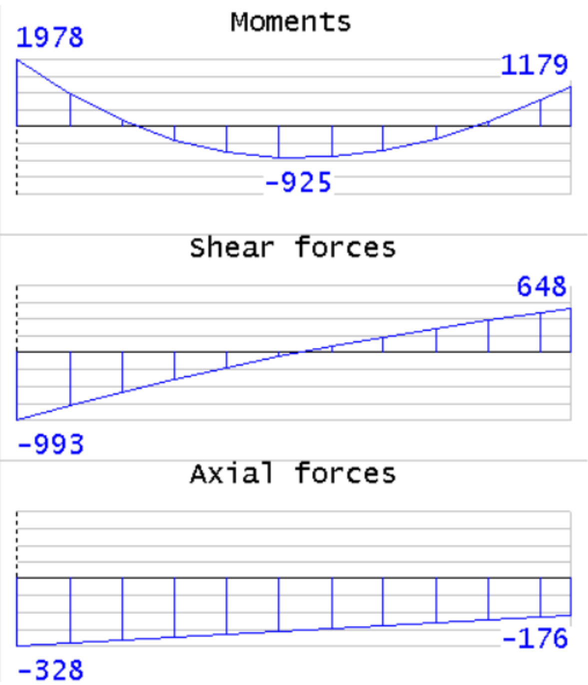

Figure 42. Result of Beam 1 characteristics

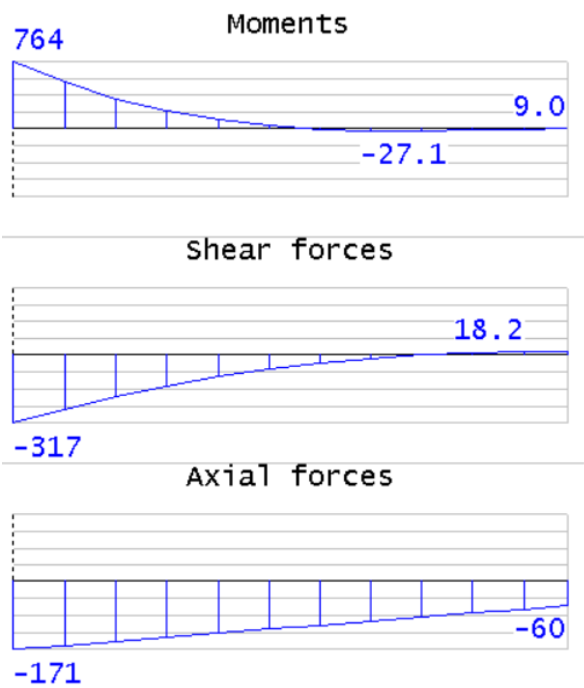

Figure 41. Results of Beam 2 characteristics

The Dutch standard TGB 1990 prescribes a shear stress criterion:

$\tau = \frac{3}{2}\frac{V}{b \cdot t} \leq \tau_1$ with $\tau_1 = 0.4 f_b \cdot 0.15 \sigma_{bmd'}$

With	τ_1	[N/mm^2]	the maximum allowable shear stress
	f_b	[N/mm^2]	the tensile strength of the concrete class
	$\sigma_{bmd'}$	[N/mm^2]	the average design value of concrete compressive strength

In the vicinity of supports, loads are transferred by compression directly to those supports (Figure 44), and the maximum shear force is therefore somewhat less than the computed maximum value. In the design of wood and reinforced concrete beams, the shear force within a distance, d, of the face of the supports can be considered equal to the value of the shear force at that distance, d (Ochshorn, 2010).

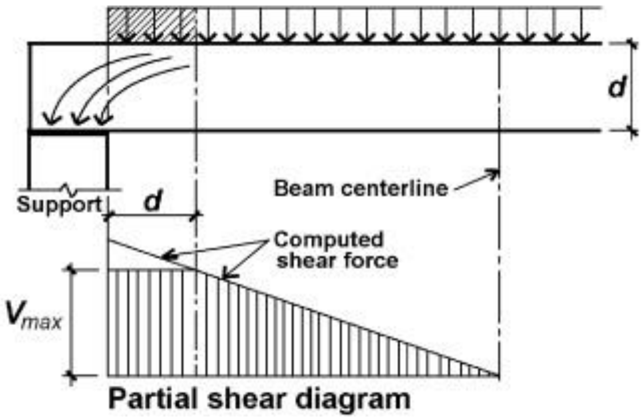

Figure 44. Reduction of shear force, Vmax, in the vicinity of the beam's reaction (support) (Ochshorn, 2010)

Therefore, $b = 0.5\ m$, $t = 0.5\ m$, thus $V = 900.16\ kN$

$$\tau_{beam1} = 5.40\ N/mm^2$$

Choosing a concrete class of C45/55, with $f'_{ck} = 55\ N/mm^2$ the tensile strength is calculated with in NEN6720:

$$f_b = \frac{f_{brep}}{\gamma_m}$$

With	$f_{brep} = 0.7 * (1.05 + 0.05 f'_{ck})$	[N/mm^2]	
	$\gamma_m = 1.2$	[-]	the material factor

So, $f_b = 1.90\ N/mm^2$ and $\sigma_{bmd'} = 67.95\ N/mm^2$ conform to NEN-EN 1015-11.

Thus, the maximum allowable shear stress $\tau_1 = 11.71\ N/mm^2$ is higher than the design value of the shear strength.

For the moment, the total resulting field moment in the middle of the bottom plate is $M_d = -925\ kNm/m$. The wall thickness can be estimated using the following chart:

$\frac{M_d}{bd^2 f_{cd}}$	ψ	k_x	k_z	ρ [%] C20/25	C28/35	C35/45	C45/55	C53/65
10	0,010	0,013	0,99	*0,03*	*0,05*	*0,06*	*0,08*	*0,09*
20	0,020	0,027	0,99	*0,07*	*0,10*	*0,13*	*0,15*	*0,18*
30	0,030	0,240	0,98	*0,10*	*0,15*	*0,19*	*0,23*	*0,27*
40	0,041	0,055	0,98	*0,14*	0,20	0,25	0,31	0,37
50	0,051	0,068	0,97	0,18	0,25	0,32	0,39	0,46
60	0,062	0,083	0,97	0,21	0,30	0,39	0,47	0,56
70	0,073	0,097	0,96	0,25	0,35	0,45	0,55	0,66
80	0,084	0,112	0,96	0,29	0,41	0,52	0,64	0,75
90	0,095	0,127	0,95	0,33	0,46	0,59	0,72	0,85
100	0,106	0,141	0,94	0,37	0,51	0,66	0,81	0,95
110	0,117	0,156	0,94	0,40	0,56	0,73	0,89	1,05
120	0,129	0,172	0,93	0,44	0,62	0,80	0,98	1,16
130	0,140	0,187	0,93	0,48	0,68	0,87	1,06	1,26
140	0,152	0,203	0,92	0,52	0,73	0,94	1,15	1,36
150	0,164	0,219	0,91	0,57	0,79	1,02	1,24	1,47
160	0,176	0,235	0,91	0,61	0,85	1,09	1,34	1,58
170	0,188	0,251	0,90	0,65	0,91	1,17	1,43	1,69
180	0,201	0,268	0,90	0,69	0,97	1,25	1,53	1,80
190	0,214	0,285	0,89	0,74	1,03	1,33	1,62	1,92
200	0,227	0,303	0,88	0,78	1,10	1,41	1,72	2,04
210	0,240	0,320	0,88	0,83	1,16	1,49	1,82	2,16
220	0,253	0,337	0,87	0,87	1,22	1,57	1,92	2,27
230	0,267	0,356	0,86	0,92	1,29	1,66	2,03	2,39
240	0,281	0,375	0,85	0,97	1,35	1,75	2,13	2,52
250	0,295	0,393	0,85	1,02	1,43	1,83	2,24	2,64
260	0,310	0,413	0,84	1,07	1,50	1,93	2,35	2,78
270	0,325	0,433	0,83	1,12	1,57	2,02	2,47	2,91
280	0,340	0,453	0,82	1,17	1,64	2,11	2,58	3,05
290	0,356	0,475	0,81	1,23	1,72	2,21	2,70	3,19
300	0,372	0,496	0,81	1,28	1,80	2,31	2,82	3,34
310	0,388	0,517	0,80	1,34	1,87	2,41	2,94	3,48
320	0,405	0,540	0,79	*1,40*	*1,96*	*2,51*	*3,07*	*3,63*

Figure 45. Reinforcement percentages for rectangular cross-sections, reinforced with B500B, loaded by bending without normal force, With Mu in kNm; b and d in m and fcd in N/mm²

For the concrete class of C45/55, and a reasonable assumption of 1% for the economic reinforcement percentage, $\frac{M_d}{b \cdot t^2 \cdot f'_b} = 130$.

With	$f'_b = \frac{f'_{brep}}{\gamma_m}$	[N/mm²]	the compressive strength of the concrete class
With	$f'_{brep} = 0.72 f'_{ck}$	[N/mm²]	
	$\gamma_m = 1.4$	[-]	the material factor

So, $f'_b = 33.00\ N/mm^2$

Therefore, $t_{beam1} = \sqrt{\frac{M_d}{b \cdot 130 \cdot f'_b}} = 0.46\ m\ < 0.50\ m.$

The thickness of the wall is then sufficient to withstand the acting forces if the chosen load situation is the governing one. Further investigation into 3D Finite Elements calculations should be carried to assess the wall and slab thicknesses.

4.3.5 Bed protection

Foundation bed

The rubble mound foundation under the caissons is a necessary protective measure to avoid structure instability over time. The stability of the of the armor units are then paramount to an overall protection. From the stability coefficient of the armor unit, the armor nominal diameter $D_{n50} = 0.09877\ m$ is calculated (see in the 4.3.3 Wave impact paragraph).

The 2.00 m thick sill is then assumed to be made of this armor material. Further investigation should be made to identify all the different necessary layers.

Scour protection

In order to find the required length of the bottom protection, the maximum scouring depth must be calculated. To find it, the depth-averaged flow velocity at the end of the bed protection must be computed. However, it is assumed that this velocity is equal to the governing outflow velocity coming out of the shafts of the tidal power plant. As this velocity enters a large body of water it is clear it would lead to its reduction. Thus, a much higher scour development would be observed increasing the safety of the structure.

The outflow velocities are calculated using the previously calculated design flow rate for the ducted setup turbine in which is included a loss coefficient due to friction and turbulence in the passage opening:

$$u_{out} = \frac{Q_{sred}}{A_s} = 2.80\ m/s$$

Using Shields equation, $u_c = C\sqrt{\psi_c \cdot \Delta \cdot D_{n50}}$, the critical velocity can be calculated.

From the boreholes surveys collected from DINOloket, the grain size analysis providing the particle size distribution of the sand can be retrieved. Because the sea bed is dredged to a depth of -16.70 m NAP for the ducted setup, the analysis from 8.00 m to 9.00 m from the sea bed level of -8.60 m NAP is needed.

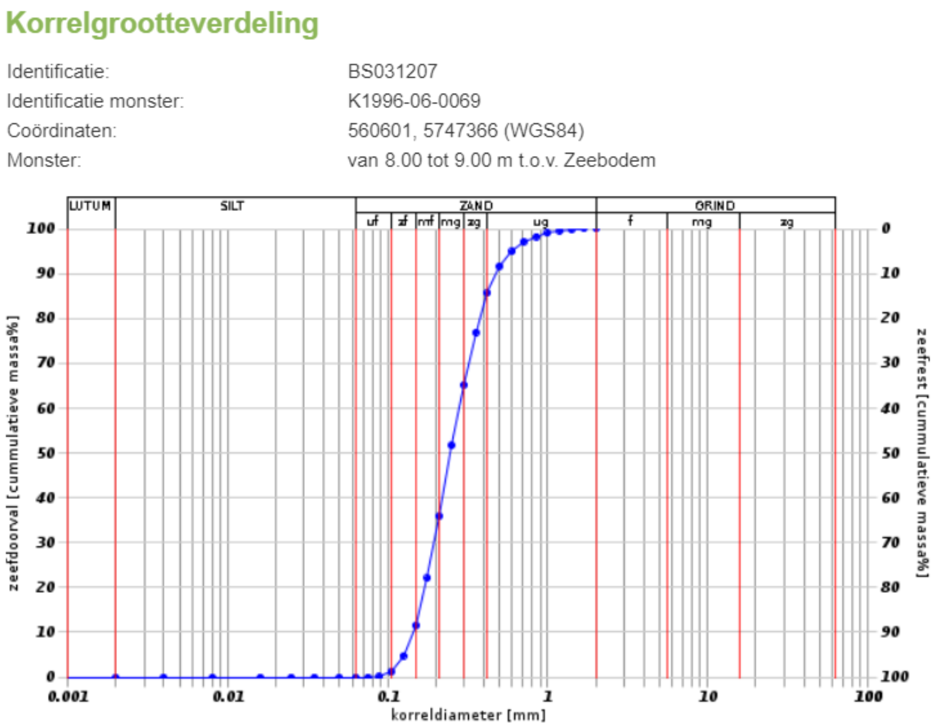

Figure 46. Grain size distribution for the 8.00 to 9.00 m subsoil layer (Netherlands Organization for Applied Natural Sciences Research TNO, 2019)

For this layer, $D_{50} = 0.25\ mm$.

ψ_c, Shields parameter, is found using the following graph, previously presented as Figure 25.

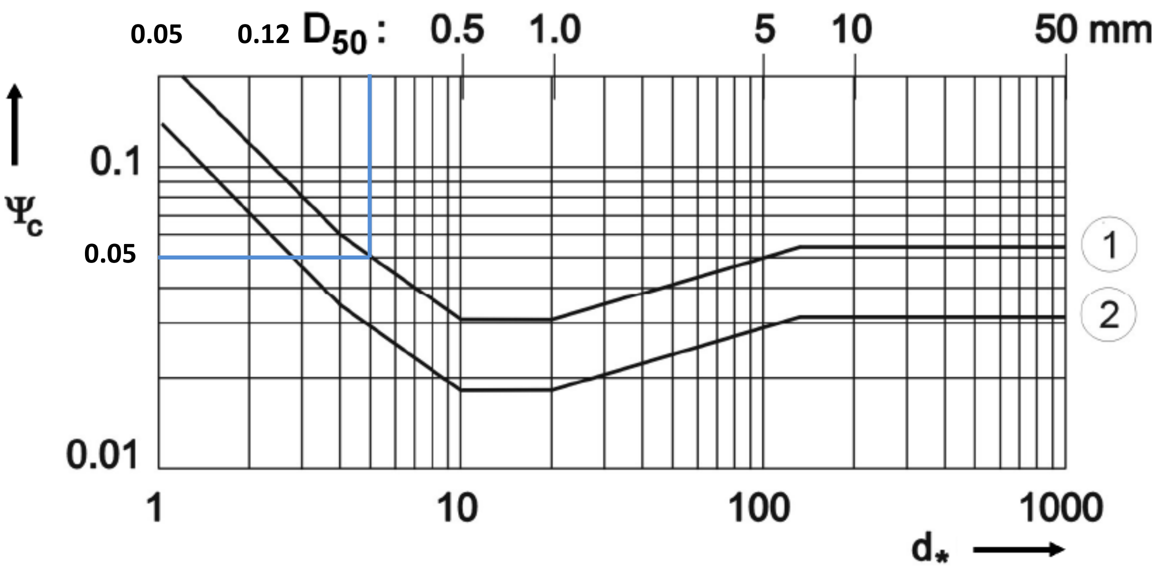

Figure 47. Computation of the Shields parameter

Parameter	Symbol	Value
Median nominal diameter of sand particles [m]	D_{n50}	0.00021
Equivalent sand roughness [m]	k_r	0.00042
Hydraulic radius [m]	R	9.39
Chézy coefficient [√m/s]	C	97.71
Relative density [-]	Δ	1.02
Sheilds parameter [-]	ψ_c	0.05
Critical velocity [m/s]	u_c	0.32

Table 38. Critical velocity calculation

With the critical velocity, the maximum scour depth can be calculated:

$$h_{max} = \frac{((0.5 \cdot \alpha \cdot u) - u_c) \cdot h_0}{u_c}$$

With α in the order of 3 and the initial water depth $h_0 = 19.70\ m$ when taking a maximum water level of +3.00 m NAP on each side:

$$h_{max} = 238.62\ m$$

Therefore, the length of the bed protection should be checked with the following formula:

$$L \geq \gamma \cdot n_s \cdot h_{max}$$

Assuming a safety factor of 1 due to the fact that the velocity for the maximum scour depth is already overestimated and the slope factor $n_s \approx 15$ for loosely packed material:

$L \geq 3{,}579.34\ m$

Largely because of the use of the outgoing velocities from the shafts of the tidal power plant as the high averaged vertical velocities, the scour development is overly big. The resulting necessary protection length is proportionally huge and thus disregarded. Further investigation of the behavior of the water velocities exiting the sluiceways should be executed to determine the correct required length of the protection bed. An estimation of $L = 8h_0$ is used as an assumption for this project. Thus, the length for the protection bed $L = 157.6\ m$.

4.3.6 Preliminary design drawings

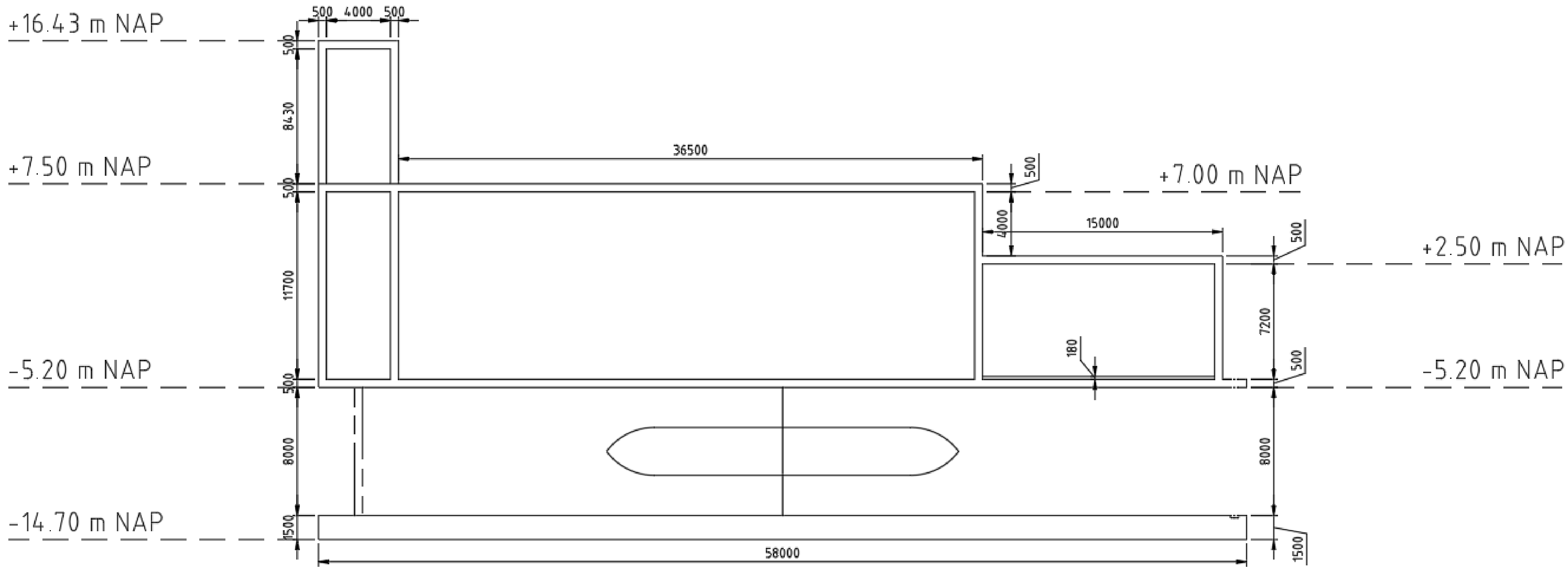

Figure 48. Transversal cross section of the tidal power plant

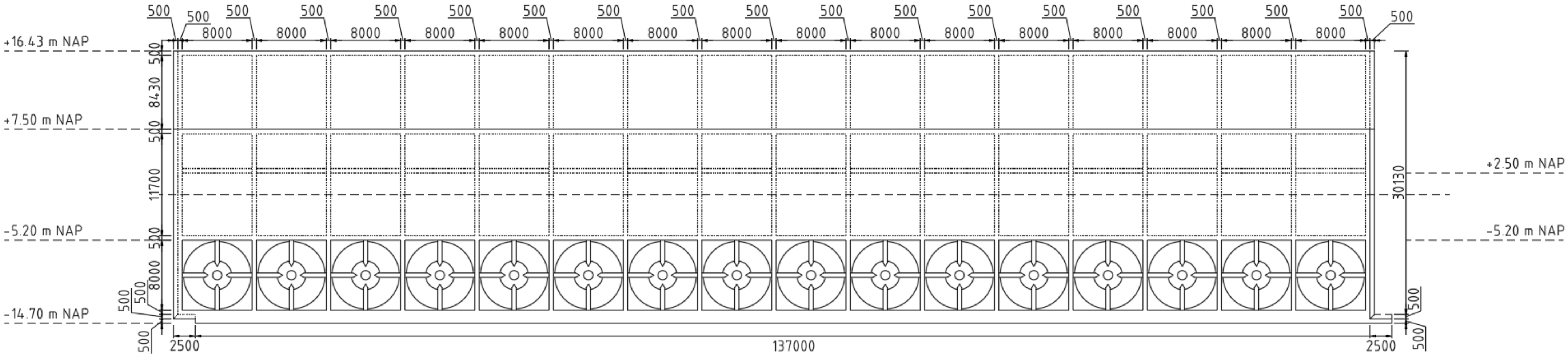

Figure 49.Detailed front view of the middle caisson of the tidal power plant

TIDAL BASIN SIDE

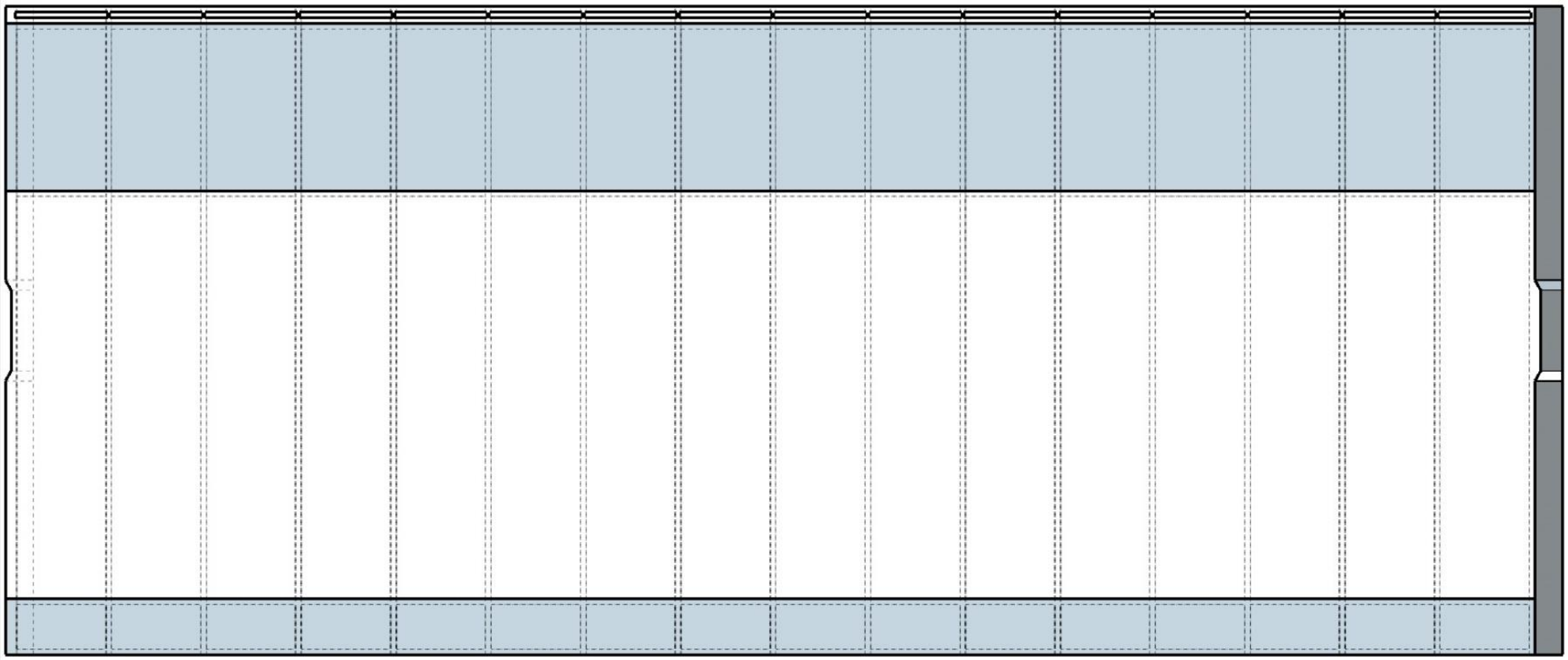

NORTH SEA SIDE

Figure 50. Top view of the tidal power plant from the SketchUp model

Following is the front view of the tidal power plant with the two side caissons. Those side caissons are 131.50 m long to fit the 400.00 m long tidal power plant requirement. The middle caisson hosts 16 turbines therefore, the two side caissons host 12 turbines each. It is assumed that the middle caisson is the governing caisson for all the checks being the longest and heaviest. The two side caissons have three closed empty shafts that can be ballasted to counterweight the turbines and ensure stability.

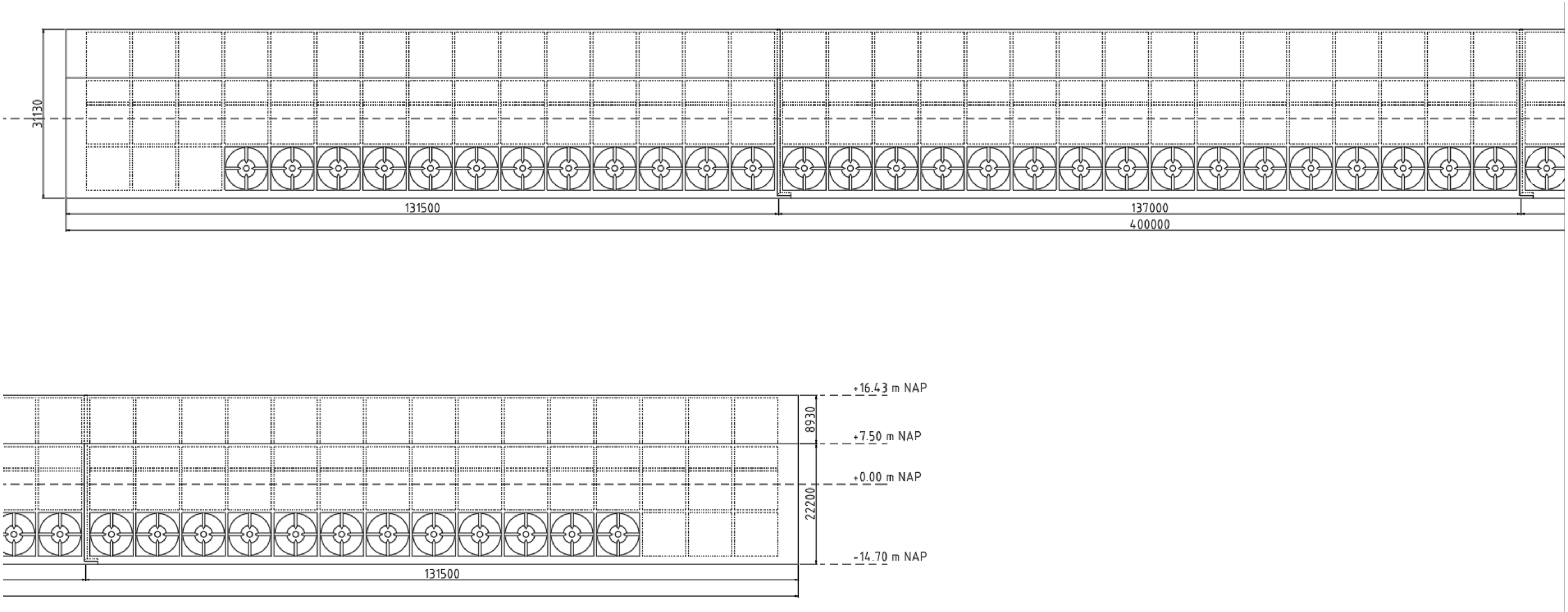

Figure 51. Front view of the tidal power plant

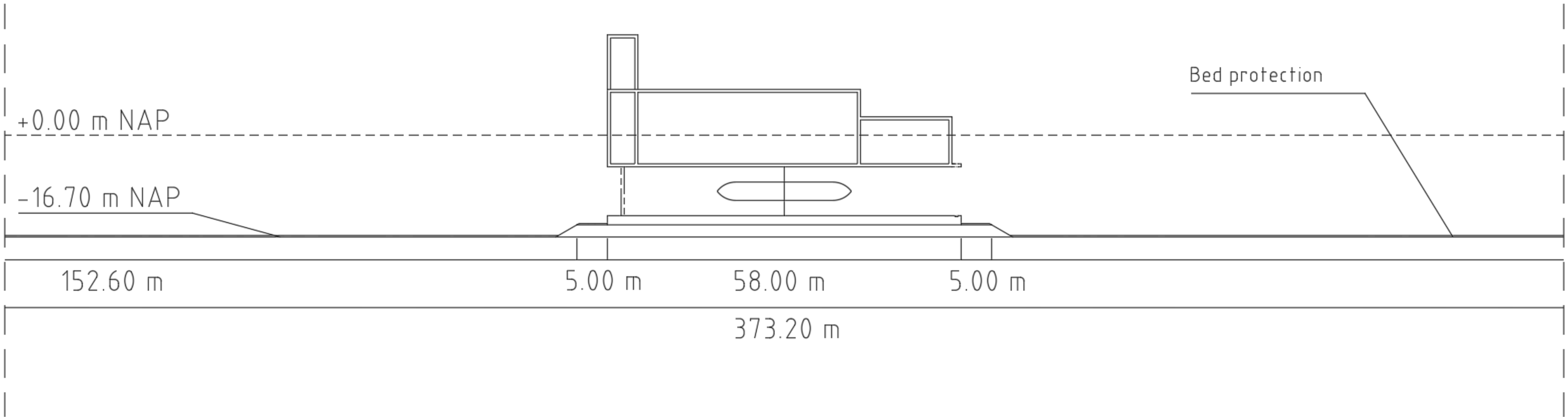

Figure 52. Tidal power plant cross-section with bed protection length

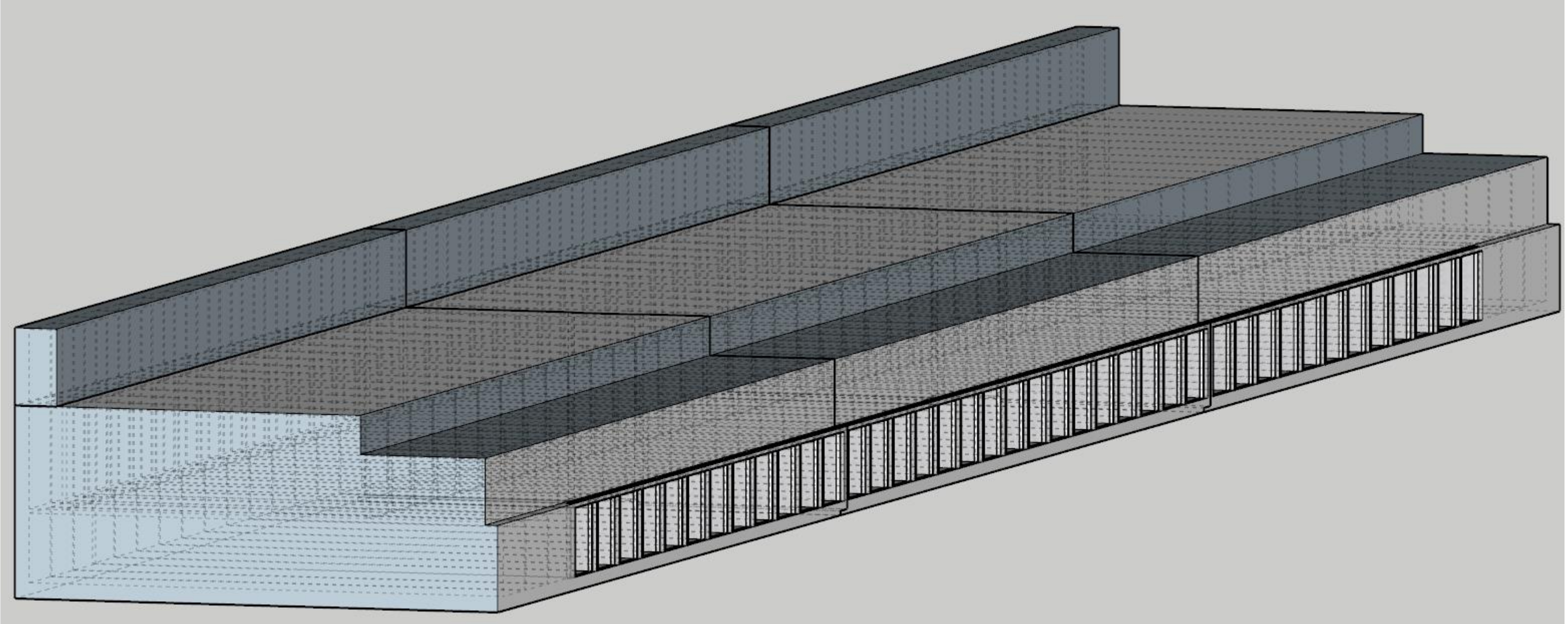

Figure 53.SketchUp model of the total tidal power plant at an angle

5. Discussions

In this chapter, the results of the research are discussed followed by an overview of its strong and weak points.

The calculations provide a reasonably accurate indication of the dimensions of the concrete caisson forming the tidal power plant. However, given that the structure is schematized into a one dimension or even two dimensions element, a more detailed, precise and complete calculation should be carried out as the current design is only preliminary. This calculation should take into account the spread of the forces in the structure into multiple directions for example by performing 3D FE (finite element) calculations.

On the whole, I believe the results are strong as they are grounded by realistic boundary conditions, found in specialized sources such as the Rijkswaterstaat, although assumptions are made concerning the geological setting and the wave behavior among others. Moreover, the formulas and logic used are compliant with the methods applied to calculate such structures. This research will hopefully provide some insight and starting points to the Delta21 full scale project with the boundary conditions and the functional and technical requirements of the tidal power plant.

However, there are also some weak points which could be furthered and improved. As this research is only a preliminary approach, it does provide a groundwork on the tidal power plant for the Delta21 project, but it does remain limited. Due to the many assumptions and uncertainties some of the results are unrealistic and thus require more accurate analysis of data that are not necessarily available to a bachelor student. Moreover, no reinforcement calculations were done but just assumptions and thus should be considered in further investigation.

Because I am not proficient with the Dutch language and I was not assigned to any company offices but worked alone, it made it harder to use certain software or to research specific literature even with the fairly accurate Dutch to English translation from Google Translate.

6. Conclusion and recommendation

This research studied three different alternatives of sluiceway setups for a tidal power plant towards an optimal design that fulfilled the requirements set in accordance with the Delta21 project. Through a Multi-Criteria Analysis the optimum setup was highlighted and calculated.

From the three covered alternatives, the ducted setup was proven to be the optimal variant as it scored the highest in three out of five criteria in the Multi-Criteria Analysis even after the sensibility checks were performed. It is the most fish friendly, which is a paramount factor for the Delta21 project, the most energy efficient and the least susceptible alternative to require dredging activities and thus additional costs during the transporting phase.

All the different stability checks were also performed and proved to be compliant, as long as the boundary conditions are correct, apart from the scour protection length calculations which was overestimated due to an assumption. Therefore, more data on the current velocities should be researched and input. A better and more detailed insight to the important parameters is thus recommended. Moreover, only a small portion of the design of the tidal power plant was completed in this thesis, much more work from a full team of engineers with different specialties would be required to determine stronger and perfected design of the structure.

The gate design on the North Sea side should be looked into in depth to create an element capable of withstanding storm conditions as well as the lifting mechanism from both the gates and the turbines that are intended to be lifted in the turbine housing for maintenance and replacement of parts. Provision was made for hanging cranes to be able to slide out of the turbine housing onto the service road for parts transportation for repair or replacement via trucks, but this would require feasibility investigations.

Moreover, the morphology of the seabed should be researched further into details for more accurate dredging activities and transportation routes as well as to find the location of original channels for the best turbine positioning.

Also, the use of HydraNL, that replaced the *Hydraulische Randvoorwaarden primaire waterkeringen* documents, should be looked into, as it requires the use of the Dutch language, for a better analysis of the water and waves behavior as well as for more precise boundary conditions.

Bibliography

Bodemrichtlijn. (2019, 7 9). Opgehaald van www.bodemrichtlijn.nl: https://www.bodemrichtlijn.nl/Bibliotheek/bodemsaneringstechnieken/g-baggeren-en-transporteren/g6-sleephopperzuiger/baggeren-en-transporteren-kosten-sleephopperzuiger

Bowles, J. E. (1997). *Foundation analysis and design (5th Edition).* McGraw-Hill.

Braam, C., & Lgendijk, P. (2008). *Constructieleer Gewapend Beton.* 's-Hertogenbosch: BowPrint International BV.

Clark, R. H. (2007). *Elements of Tidal-Electric Engineering.*

Delta21. (2017). *Deskstudie: Delta21 en Energie.*

Deltacommissie. (2008). *Working together with water, A living land builds for its future .*

Deltadienst. (1957-1987). *Driemaandelijks Bericht Deltawerken.*

Edwards, J. T. (1990). *Civil Engineering for Underground Rail Transport.* Butterworth & Co.

El-Reedy, M. A. (2012). *Offshore Structures.* Gulf Professional Publishing.

Garmin. (2019). *Navionics*. Opgehaald van webapp.navionics.com: https://webapp.navionics.com/?lang=en#boating@10&key=q%60s%7BH%7DjgW

Hawkswood, M., & Allsop, W. (2009). *Foundations to Precast Marine Structures.*

Katsman, C. A., Sterl, A., Beersma, J. J., & al. (2011). Exploring high-end scenarios for local sea level rise to develop flood protection strategies for a low-lying delta—the Netherlands as an example. In *Climate Change* (pp. 617-645).

Lewin, J. (2001). *Hydraulic gates and valves - In Free Surface Flow and Submerged Outlets.* Thomas Telford Publishing.

Mack, D. L., Slack, C., & Llorca, J. (2004). *Water Control Structures - Selected Design Guidelines.*

Meijnen, R., & Arnold, J. (2015). *Conceptual Design and Comparison of Two Propeller Turbine Configurations.* Pro-Tide.

Molenaar, W. F., & Voorendt, M. Z. (2016). *Manual Hydraulic Structures.* TU Delft, Department Hydraulic Engineering.

Netherlands Organization for Applied Natural Sciences Research TNO. (2019). *DINOloket*. Opgehaald van www.dinoloket.nl: https://www.dinoloket.nl/ondergrondgegevens

Ochshorn, J. (2010). Beams. In J. Ochshorn, *Structural Elements for Architects and Builders.*

Professional Diving Academy. (2019, 7 9). Opgehaald van http://www.professionaldivingacademy.com: http://www.professionaldivingacademy.com/careers-in-diving/

Rijkswaterstaat. (2019). *Waterinfo Rijkswaterstaat*. Opgehaald van waterinfo.rws.nl: https://waterinfo.rws.nl/#!/kaart/astronomische-getij/

Schiereck, G. J. (1993). *Introduction to bed bank shore protection- Engineering the interface of soil and water.*

Sung Hoon, S., Min Su, P., Youn Ju, J., & Yoon Koog, H. (2019). Dispersion Effects of Wave Force on Interlocking Caisson Breakwater with shear-key. *Journal of the Korean Society of Civil Engineers*.

Tanimoto, K., & Takahashi, S. (1994). *Design and construction of caisson breakwater - the Japanese experience.*

van der Meer, J. W., Allsop, N. W., Bruce, T., De Rouck, J., Kortenhaus, A., Pullen, T., . . . Zanuttigh, B. (2018). *Manual on wave overtopping of sea defences and related structures. An overtopping manual largely based on European research, but for worldwide application.* EurOtop.

van Esch, B. P. (2015). *Model-based study of fish damage for the Pentair Fairbanks Nijhuis Modified Bulb Turbine and the Water2Energy Cross Flow turbine.* Pro-Tide.

van Saase, M. H. (2018). *The Conceptual Design of a Tidal Power Plant in the Brouwersdam.*

Van Saase, M. H. (2018). *The Conceptual design of a Tidal Power Plant in the Brouwersdam.*

Voorendt, M. Z., Bezuyen, K. G., & Molenaar, W. F. (2011). *Hydraulic structures: Caissons.*

Waterstaat, M. v. (2007). *Hydraulische Randvoorwaarden primaire waterkeringen.*

Windfinder. (2019). *Windfinder*. Opgehaald van www.windfinder.com: https://www.windfinder.com/windstatistics/renesse

Appendix 1a: Venturi setup preliminary design A-A' cross-section

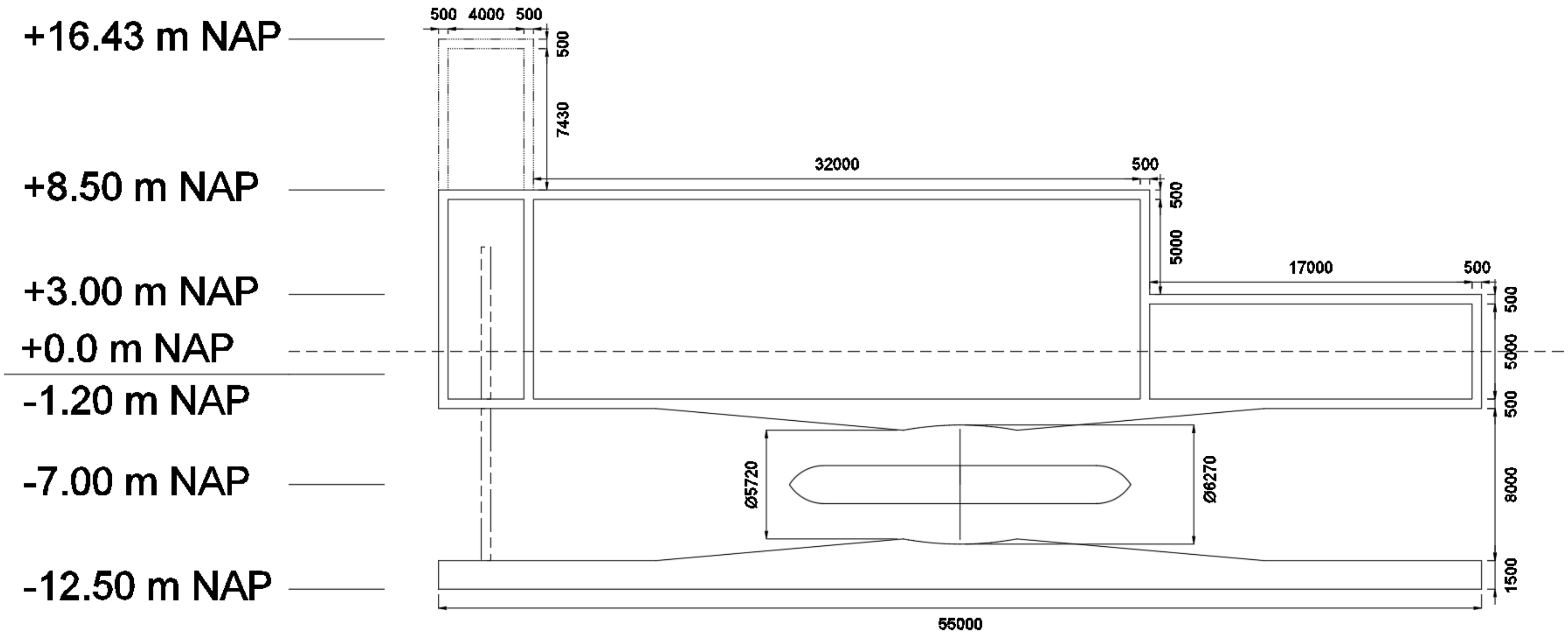

Appendix 1b: Venturi setup preliminary design front view

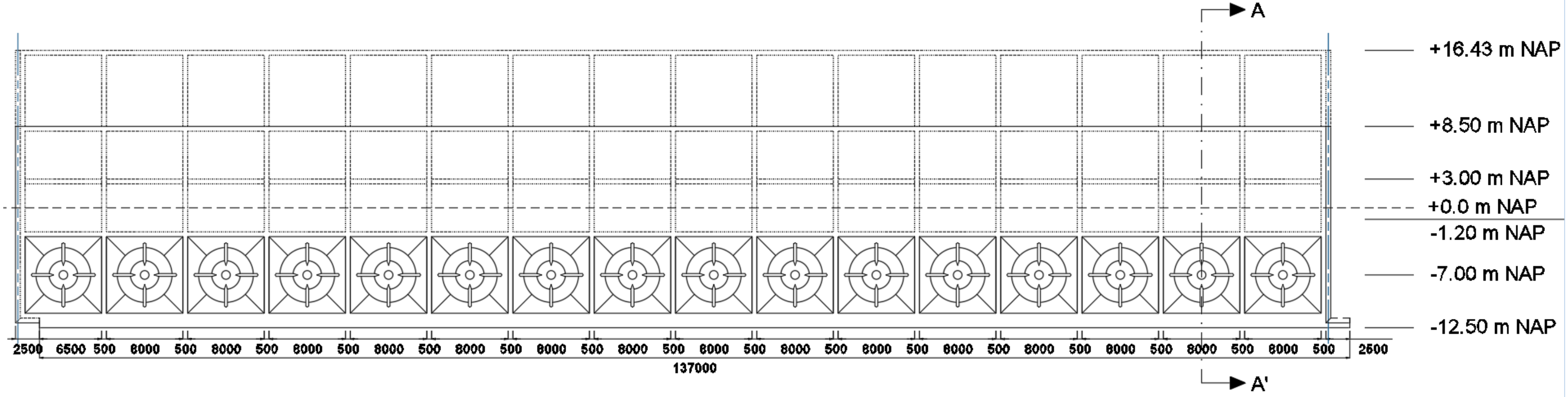

Appendix 2a: Ducted setup preliminary design A-A' cross-section

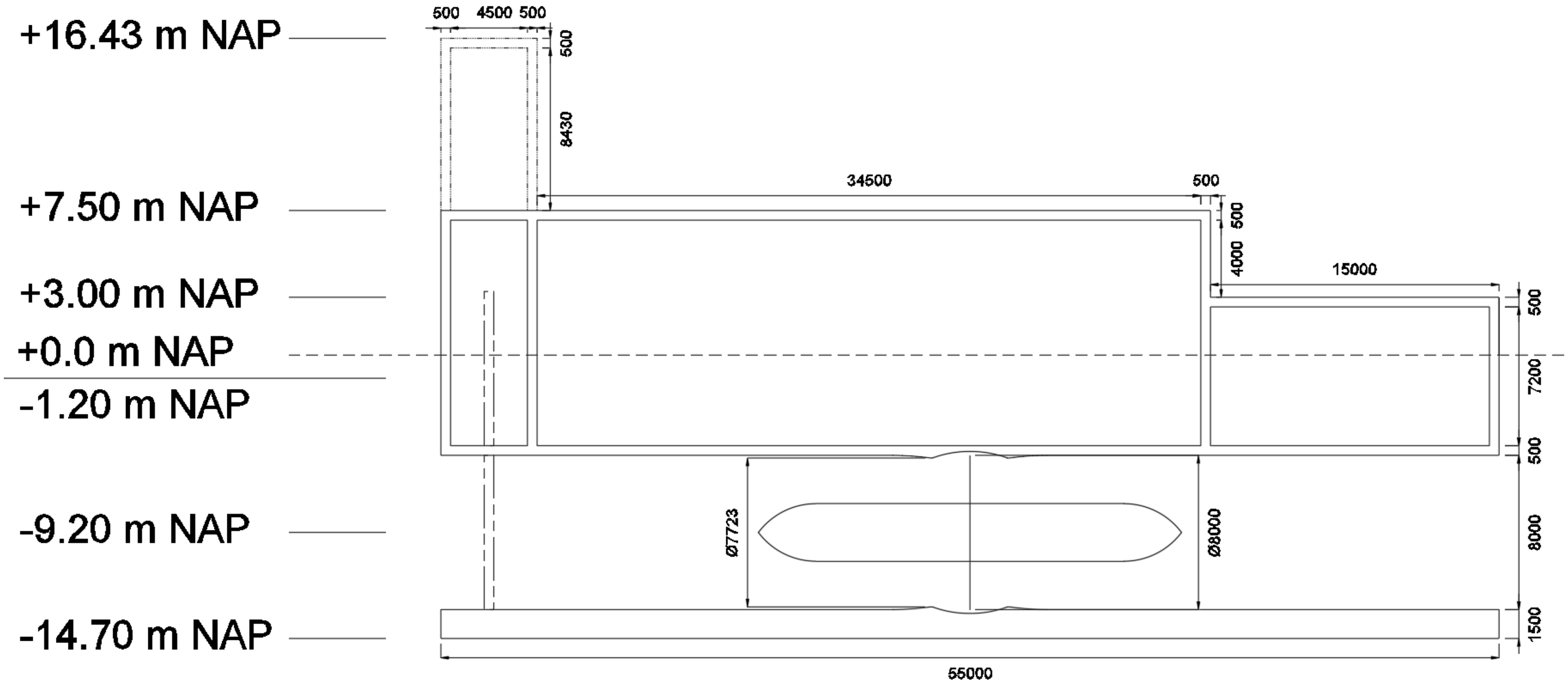

Appendix 1b: Ducted setup preliminary design front view

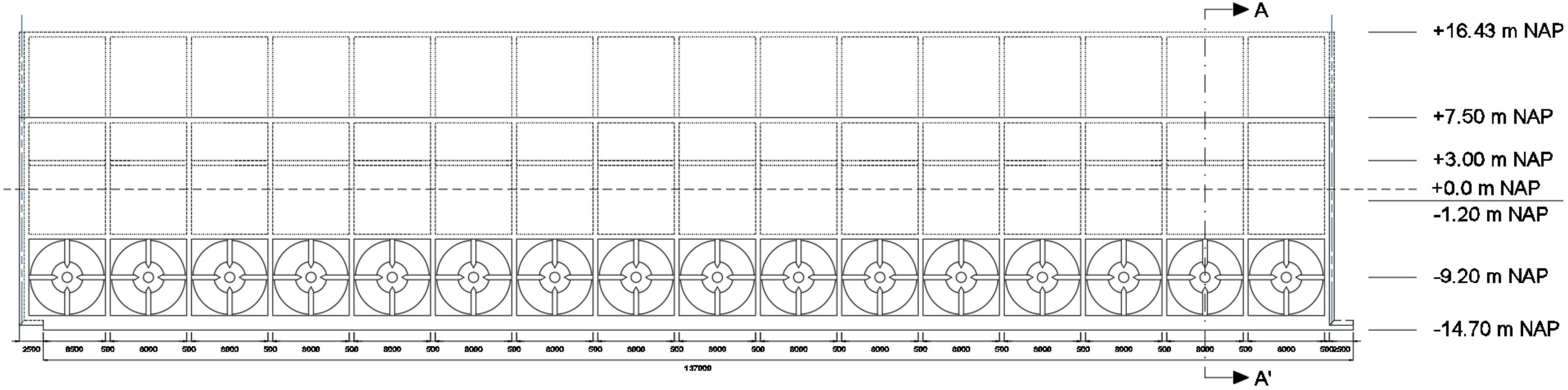

Appendix 3a: Hybrid setup preliminary design A-A' cross-section

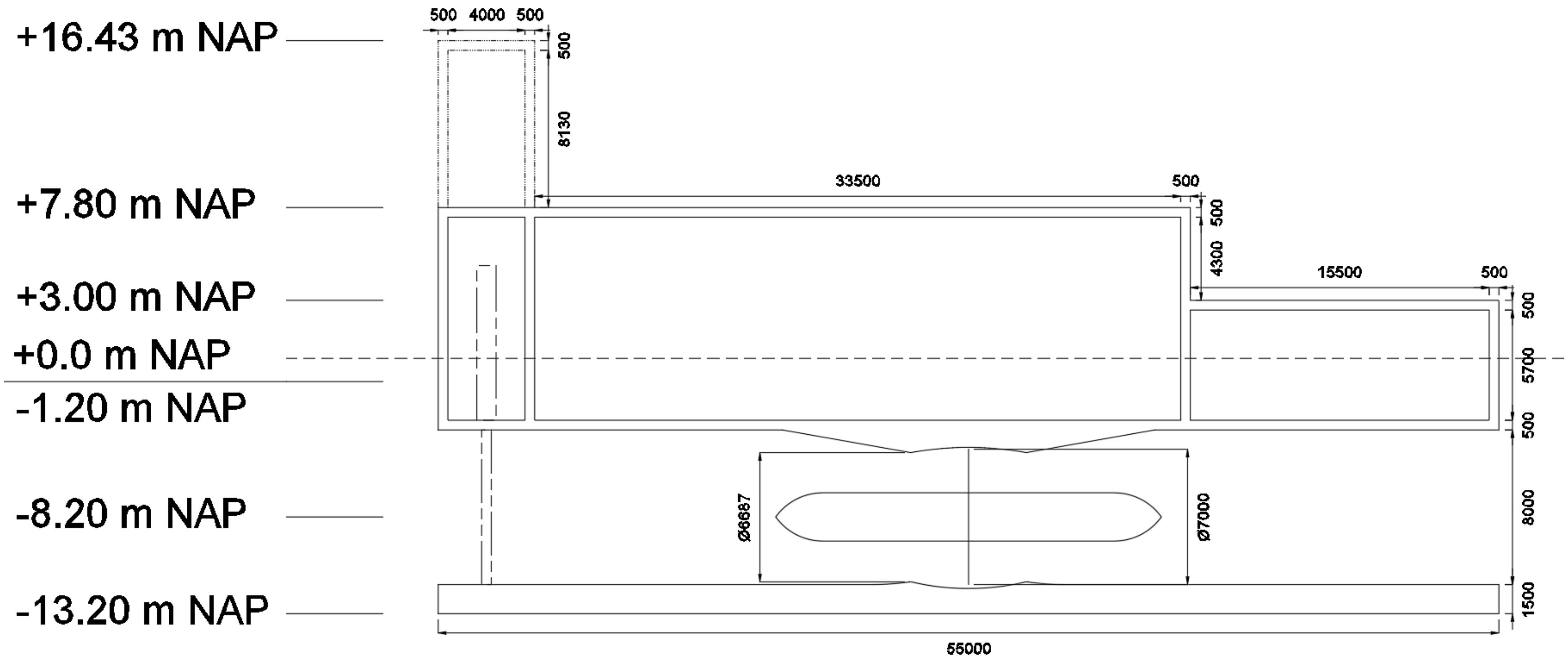

Appendix 3b: Ducted setup preliminary design front view

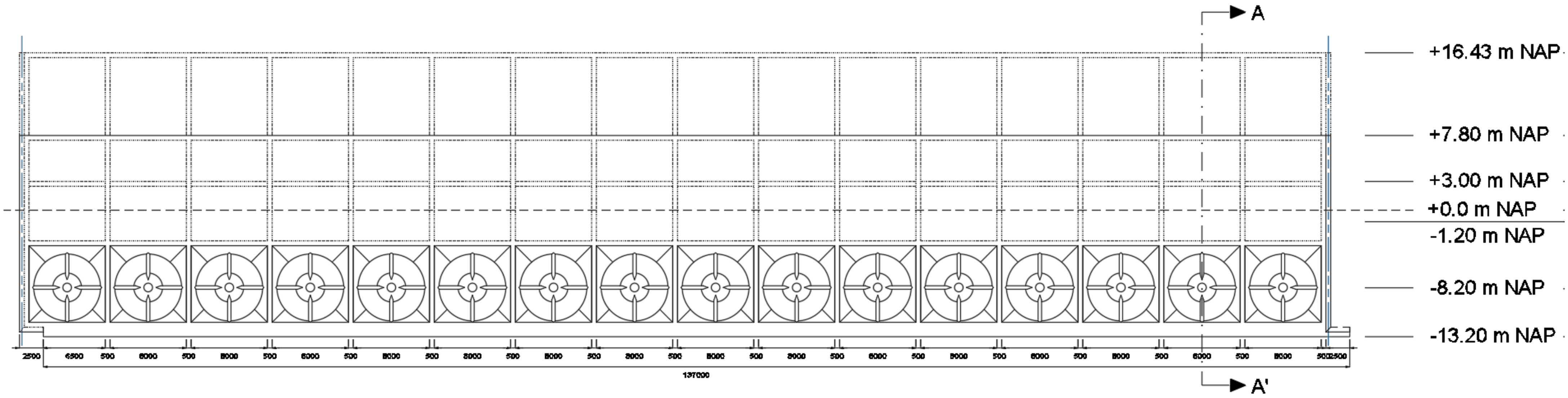

Appendix 4: SketchUp model of the Venturi setup in parallel projection from the front, the side and at an angle

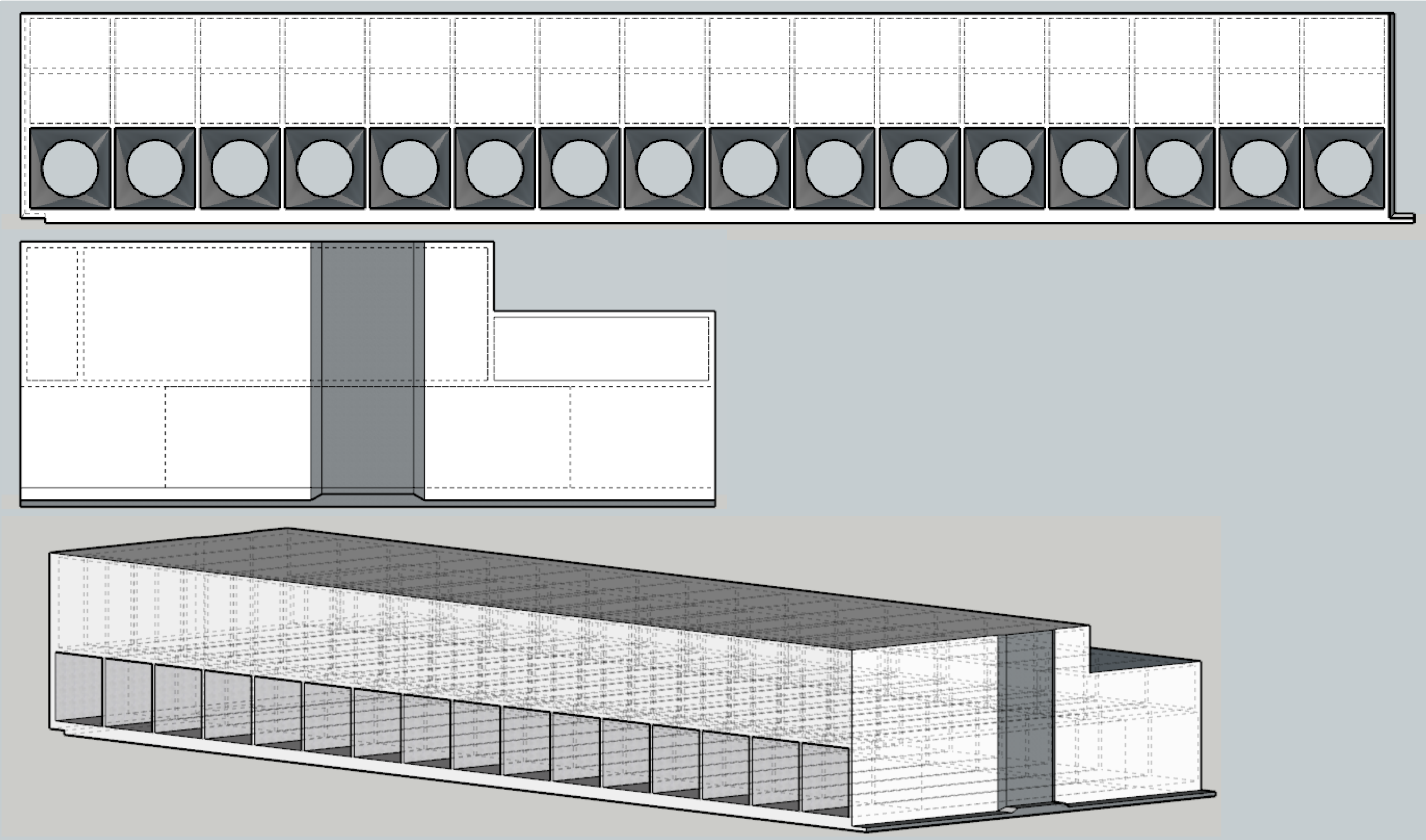

Appendix 5: SketchUp model of the Ducted setup in parallel projection from the front, the side and at an angle

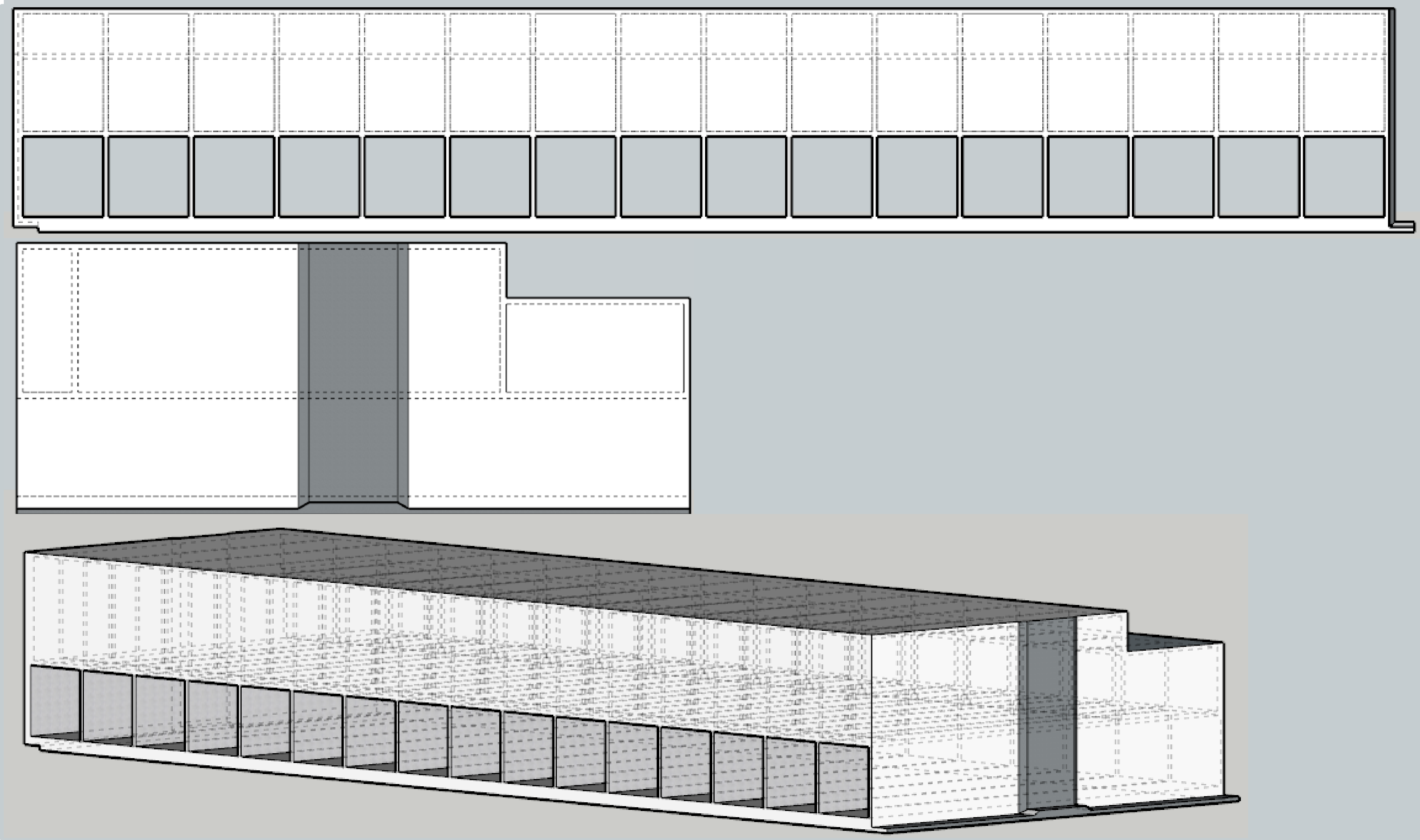

Appendix 6: SketchUp model of the Hybrid setup in parallel projection from the front, the side and at an angle

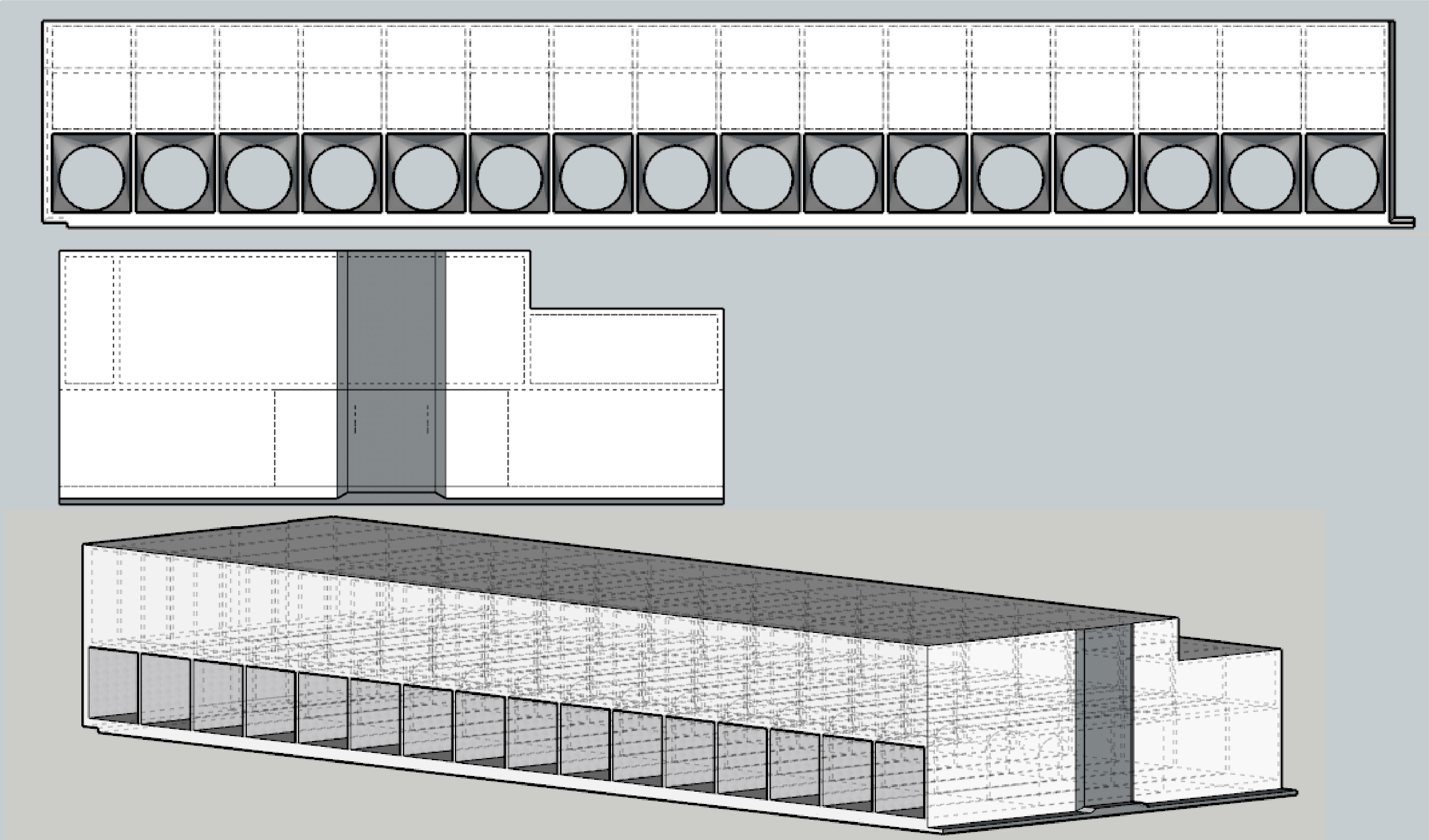

Appendix 7: SketchUp model of the optimal ducted setup in parallel projection from the front, the side and at an angle